

BOLU ABANT IZZET BAYSAL UNIVERSITY
THE GRADUATE SCHOOL OF NATURAL AND APPLIED
SCIENCES
DEPARTMENT OF CHEMISTRY



SYNTHESIS AND CHARACTERIZATION OF BISMUTH
CONTAINING NOVEL TYPE OXYPHOSPHATES

MASTER OF SCIENCE

BURCU KARTAV

BOLU, MAY 2019

APPROVAL OF THE THESIS

**SYNTHESIS AND CHARACTERIZATION OF BISMUTH CONTAINING NOVEL
TYPE OXYPHOSPHATES** submitted by **Burcu KARTAV** in partial fulfillment of the
requirements for the degree of **MASTER OF SCIENCE** in **DEPARTMENT OF
CHEMISTRY, The Graduate School of Natural and Applied Sciences of BOLU
ABANT IZZET BAYSAL UNIVERSITY** in 24/05/2019 by,

Examining Committee Members

Signature

Supervisor
Assoc. Prof. Dr. Sevim DEMİRÖZÜ ŞENOL
BOLU ABANT IZZET BAYSAL
UNIVERSITY

.....

Member
Asst. Prof. Dr. Erhan BUDAK
BOLU ABANT IZZET BAYSAL
UNIVERSITY

.....

Member
Asst. Prof. Dr. Elif AŞIKUZUN
KASTAMONU UNIVERSITY

.....

Graduation Date

Prof. Dr. Ömer ÖZYURT



Director of Graduate School of Natural and Applied Sciences

To my parents and my brother



DECLARATION

I hereby declare that all information in this document has been obtained and presented in accordance with academic rules and ethical conduct. I also declare that, as required by these rules and conduct, I have fully cited and referenced all material and results that are not original to this work.



BURCU KARTAV



ABSTRACT

SYNTHESIS AND CHARACTERIZATION OF BISMUTH CONTAINING NOVEL TYPE OXYPHOSPHATES

MSC THESIS

BURCU KARTAV

BOLU ABANT IZZET BAYSAL UNIVERSITY GRADUATE SCHOOL OF
NATURAL AND APPLIED SCIENCES

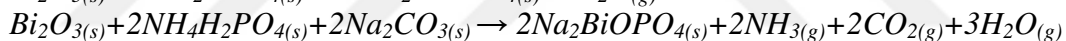
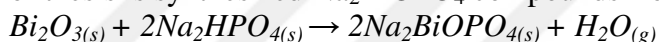
DEPARTMENT OF CHEMISTRY

(SUPERVISOR: ASSOC. PROF. DR SEVİM DEMİRÖZÜ ŞENOL)

BOLU, MAY 2019

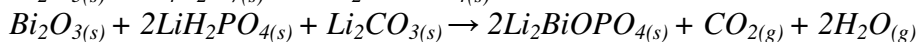
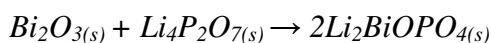
The thesis is about the synthesis of new bismuth-alkali oxy-phosphates which type of M_2BiOPO_4 ($M= Na, Li$). The obtained compounds have been characterized by X-Ray powder diffraction (XRD), Infrared spectroscopy (IR), and Scanning Electron Microscopy (SEM/EDX). And in the results of calculations (refinement) by Jana2006 and Match!3 Softwares, for the

$Bi_2O_3(s) + Na_4P_2O_7(s) \rightarrow 2Na_2BiOPO_4(s)$ solid-state reaction the unit cell parameters of synthesized compound are $a = 15.4658$, $b = 10.8601$, $c = 12.6592$ Å, the space group is detected as Pmm_2 and it crystallizes in orthorhombic system. Another work of thesis is synthesized Na_2BiOPO_4 compounds from



solid-state reactions. When the examination of obtained products in XRD and FTIR data, Na_2BiOPO_4 was found to be orthorhombic. According to Rietveld calculation results by using Jana2006 and Match!3 softwares the unit cell parameters are calculated as $a = 15.932$, $b = 10.913$, $c = 13.128$ Å and $a = 15.324$, $b = 10.746$, $c = 13.011$ Å respectively and space groups of compounds determined as Pmm_2 .

Also finally, the lithium-bismuth oxyphosphate compound was synthesized from the following solid-state reactions.



The obtained compounds were found to be monoclinic structure and found to be isomorphous with $Li_2Bi_{14.67}(PO_4)_6O_{14}$ compound. And the unit cell parameters were calculated as $a = 10.738$, $b = 12.2486$, $c = 10.4148$ Å, $\hat{a}^\circ = 93.088$, $a = 24.0345$, $b = 4.3912$, $c = 11.3362$, $\hat{a} = 101.802$ respectively and the space group determined as $P2_1$.

KEYWORDS: Oxyphosphates, XRD, IR, SEM, Sodium bismuth oxyphosphate, Lithium bismuth oxyphosphate.

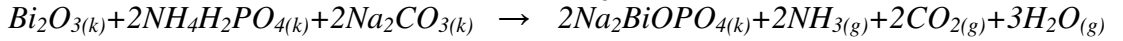
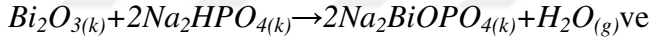
ÖZET

**BİZMUT İÇEREN YENİ TİP OKSİFOSFATLARIN SENTEZİ VE
KARAKTERİZASYONU
YÜKSEK LISANS TEZİ
BURCU KARTAV
BOLU ABANT İZZET BAYSAL ÜNİVERSİTESİ
FEN BİLİMLERİ ENSTİTÜSÜ
KİMYA ANABİLİM DALI
(TEZ DANIŞMANI: DOÇ. DR. SEVİM DEMİRÖZÜ ŞENOL)**

BOLU, MAYIS - 2019

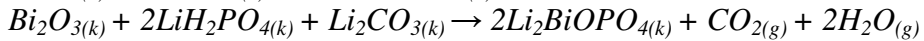
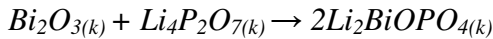
Bu tez çalışması, M_2BiOPO_4 (M= Na, Li) tipinde oluşturulan yeni bizmut alkali oksifosfatların sentezi hakkındadır. Elde edilen bu ürünler X-Işını Toz Difraksiyonu (XRD), İnfrared Spectrumu (FTIR) ve Taramalı Elektron Mikroskop (SEM/EDX) analiz yöntemleriyle karakterize edildi. Jana2006 ve Match!3 Programları (refinement) kullanılarak gerçekleştirilen hesaplamalar sonucunda,

$Bi_2O_3 (k) + Na_4P_2O_7 (k) \rightarrow 2Na_2BiOPO_4(k)$ katı hal reaksiyonu için sentezlenen bileşiğin birim hücre parametreleri $a = 15.4658$, $b = 10.8601$, $c = 12.6592$ Å olarak hesaplandı ve muhtemel simetri grubu Pmm_2 ile ortorombik sistemde kristallendiği ilk kez bu çalışma ile belirlendi. Tezin diğer bir çalışması ise katı hal yöntemi kullanılarak sentezlenen



reaksiyonlarıdır. Bu reaksiyonlar sonucunda elde edilen ürünlerin XRD ve FTIR verileri incelendiğinde, Na_2BiOPO_4 'ın ortorombik yapıda olduğu görüldü. Jana2006 ve Match!3 Programları kullanılarak gerçekleştirilen hesaplamalar sonucunda bileşiklerin birim hücre parametrelerinin sırasıyla $a = 15.932$, $b = 10.913$, $c = 13.128$ Å ve $a = 15.324$, $b = 10.746$, $c = 13.011$ Å olduğu hesaplandı ve simetri gruplarının Pmm_2 olduğu belirlendi.

Son olarak, lityum-bizmut oksifosfat bileşiği aşağıdaki katı hal reaksiyonu kullanılarak sentezlendi.



Elde edilen bileşiklerin monoklinik yapıda oldukları görüldü ve $Li_2Bi_{14.67}(PO_4)_6O_{14}$ bileşiği ile izomorf yapıda olduğu bulundu. Birim hücre boyutları sırasıyla $a = 10.738$, $b = 12.2486$, $c = 10.4148$ Å ve $\beta = 93.088^\circ$, $a = 24.0345$, $b = 4.3912$, $c = 11.3362$, $\beta = 101.802$ olarak hesaplandı ve muhtemel simetri grubunun $P2_1$ olduğu belirlendi.

ANAHTAR KELİMELER: Oksifosfat, XRD, IR, SEM, Sodyum bizmut oksifosfat, Lityum bizmut oksifosfat.

TABLE OF CONTENTS

| | <u>Page</u> |
|---|-------------|
| ABSTRACT | v |
| ÖZET | vi |
| TABLE OF CONTENTS | vii |
| LIST OF FIGURES | ix |
| LIST OF TABLES | xii |
| LIST OF ABBREVIATIONS AND SYMBOLS | xiii |
| 1. INTRODUCTION | 1 |
| 1.1 Phosphorous | 1 |
| 1.1.1 Historical Definition and Usage | 2 |
| 1.1.2 General Properties | 3 |
| 1.2 Phosphates | 4 |
| 1.2.1 General Usage | 5 |
| 1.3 Bismuth | 6 |
| 1.3.1 Definition and Properties | 6 |
| 1.3.2 Usage and Importance | 7 |
| 1.4 Oxy-phosphates | 9 |
| 1.4.1 KTiOPO_4 (KTP) | 9 |
| 1.4.2 General Properties and Definition of Oxyphosphates | 10 |
| 1.5 Bismuth-Oxyphosphates | 12 |
| 2. PURPOSE OF WORK | 14 |
| 2.1 Reactions | 14 |
| 3. MATERIALS AND METHODS | 16 |
| 3.1 Chemicals | 16 |
| 3.2 Preparation of Samples | 16 |
| 3.2.1 Agate Mortar and Pestle | 16 |
| 3.2.2 Chamber Furnace | 17 |
| 3.3 Experimental Procedure | 18 |
| 3.3.1 Solid-State Reaction of Bi_2O_3 (s) + $\text{Na}_4\text{P}_2\text{O}_7$ (s) | 18 |
| 3.3.2 Solid-State Reaction of Bi_2O_3 (s) + $2\text{Na}_2\text{HPO}_4$ (s) | 19 |
| 3.3.3 Solid-State Reaction of Bi_2O_3 (s) + $2\text{NH}_4\text{H}_2\text{PO}_4$ (s) + $2\text{Na}_2\text{CO}_3$ (s) | 20 |
| 3.3.4 Synthesis of $\text{Li}_4\text{P}_2\text{O}_7$ (s) | 20 |
| 3.3.5 Solid-State Reactions of Bi_2O_3 (s) + $\text{Li}_4\text{P}_2\text{O}_7$ (s) | 20 |
| 3.3.6 Solid-State Reaction of Bi_2O_3 (s) + $2\text{LiH}_2\text{PO}_4$ (s) + Li_2CO_3 (s) | 21 |
| 3.3.7 Solid-State Reaction of Bi_2O_3 (s) + $2\text{Li}_2\text{CO}_3$ (s) + $2\text{NH}_4\text{H}_2\text{PO}_4$ (s) | 21 |
| 3.3.8 Solid-State Reaction of Bi_2O_3 (s) + $2(\text{NH}_4)_2\text{HPO}_4$ (s) + $2\text{Li}_2\text{CO}_3$ (s) | 22 |
| 3.4 Characterization | 22 |
| 3.4.1 X-Ray Powder Diffraction | 22 |
| 3.4.2 Fourier Transform Infrared (FTIR) Spectroscopy | 23 |
| 3.4.3 Scanning Electron Microscopy (SEM) and Energy Dispersive X-Ray (EDX) Analysis | 24 |
| 3.5 Calculations | 25 |
| 3.5.1 Weight Loss Calculation | 25 |

| | | |
|-----------|---|-----------|
| 4. | RESULT AND DISCUSSION..... | 27 |
| 4.1 | Solid State Reaction of $\text{Bi}_2\text{O}_3(s) + \text{Na}_4\text{P}_2\text{O}_7(s)$ | 27 |
| 4.1.1 | Infrared (IR) Studies of $\text{Bi}_2\text{O}_3(s) + \text{Na}_4\text{P}_2\text{O}_7(s)$ | 27 |
| 4.1.2 | X-Ray Diffraction (XRD) Studies..... | 29 |
| 4.1.3 | Scanning Electron Microscopy (SEM) and (EDX) Studies | 32 |
| 4.2 | Solid State Reaction of $\text{Bi}_2\text{O}_3(s) + 2\text{Na}_2\text{HPO}_4(s)$ | 36 |
| 4.2.1 | Infrared (IR) Studies of $\text{Bi}_2\text{O}_3(s) + 2\text{Na}_2\text{HPO}_4(s)$ | 36 |
| 4.2.2 | X-Ray Diffraction (XRD) Studies..... | 37 |
| 4.2.3 | Scanning Electron Microscopy (SEM) and (EDX) Studies | 42 |
| 4.3 | Solid State Reaction of $\text{Bi}_2\text{O}_3(s) + 2\text{NH}_4\text{H}_2\text{PO}_4(s) + 2\text{Na}_2\text{CO}_3(s)$ | 43 |
| 4.3.1 | Infrared (IR) Studies of $\text{Bi}_2\text{O}_3(s) + 2\text{NH}_4\text{H}_2\text{PO}_4(s) + 2\text{Na}_2\text{CO}_3(s)$ | 44 |
| 4.3.2 | X-Ray (XRD) Studies..... | 46 |
| 4.3.3 | Scanning Electron Microscopy (SEM) and (EDX) Studies | 49 |
| 4.4 | Synthesize of $\text{Li}_4\text{P}_2\text{O}_7$ | 51 |
| 4.4.1 | Infrared (IR) Studies..... | 51 |
| 4.4.2 | X-Ray (XRD) Studies..... | 53 |
| 4.5 | Solid-State Reaction of $\text{Bi}_2\text{O}_3(s) + \text{Li}_4\text{P}_2\text{O}_7(s)$ | 56 |
| 4.5.1 | Infrared (IR) Studies..... | 57 |
| 4.5.2 | X-Ray Diffraction (XRD) Studies..... | 58 |
| 4.5.3 | Scanning Electron Microscopy (SEM) and (EDX) Study..... | 63 |
| 4.6 | Solid-State Reaction of $\text{Bi}_2\text{O}_3(s) + 2\text{LiH}_2\text{PO}_4(s) + \text{Li}_2\text{CO}_3(s)$ | 65 |
| 5. | CONCLUSIONS | 70 |
| 6. | REFERENCES..... | 72 |
| 7. | APPENDICES | 78 |
| 7.1 | Appendix A FTIR Spectrums of Samples..... | 78 |
| 8. | CURRICULUM VITAE..... | 81 |

LIST OF FIGURES

| | <u>Page</u> |
|--|-------------|
| Figure 1.1. A Phosphorous rock and a crystal structure of a Phosphorous element which was drawn with Diamond4 Crystal and Molecular Structure Visualization software..... | 1 |
| Figure 1.2. Picture of powder white, red, black Phosphorous. | 3 |
| Figure 1.3. 3D representation of some phosphate compounds. | 4 |
| Figure 1.4. A crystal bismuth view and a crystal structure of a Bismuth element which is drawn with Diamond4 Crystal Structure Visualization software | 6 |
| Figure 1.5. Bismuth usage areas in the industry. | 7 |
| Figure 1.6. A crystal KTP view and crystal structure of a KTiOPO_4 -orthorhombic structure drawn with Diamond 4 Crystal and Molecular Structure Visualization software. | 9 |
| Figure 3.1. KERN Analytical balance ABS-N/ABJ-NM..... | 17 |
| Figure 3.2. The Protherm Chamber Furnace-PLF Series (150/5)..... | 18 |
| Figure 3.3. Rigaku MultiFlex X-Ray Diffractometer | 23 |
| Figure 3.4. PerkinElmer Spectrum Two FT-IR Spectroscopy | 24 |
| Figure 3.5. Jeol model-JSM 6390 LV Scanning Electron Microscope..... | 25 |
| Figure 4.1. IR Spectra of the Initial Pure Compounds $\text{Na}_4\text{P}_2\text{O}_7$ and Bi_2O_3 | 28 |
| Figure 4.2. IR Spectra of the products of $\text{Bi}_2\text{O}_3(s) + \text{Na}_4\text{P}_2\text{O}_7(s)$ at 350°C (6h), 500°C (6h), 600°C (6h), 700°C (6h), and twice at 800°C (12h). | 28 |
| Figure 4.3. X-Ray Powder Diffraction Pattern of $\text{Bi}_2\text{O}_3(s) + \text{Na}_4\text{P}_2\text{O}_7(s)$ at 800°C (12h)..... | 30 |
| Figure 4.4. X-Ray Powder Diffraction Pattern of $\text{Bi}_2\text{O}_3(s) + \text{Na}_4\text{P}_2\text{O}_7(s)$ at 350°C (6h), 500°C (6h), 600°C (6h), 700°C (6h) and two times at 800°C (6h)..... | 30 |
| Figure 4.5. Jana2006 refinement pattern for Bi_2O_3 and $\text{Na}_4\text{P}_2\text{O}_7$ | 31 |
| Figure 4.6. SEM images of $\text{Bi}_2\text{O}_3(s) + \text{Na}_4\text{P}_2\text{O}_7(s)$ reaction at 800°C a) $10\ \mu\text{m}$ b) $5\ \mu\text{m}$ | 33 |
| Figure 4.7. EDS Spectrum of the Products obtained from the $\text{Bi}_2\text{O}_3(s) + \text{Na}_4\text{P}_2\text{O}_7(s)$ reaction at 800°C (12h)..... | 33 |
| Figure 4.8. The IR Spectrum of the decomposed $\text{Na}_2\text{BiOPO}_4$ compound to $\gamma\text{-Na}_3\text{Bi}(\text{PO}_4)_2$ from the reaction of $\text{Bi}_2\text{O}_3(s) + \text{Na}_4\text{P}_2\text{O}_7(s)$ at 900°C | 34 |
| Figure 4.9 a) X-Ray Powder Diffraction Pattern of the decomposed $\text{Na}_2\text{BiOPO}_4$ compound to $\gamma\text{-Na}_3\text{Bi}(\text{PO}_4)_2$ from the reaction of $\text{Bi}_2\text{O}_3(s) + \text{Na}_4\text{P}_2\text{O}_7(s)$ at 900°C b) Shows the simplified quantitative analysis of difference plot of the reaction product and $\gamma\text{-Na}_3\text{Bi}(\text{PO}_4)_2$ ICDD: 41-0178. | 35 |
| Figure 4.10. IR Spectra of the products of $\text{Bi}_2\text{O}_3(s) + 2\text{Na}_2\text{HPO}_4(s)$ reaction at 350°C (6h), 500°C (6h), 600°C (6h), 700°C (6h) and twice at 800°C (12h)..... | 37 |
| Figure 4.11. X-Ray Powder Diffraction Pattern of $\text{Bi}_2\text{O}_3(s) + 2\text{Na}_2\text{HPO}_4(s)$ at 800°C (12h)..... | 38 |

| | |
|---|----|
| Figure 4.12. X-Ray Powder Diffraction Pattern of $Bi_2O_3(s) + 2Na_2HPO_4(s)$ at 350°C(6h), 500°C(6h), 600°C(6h), 700°C(6h), and two times at 800°C(12h)..... | 39 |
| Figure 4.13. Jana2006 refinement XRD pattern of product | 40 |
| Figure 4.14. SEM images of $Bi_2O_3(s) + 2Na_2HPO_4(s)$ reaction at 800°C a) 20 μm b) 10 μm c) 5 μm..... | 42 |
| Figure 4.15. EDS Spectrum of the Product obtained from the $Bi_2O_3(s) + 2Na_2HPO_4(s)$ reaction at 800°C (12h). | 43 |
| Figure 4.16. IR Spectra of the Initial Pure Compounds Na_2CO_3 and $NH_4H_2PO_4$ | 45 |
| Figure 4.17. IR Spectra of the products of $Bi_2O_3(s) + 2NH_4H_2PO_4(s) + 2Na_2CO_3(s)$ reaction at 350°C (6h), 500°C (6h), 600°C (6h), 700°C (6h) and twice at 800°C (6h)..... | 45 |
| Figure 4.18. X-Ray Powder Diffraction Pattern of $Bi_2O_3(s) + 2NH_4H_2PO_4(s) + 2Na_2CO_3(s)$ solid-state reaction at 800°C (12h)..... | 46 |
| Figure 4.19. X-Ray Powder Diffraction Pattern of $Bi_2O_3(s) + 2NH_4H_2PO_4(s) + 2Na_2CO_3(s)$ at 350°C(6h), 500°C(6h), 600°C(6h), 700°C(6h) and two times at 800°C(12h). | 47 |
| Figure 4.20. Jana2006 refinement pattern for $Bi_2O_3 + Na_2CO_3 + NH_4H_2PO_4$ | 48 |
| Figure 4.21. SEM images of $Bi_2O_3(s) + 2NH_4H_2PO_4(s) + 2Na_2CO_3(s)$ reaction at 800°C a) 10 μm b) 5 μm..... | 50 |
| Figure 4.22. EDS Spectrum of the Product obtained from the $Bi_2O_3(s) + NH_4H_2PO_4(s) + 2Na_2CO_3(s)$ reaction at 800°C (12h). | 50 |
| Figure 4.23. IR Spectra of the Initial Pure Compounds Li_2CO_3 and $NH_4H_2PO_4$ | 52 |
| Figure 4.24. IR Spectra of the reaction $Li_2CO_3 + NH_4H_2PO_4$ at 300°C (8h), 500°C (8h), and 750°C (8h)..... | 52 |
| Figure 4.25. X-Ray Powder Diffraction Pattern of $Li_4P_2O_7(s)$ at 750°C (8h) | 57 |
| Figure 4.26. X-Ray Powder Diffraction Pattern of $Li_4P_2O_7(s)$ at 300°C(8h), 500°C(8h), and 750°C(8h)..... | 57 |
| Figure 4.27. Jana2006 refinement pattern of synthesized $Li_4P_2O_7$ | 56 |
| Figure 4.28. IR Spectra of the products of $Bi_2O_3(s) + Li_4P_2O_7(s)$ reaction at 350°C (6h), 500°C (6h), 600°C (6h), 700°C (6h), and three times at 800°C (20h)..... | 58 |
| Figure 4.29. X-Ray Powder Diffraction Pattern of $Bi_2O_3(s) + Li_4P_2O_7(s)$ at 800°C (20h)..... | 60 |
| Figure 4.30. X-Ray Powder Diffraction Pattern of $Bi_2O_3(s) + Li_4P_2O_7(s)$ at 350°C(6h), 500°C(6h), 600°C(6h), 700°C(6h), and first heating at 800°C. | 60 |
| Figure 4.31. Jana2006 refinement pattern for $Bi_2O_3(s) + Li_4P_2O_7(s)$ | 62 |
| Figure 4.32. SEM images of $Bi_2O_3(s) + Li_4P_2O_7(s)$ reaction at 800°C (20h) a) 5 μm b) 10 μm c) EDX Spectrum..... | 64 |
| Figure 4.33. IR Spectra of the product of $Bi_2O_3(s) + 2LiH_2PO_4(s) + Li_2CO_3(s)$ at 350°C (6h), 500°C (6h), 800°C (24h), 850°C(6h)..... | 65 |
| Figure 4.34. X-Ray Powder Diffraction Pattern of $Bi_2O_3(s) + 2LiH_2PO_4(s) + Li_2CO_3(s)$ at 850°C (6h)..... | 66 |
| Figure 4.35. Jana2006 refinement pattern for $Bi_2O_3(s) + 2LiH_2PO_4(s) + Li_2CO_3(s)$ | 67 |
| Figure 4.36. X-Ray Powder Diffraction Pattern of $Bi_2O_3(s) + 2Li_2CO_3(s) + 2(NH_4)_2HPO_4(s)$ at 850°C (12h) shown on the top of figure and $Bi_2O_3(s) + 2Li_2CO_3(s) + 2NH_4H_2PO_4(s)$ at 850°C (6h) shown on the below of figure..... | 69 |

| | |
|---|----|
| Figure A.1. IR Spectrum of the product of $Bi_2O_3 (s) + Na_4P_2O_7 (s)$ at $800^\circ C$ (12h)..... | 78 |
| Figure A.2. IR Spectrum of the product of $Bi_2O_3 (s) + 2Na_2HPO_4(s)$ at $800^\circ C$ (12h)..... | 78 |
| Figure A.3. IR Spectrum of the product of $Bi_2O_3 (s) + 2NH_4H_2PO_4(s) + 2Na_2CO_3(s)$ at $800^\circ C$ (12h)..... | 79 |
| Figure A.4. IR Spectrum of the product of $Bi_2O_3(s) + Li_4P_2O_7(s)$. at $800^\circ C$ (20h)..... | 79 |
| Figure A.5. IR Spectrum of the product of $Li_4P_2O_7(s)$ at $750^\circ C$ (8h)..... | 80 |
| Figure A.6. IR Spectrum of the product of $Bi_2O_3(s) + LiH_2PO_4(s) + Li_2CO_3(s)$ at $850^\circ C$ (6h)..... | 80 |



LIST OF TABLES

| | <u>Page</u> |
|---|-------------|
| Table 1.1. Representations and general usage of Phosphate compounds..... | 5 |
| Table 1.2. Explanation of Bismuth industry with some related examples..... | 9 |
| Table 1.3. Some important oxyphosphates which used in the industry. | 11 |
| Table 3.1. a) Weight Loss results of the last temperature of each reaction product was charted. b) Weight Loss results of each reaction temperatures from starting temperature to ending temperature for each reaction were charted. | 26 |
| Table 4.1. The observed IR frequencies of reagents Bi_2O_3 and $\text{Na}_4\text{P}_2\text{O}_7$ | 27 |
| Table 4.2. Refinement and structural parameters of product recorded from Jana2006..... | 31 |
| Table 4.3. X-Ray powder diffraction data of orthorhombic $\text{Na}_2\text{BiOPO}_4$ from the reaction of $\text{Bi}_2\text{O}_3 (s) + \text{Na}_4\text{P}_2\text{O}_7 (s)$, with the refined cell parameters (see Table 4.2). | 32 |
| Table 4.4. Refinement and structural parameters of product recorded from Jana2006..... | 40 |
| Table 4.5. X-Ray powder diffraction data of orthorhombic $\text{Na}_2\text{BiOPO}_4$ from the reaction of $\text{Bi}_2\text{O}_3 (s) + 2\text{Na}_2\text{HPO}_4 (s)$, with the refined cell parameters (see Table 4.4)..... | 41 |
| Table 4.6. The observed IR frequencies of reagents Na_2CO_3 and $\text{NH}_4\text{H}_2\text{PO}_4$ | 44 |
| Table 4.7. Refinement and structural parameters of product recorded from Jana2006..... | 48 |
| Table 4.8. X-Ray powder diffraction data of orthorhombic $\text{Na}_2\text{BiOPO}_4$ from the reaction of $\text{Bi}_2\text{O}_3 (s) + 2\text{NH}_4\text{H}_2\text{PO}_4 (s) + 2\text{Na}_2\text{CO}_3 (s)$ with the refined cell parameters (see Table 4.7.) | 49 |
| Table 4.9. The observed IR frequencies of reagents Li_2CO_3 and $\text{NH}_4\text{H}_2\text{PO}_4$ | 51 |
| Table 4.10. X-Ray Powder Data for Triclinic $\text{Li}_4\text{P}_2\text{O}_7$ compound by the $2\text{Li}_2\text{CO}_3 (g) + 2\text{NH}_4\text{H}_2\text{PO}_4 (s)$ solid-state reaction at 750°C (8h) from Rietveld Calculation..... | 54 |
| Table 4.11. Refinement and structural parameters of product recorded from Jana2006..... | 56 |
| Table 4.12. The observed IR frequencies of reagents Bi_2O_3 and $\text{Li}_4\text{P}_2\text{O}_7$ | 57 |
| Table 4.13. X-Ray Powder Data for Monoclinic compound by the solid-state reaction of $\text{Bi}_2\text{O}_3 (s) + \text{Li}_4\text{P}_2\text{O}_7 (s)$ at 800°C (20h) from Rietveld Calculation. | 61 |
| Table 4.14. Refinement and structural parameters of product recorded from Jana2006..... | 63 |
| Table 4.15. X-Ray Powder Data for Monoclinic compound by the solid-state reaction of $\text{Bi}_2\text{O}_3 (s) + 2\text{LiH}_2\text{PO}_4 (s) + \text{Li}_2\text{CO}_3 (s)$ at 850°C (6h) from Rietveld Calculation. | 75 |

LIST OF ABBREVIATIONS AND SYMBOLS

| | |
|--|---|
| XRD | : X-Ray Diffractometer |
| IR | : Infrared |
| SEM | : Scanning Electron Microscopy |
| EDX | : Energy Dispersive X-Ray |
| Na₂BiOPO₄ | : Sodium Bismuth Oxyphosphate |
| Li₂BiOPO₄ | : Lithium Bismuth Oxyphosphate |
| COD | : Crystallography Open Database |
| ICDD | : International Centre for Diffraction Data |



ACKNOWLEDGEMENTS

I would like to thank my supervisor, Assoc. Prof. Dr. Sevim DEMİRÖZÜ ŞENOL, for her inspiration and all her support during my study at Bolu Abant İzzet Baysal University. Also, I would like to thank her for helping about writing a thesis with her own master thesis (Thesis No: 131663).

I would like to thank my university for all providing opportunities.

I would like to thank my family for all financial and moral support during my education.



1. INTRODUCTION

1.1 Phosphorous

Elemental phosphorous (known as white phosphorus) exists as P_4 molecules when the oxides P_4O_6 and P_4O_{10} are formed, the phosphorous atoms retain their tetrahedral arrangement. It is solid, highly reactive, poisonous and the name of phosphorus comes from the phos- meaning light, -phoros meaning bearer creating the term bringing light.

Phosphorus occurs broadly in nature and it is the sixth most abundant element in all living organisms. And it is present in our teeth, genes, bones, and muscles work in our body, in case of the phosphorus in adenosine triphosphate (ATP). Also phosphorous is present naturally in water and food and it is found in diet supplements (Phosphates, 2019).

Phosphorus (P), one of the non-metallic chemical element of the nitrogen family that at room temperature is a colorless solid, semi-transparent, soft, waxy solid that glows in the dark.

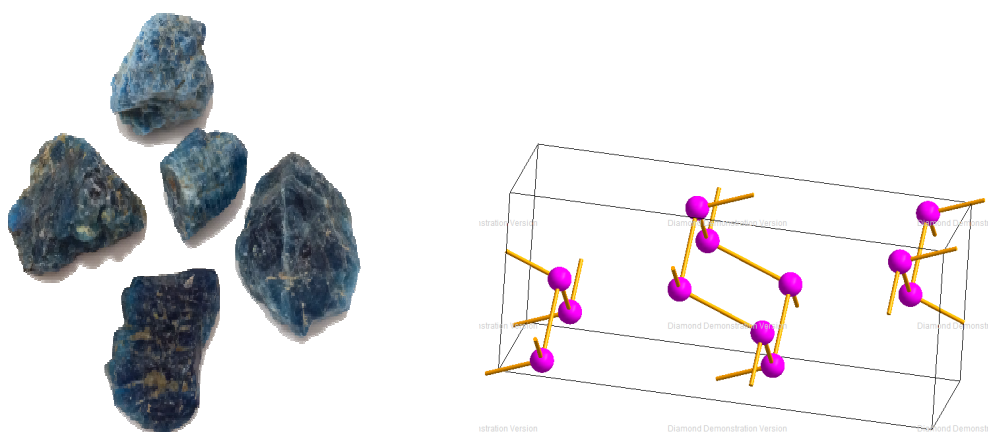


Figure 1.1. A Phosphorous rock and a crystal structure of a Phosphorous element which was drawn with Diamond4 Crystal and Molecular Structure Visualization software.

1.1.1 Historical Definition and Usage

The growth of phosphorous was beginning with Hennig Brand who was the discoverer of phosphorus accidentally in Germany, 1669 with preparing phosphorous from urine (Urine that naturally contains many amounts of unsolved phosphates). Brand called of phosphorous substance as 'cold-fire' in the case of phosphorous was luminous and so glowing in the dark (Weeks, 1933).

Brand's method is believed to have consisted of evaporating urine to leave a black residue that was then left for a few months. Then the residue was heated with sand and driving off a variety of gases and oils which were condensed in water. The final substance to be driven off, condensing as a white solid was phosphorus. (Weeks, 2000).

Phosphorous produced in its elemental form from phosphate bearing ore is the mother element of this industry and growing family of phosphates. Most of the food-grade phosphoric acids and phosphates are produced by processors of elemental phosphorous from electric furnace operations (Erhan, 1946).

Today, an elementary phosphorus compound can be used in different type of applications, such as pharmaceuticals, industrial & institutional cleaners, personal care products, and other technical uses such as fire extinguishers. Phosphorous and its compounds used in plastics, sealants, flame-retardant, toothpaste, detergents, steel, mating matchbook strikers. It is also used in making weapons like incendiary bombs from white phosphorus during World War 2.

In addition to their versatility, government authorities also recognize them as safe for worker exposure and handling and for use in the home. Phosphates are generally used as compounds of phosphate ions in combination with one or more elements, such as sodium, calcium, potassium, and aluminum. In generally, phosphates can be separated into several primary groups based on the number of phosphorus molecules. Each of these groups has functional properties ideal for many applications (Phosphates, 2019).

1.1.2 General Properties



Figure 1.2. Picture of powder white, red, black Phosphorous.

While the specifying of Phosphorous, there are three allotropes which are white, black and red phosphorus.

Red phosphorus is an amorphous non-toxic solid that can vary in color from orange to purple, cause of slight variations in its chemical structure. It does not dissolve in many liquids. Red phosphorous is the most stable among three forms of phosphorus and it is chemically the least reactive. For this reason, unlike white phosphorus, red phosphorous does not ignite spontaneously. Also, it is the densest type of phosphorous.

White phosphorus is used in incendiary devices and flares. It is a poisonous waxy solid and when contact with skin can cause severe burns. It glows in the dark and it is spontaneously flammable when exposed to air. White phosphorus does not react with water and can be easily stocked, melted or transported when protected by a layer of water. It is soluble in some of the classical solvents such as benzene and carbon disulfide. White phosphorus is manufactured industrially by heating phosphate rock in the presence of carbon and silica in a furnace (Emsley John, 2011).

Black Phosphorus which is thermodynamically the most stable allotrope of phosphorous is a layered semiconducting material. It is existing into three crystalline modifications which are rhombohedral, orthorhombic, and simple cubic forms.

Black phosphorus atomic layers, phosphorene, is a two-dimensional material. It has anisotropic and high mobility properties, also other particular characteristics.

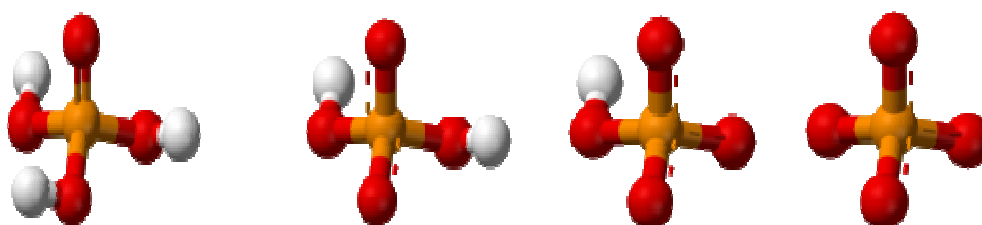
Black phosphorous is non-flammable and it is insoluble in many solvents. Also, it is chemically inert in appearance to graphite and with numerous uses in optoelectronic-optical polarizers, semiconductor, thin-film solar cells, nano-electromechanical oscillators, gas sensors, and photovoltaic applications. In a two-dimensional form, black phosphorus is known as Phosphorene and has similar properties to other 2D semiconductor materials such as graphene (Zhao et al., 2017).

1.2 Phosphates

Phosphates are salt of phosphoric acids. Phosphorus existed on Earth crust in numerous compound forms, such as the phosphate ion (PO_4^{3-}), located in water, soil and sediments. This inorganic phosphate is then distributed in soils and water. Rain and weathering cause rocks to release phosphate ions and other minerals.

In soil, there is a small amount of phosphorous, and this often limits plant growth. Animals absorb phosphates by eating plants or plant-eating animals (Pokapū Akoranga Pūtaiao, 2013).

In an aqueous solution, phosphate exists in four forms. Also, it can form polymeric ions like diphosphate and pyrophosphate (McMurry, Fay, and McCarty, 2004).



H_3PO_4 (Main form) H_2PO_4^- (Most Common) HPO_4^{2-} (Prevalent) PO_4^{3-} (Predominate)

Figure 1.3. 3D representation of some phosphate compounds.

Phosphate materials can be specified into four classes without allotropes of phosphate which are mono-phosphates, condensed phosphates (poly-phosphates, cyclo-phosphates, ultra-phosphates), adducts and hetero-polyphosphates. Monophosphates is given to compounds which anionic entity PO_4^{3-} and monophosphates are the most stable and the only phosphates to be found in nature. Condensed phosphates which phosphoric anion including P-O-P bonds are applied to salts (Averbuch-Pouchot and Durif, 1996).

1.2.1 General Usage

Table 0.1. Representations and general usage of Phosphate compounds.

| | | |
|--|---------------------|--|
| PO_4^{-3} | • Monophosphates | Buffering – detergents. |
| $\text{P}_2\text{O}_7^{-4}$ | • Pyrophosphates | Sequestering – water treatment, metal cleaning. |
| $\text{P}_n\text{O}_{3n}^{-n}$ | • Metaphosphate | An alternative of white phosphorus in organic synthesize. Some types of metaphosphate salts use in foods and toiletries. |
| $\text{P}_n\text{O}_{(3n+1)}^{-(n+2)}$ | • Polyphosphates | Dispersant – kaolin production. Paints and coatings. Such as Tetrasodium Pyrophosphate (TSPP). |
| $\text{P}_3\text{O}_{10}^{-5}$ | • Tripolyphosphates | Dispersant – meat processing, dish detergent. Such as Potassium Tripolyphosphate (KTPP). |
| $\text{P}_6\text{O}_{19}^{-8}$ | Hexametaphosphate | Kaolin clay deflocculants for the production of paper coatings (Kaolin is the predominant pigment used in coatings). |

(Phosphates, 2019)

Mainly the usage areas of Phosphate are Building and Construction, industrial and institutional cleaning, pharmaceuticals and personal care products, agriculture, water treatment, fire, metal treatment, specialty industrial applications like ceramics, clay processing, paper processing, photocopier toner, integrated circuitry, etc (Paints & Coatings n.d.).

In the earth crust, there are hundreds of phosphate minerals which have been separated into various groups depending upon the cationic elements present in them. On the other hand, all the naturally occurring phosphates are represented by one anionic group which is orthophosphate (Byrappa, 1986).

Phosphorus occurs extensively in nature, the most common materials which are being phosphate rocks and minerals, bones, and teeth. The most important phosphate rocks are calcium phosphate- $\text{Ca}_3(\text{PO}_4)_2$, apatite- $\text{Ca}_5(\text{PO}_4)_3\text{OH}$, fluoroapatite- $\text{Ca}_5(\text{PO}_4)_3\text{F}$, and chloroapatite- $\text{Ca}_5(\text{PO}_4)_3\text{Cl}$. Phosphoric acid mainly for use in manufacturing fertilizers and other chemicals are processing by treating phosphate rock with sulfuric acid. Huge quantities of phosphorus compounds are used in the production of fertilizers. Such as calcium phosphate which has many fields of the world, but its direct use as a fertilizer is not very effective because of its low solubility so sulfuric acid plays an important role in fertilizer production and approximately 65% of the sulfuric acid manufactured is used for this reason (House and House, 2016).

Hydrophosphates of calcium $\text{Ca}(\text{H}_2\text{PO}_4)_2\text{H}_2\text{O}$ and ammonium $(\text{NH}_4)_2\text{HPO}_4$ and $(\text{NH}_4)\text{H}_2\text{PO}_4$ are the most commonly used fertilizers, while potassium hydro phosphate KH_2PO_4 is also used where the soil needs potash (potassium compounds such as carbonates, nitrates, and sulfates). Also, other applications and fertilizer usage described with related compounds found in the literature (Naito, Shinohara, and Uematsu, 2003).

1.3 Bismuth

1.3.1 Definition and Properties

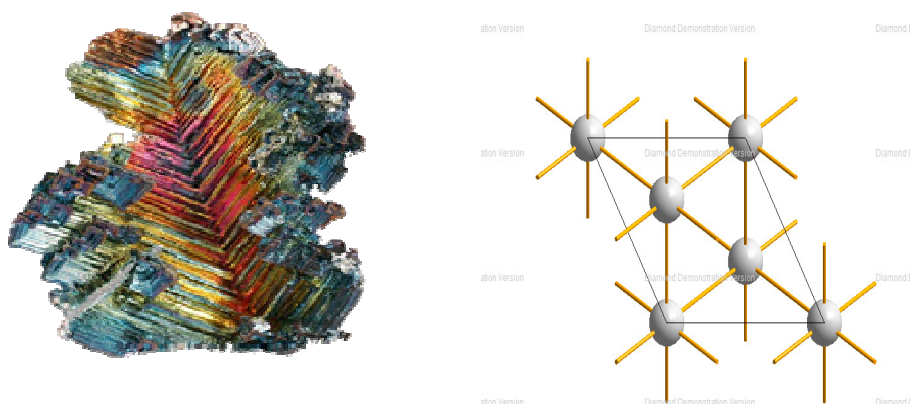


Figure 1.4. A crystal bismuth view and a crystal structure of a Bismuth element which is drawn with Diamond4 Crystal Structure Visualization software.

Bismuth was isolated in the 15th century, and it was first used as making movable type for printing shortly after the invention of the Gutenberg printing process in 1440. It was confused with other elements like lead, tin, antimony. Bismuth is used in printing because it is one of the few substances known whose solid state is less dense than the liquid (DeCoste, 2013).

After that, bismuth was first determined to be a distinct element in 1753 by Claude Geoffroy the Younger. It is a white crystalline, brittle metal and occurs free in nature and in such minerals as bismuthinite (Bi_2S_3) which is the most source of bismuth and bismite (Bi_2O_3) ores. The largest deposits of bismuth are found in Bolivia, although bismuth is usually obtained as a by-product of mining and refining lead, copper, tin, silver, and gold. Bismuth (Bi) is the most diamagnetic metal “Bismanol” is a permanent magnet of high coercive force, made of MnBi and has the lowest thermal conductivity in all metals (except mercury) (Haynes n.d.).

It is also the least abundant (2×10^{-5} weight percent of Earth’s crust) of the elements in the nitrogen group. And bismuth is the 70th most abundant element in the Earth’s crust.

1.3.2 Usage and Importance

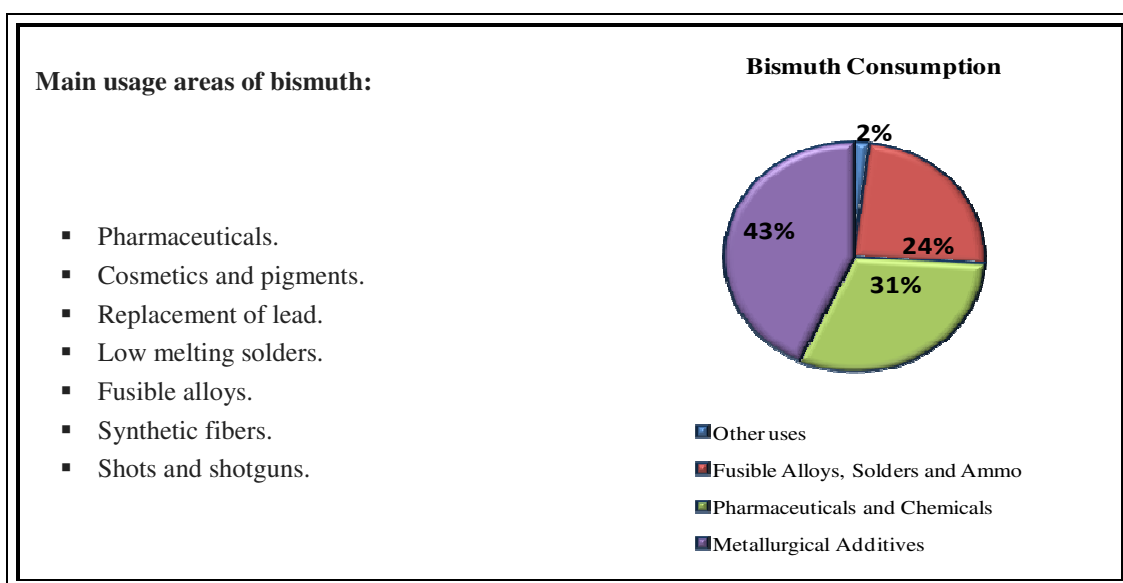


Figure 0.5. Bismuth usage areas in the industry.
(Bismuth: Not Just for Heartburn | Seeking Alpha n.d.)

1.3.2.1 Medical Usage

Bismuth unusually has the lowest toxicity of all heavy metals. Even most bismuth compounds have less toxicity than sodium chloride. Their insolubility in neutral aqueous solutions such as biological fluids resulting from the remarkably low toxicity. Though, low pH environment increases the solubility of bismuth compounds. Both of Bi(III) and Bi(V) complexes as cancer drugs have been developed and used for some tumor treatment. Their bioactivities in the treatment of several gastrointestinal disorders, anti-tumor, anti-microbial, and anti-bacterial activities have been investigated (Yang et al. 2015), (Ouyang et al. 2016).

1.3.2.2 Bismuth Oxide Thin Films

Most of the high performance electronic and optoelectronic devices are made of crystalline materials. Bismuth trioxide thin films, Bi_2O_3 is one of the important industrial compounds of elemental bismuth due to this type of bismuth molecules have a large energy band gap, high refractive index, high photoconductivity, photosensitivity to ultraviolet radiation depending on their structure and morphology. These properties provide Bi_2O_3 for a huge variety of applications such as solar cells, components in electronic circuitry, optical coatings, recording layers in CDs and DVDs, humidity sensors, etc. (Jeanmonod, Rebecca, and Suzuki, 2018).

1.3.2.3 Bismuth Based Nanoparticles

The application of bismuth-based nanoparticles is known as their excellent chemical, electrical, optical and especially catalytic activities. Bismuth-based nanoparticles are photocatalytic materials so, with this property, Bismuth-based nanoparticles are cost-effective and environmentally friendly nature. That nanoparticles are high visible light responsivity and efficient photocatalytic performances and they used in carbon dioxide reduction, hydrogen generation, air purification (William W. Anku and Penny P. Govender, 2018).

Table 0.2 Explanation of Bismuth industry with some related examples.

| | |
|-------------------------------|---|
| <p>MEDICAL APPLICATIONS</p> | <ul style="list-style-type: none"> • Good antibacterial properties. • Treat peptic ulcers. • Treat eye infections. • Internal deodorant to treat malodor • Milk of bismuth (an aqueous solution of bismuth hydroxide and bismuth subcarbonate) • Bismuth subcarbonate ($\text{Bi}_2\text{O}_2(\text{CO}_3)$) are also used in medicine |
| <p>COSMETICS AND PIGMENTS</p> | <ul style="list-style-type: none"> • Bismuth oxychloride (BiOCl) is occasionally used in cosmetics, as a pigment in paint for eye shadows, hair sprays and nail polishes |
| <p>METAL AND ALLOYS</p> | <ul style="list-style-type: none"> • Lead replacement for many ballistics and weighting applications. Bismuth alloys are used in soldering, thermocouple materials and magnetic memory devices, lubricating greases, thermoelectric materials, infrared spectrometers, etc. |

(Bismuth: applications and uses-Metalpedia n.d.)

1.4 Oxy-phosphates

1.4.1 KTiOPO_4 (KTP)

One of the most important oxyphosphates of the $\text{MM}'\text{OPO}_4$ type is KTiOPO_4 (KTP). The crystal structure of KTiOPO_4 was determined in 1974 by Tordjman and his coworkers (Tordjman, Masse, and Guitel, 1974). KTP is a complex with a three-dimensional network of PO_4 tetrahedra and distorted TiO_6 octahedra with one shorter and longer Ti-O bond. It crystalizes as orthorhombic. It has a high damage threshold, and high conversion efficiency, good physical and chemical resistivity, it is insoluble in hygroscopic and water (Bolt, van der Mooren, and Sebastian, 1991).

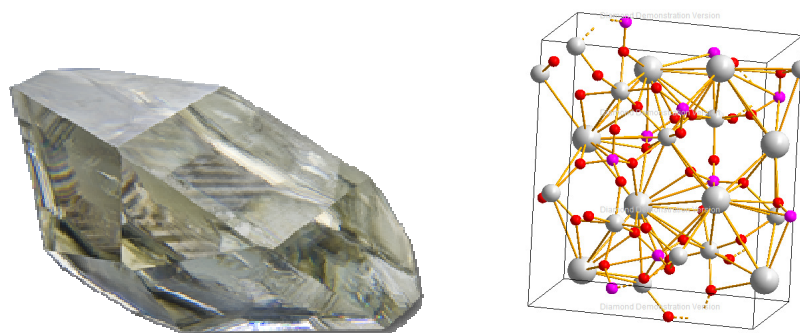


Figure 1.6. A crystal KTP view and crystal structure of a KTiOPO_4 -orthorhombic structure drawn with Diamond 4 Crystal and Molecular Structure Visualization software.

Potassium titanyl phosphate (KTiOPO₄; KTP) has superior properties for several nonlinear-optical applications and its high nonlinear-optical d coefficients, high optical damage threshold, wide acceptance angles, and thermally stable phase-matching properties. Also, KTP used in important applications in non-linear optics and electro-optics due to its high optical coefficients and low dielectric constants.

Recently low-loss optical waveguide fabrication processes were developed for KTP that, together with its large figure of merit, suggest that this material is also promising for integrated-optic applications (Bierlein and Vanherzeele, 1989). KTP is preferred for laser applications in the medical, defense, industrial and scientific areas. And also used in optical applications like Electro-Optic modulator.

1.4.2 General Properties and Definition of Oxyphosphates

The first oxyphosphate to be introduced commercially in America was announced in 1879 under the name Weston's Insoluble Cement. Dr. Weston had achieved a very important advance; his result was remarkable considering the time and the conditions under which his cement was evolved (White (Firm), 1923).

For oxyphosphates, for a time in exactly named basic phosphates, mainly two definitions are used in the chemical literature. The first one described as "oxyphosphates" which are compounds with oxygen atoms not belonging to the anionic entity, the second describe is "oxyphosphates" are salts with a global formula corresponding to a ratio O/P > 4 in the anhydrous state. The first definition is acceptable, but the second one, based on the fact that in all previous investigations the anionic entity was an isolated PO₄ tetrahedron, is not strictly acceptable. For example, M₂²⁺P₄O₁₂.2M²⁺O cyclotetraphosphate anion has the O/P ratio which is 3.5 (Selander, 1991).

Inorganic oxy phosphates with the general formula MOPO₄ (M = Nb, Mo, V, Sb or Ta and ATOPO₄) either A monovalent (K⁺, Na⁺, Li⁺, Rb⁺) or A divalent (Ni²⁺, Cu²⁺ etc.) and T tetravalent or trivalent (Bi³⁺, Fe³⁺, La³⁺ etc.) have been extensively investigated (Essehli et al. 2009).

In the literature, there are many investigations based on oxyphosphate. Oxyphosphate of rare earth and alkaline metals, $\text{Na}_2\text{GdOPO}_4$ has been synthesized and characterized by A.Uzteik for the first time (Uztetik Amour and Kızılyalli, 1995). After that, $\text{Pb}_2\text{BiO}_2\text{PO}_4$ synthesized (Mizrahi, Wignacourt, and Steinfink, 1997). And then single crystal of bismuth-oxyphosphate $\text{Bi}_{6.67}(\text{PO}_4)_4\text{O}_4$ has been isolated and characterized (Mustafa Ketatni et al., 1998), also BiCoPO_5 (M. Ketatni, Abraham, and Mentre, 1999). And in 2000, a new orthorhombic phase of $\text{Na}_2\text{GdOPO}_4$ and $\text{Na}_2\text{LaOPO}_4$ has been synthesized and showed the presence of two orthorhombic rare earth oxyphosphates (Gonen and Kizilyalli, 2000). In 2008, synthesis by solid-state reaction and characterization of novel sodium rare-earth oxyphosphates have been investigated (Seyyidođlu, Özenbaş, and Yilmaz, 2008).

The following table shows that some well-known oxyphosphates in literature with acceptable properties to be used in industrial areas.

Table 0.3 Some important oxyphosphates which used in the industry.

| | |
|--|--|
| ¹ Pd/NbOPO_4 | <ul style="list-style-type: none"> Excellent catalyst for the production of alkanes from furan-based compounds in an inert solvent and NbOx played very important role in C-O bond cleavage |
| ² BiCoOPO_4 | <ul style="list-style-type: none"> Compounds BiMPO_5 ($\text{M}^{2+} = \text{Ni}^{2+}, \text{Co}^{2+}$) are show paramagnetic properties. |
| ³ $\text{VOPO}_4 \cdot 3\text{H}_2\text{O}$ | <ul style="list-style-type: none"> Vanadium phosphate are used in industry for light hydrocarbon oxidation. |
| ⁴ $\text{Pb}_2\text{BiO}_2\text{PO}_4$ | <ul style="list-style-type: none"> $\text{Pb}^{+2} \text{M}^{+3} \text{XO}_6$ exists because they display magnetic, electro-optic, anion transport, and laser properties. |
| ⁵ $\text{M}_{0.5}\text{TiOPO}_4$ | <ul style="list-style-type: none"> ($\text{M} = \text{Ni}^{2+}, \text{Fe}^{2+}, \text{Mn}^{2+}, \text{Co}^{2+}, \text{Mg}^{2+}$) act as electrodes for Lithium batteries. |
| ⁶ WOP_2O_7 | <ul style="list-style-type: none"> As a result of it is non-toxic, it is used and described as environmentally friendly inorganic blue pigments |
| ⁷ $\text{Na}_4\text{VO}(\text{PO}_4)_2$ | <ul style="list-style-type: none"> Used as cathode material for new type low cost, less toxic than Na ion batteries. |
| ⁸ $\text{BiCa}_4\text{O}(\text{PO}_4)_3$ | <ul style="list-style-type: none"> Bismuth doped calcium phosphate is found to be potent antimicrobial agent for root canal filling. |

¹(Xia et al., 2014), ²(Mentre et al., 2008), ³(Gautier et al., 2011), ⁴(Mizrahi, Wignacourt, and Steinfink, 1997), ⁵(Belharouak and Amine, 2005), ⁶(Wendusu et al., 2013), ⁷(Deriouche et al., 2017), ⁸(Sumathi and Gopal, 2015)

1.5 Bismuth-Oxyphosphates

In the literature, single crystals of new bismuth oxy-phosphate isolated and X-Ray investigated by leading to the formula $\text{Bi}_{6.67}(\text{PO}_4)_4\text{O}_4$. The new series $\text{Bi}_6\text{M}\text{P}_4\text{O}_{20}$ ($\text{M} = \text{Sr}^{2+}, \text{Cd}^{2+}, \text{Ca}^{2+}, \text{Pb}^{2+}$) and $\text{Bi}_{6.5}\text{A}_{0.5}\text{P}_4\text{O}_{20}$ ($\text{A} = \text{Li}^+, \text{Na}^+, \text{K}^+$) has been yielded in that phase diagram study. The substitution involves only the bismuth atom labeled Bi(4) because of its peculiar role within the framework. Pure powder phases of $\text{Bi}_6\text{M}(\text{PO}_4)_4\text{O}_4$ ($\text{M} = \text{Pb}^{2+}, \text{Sr}^{2+}, \text{Ca}^{2+}, \text{Cd}^{2+}$) and $\text{Bi}_{6.5}\text{A}_{0.5}\text{P}_4\text{O}_{20}$ ($\text{A} = \text{Li}^+, \text{Na}^+, \text{K}^+$) has been prepared by thermal treatment of stoichiometric mixtures of Bi_2O_3 , $(\text{NH}_4)_2\text{HPO}_4$, and the corresponding oxide (Pb or Cd) or carbonate. By distinguishing the partially occupied Bi(4) atom, the formula of that studied compound has been described as $\text{Bi}_{2/3}\text{Bi}_6(\text{PO}_4)_4\text{O}_4$. This consideration was lead to the attractive possibility of substitution of one M^{2+} cation for $2/3\text{Bi}^{3+}$ or 0.5A^+ cation for $1/6\text{Bi}^{3+}$, yielding respectively $\text{Bi}_6\text{M}\text{P}_4\text{O}_{20}$ ($\text{M} = \text{Sr}^{2+}, \text{Cd}^{2+}, \text{Ca}^{2+}, \text{Pb}^{2+}$) and $\text{Bi}_{6.5}\text{A}_{0.5}\text{P}_4\text{O}_{20}$ ($\text{A} = \text{Li}^+, \text{Na}^+, \text{K}^+$) (Mustafa Ketatni et al., 1998).

The crystal structures of that published bismuth-transition metal oxy-phosphates are described as the association of complex infinite one-dimensional polycations and phosphate anions. And some highly disordered bismuth-transition metal oxyphosphates. They answer the formulations BiMOPO_4 which tetrahedrally coordinated by four metal atoms which are two bismuth and two M atoms. And BiM_2XO_6 ($\text{M} = \text{Ni}, \text{Co}$ and $\text{X} = \text{P}, \text{V}, \text{As}$). The first describing of the crystal structure of these compounds in terms of mixed double chains of two edge-sharing MO_6 octahedra alternating with two edge-sharing BiO_6 octahedra and connected to each other through the PO_4 tetrahedra to form a three-dimensional network. Investigations of bismuth oxyphosphates are mainly with transition metal oxy-phosphates (Abraham et al., 2002).

Many $\text{Bi}^{\text{III}}/\text{X}^{\text{V}}/\text{M}^{\text{II}}$ oxides, ($\text{X} = \text{P}, \text{V}, \text{As}$) containing many divalent M^{II} cations has been investigated reported, refined by powder X-Ray Diffraction for many reasons related with potential applications in the case of the $\text{Bi}^{3+} 6s^2$ lone pair possessing cation (ferroelectricity, ionic conductivity, non-linear optical properties,

etc.) (E. M. Ketatni et al., 2003). Studies of bismuth-oxophosphates with alkali metals which we work with are rarely in the literature.

Bismuth oxides which are bismuth-based oxo salts of inorganic acids, and bismuth oxide derivatives with transition-metal ions have a great interest because of their extended range of chemical and physical properties which are selective oxidation catalysts, luminescence property, and multiferroic behaviors. Bismuth-based oxo-salts of transition metals also have low dimensional magnetic properties. Most belong to the $\text{Bi}_2\text{O}_3\text{-MO-X}_2\text{O}_5$ ternary system (M = divalent metal; X = P, As, V) (Aksenov et al., 2018).

Bismuth-containing oxides materials have excellent physical properties such as oxygen ion conductivity, ferromagnetism, superconductivity, ferroelectricity and catalytic. Also, Bi^{3+} is a highly polarizable and stereo chemically active cation. These properties are closely related to their specific structure which is caused by the lone electron pair effect on Bi^{3+} (has electronic configuration $[\text{Xe}]4f^{14} 5d^{10} 6s^2$), hybridization of the 6s and 6p states results in interesting stereochemistry (Xun, 2002).

In this work, we reported the investigation, preparation of solid-state reactions, synthesize process, characterization of reaction samples, the crystal structure approach of new alkali earth-bismuth containing a novel type of oxophosphate.

When the indexing data processed from XRD Pattern data, we were determined refined unit cell parameters, the goodness of fit (GOF) which is the fitness between calculated and experimental data, and other R_p (expected profile), R_{wp} (weighed profile) agreement factors. For the best fit, this (x represents GOF Factor) $\chi^2 = (R_{wp}/R_p)^2$ Toby (2006), formula mainly could be considered. And the square of GOF value (χ^2 Chi-squared) may be less than 5. And in this work, all indexed profiles agreed with this formula which all agreement factors is given in section 4 separately.

2. PURPOSE OF WORK

Oxyphosphates have gained a respectable amount of importance in the area of laser and communication technology. MOPO₄ type of materials have been used for catalytic, ion exchange and electronic applications. These molecules are classified and defined as advanced technology materials.

This work gains to synthesize, and investigate novel types of bismuth oxyphosphates with alkali metals (Na, Li). Hence that these compounds can be specify as MBiPO₅ (M= Na⁺, Li⁺, K⁺, Rb⁺, Cs⁺, Rb⁺) series. Our purpose is to synthesize pure sodium and lithium bismuth oxyphosphate. Also, we were gained to reach and prove the crystal approach of the compound of *Na₂BiOPO₄* and *Li₂BiOPO₄* from different solid-state reactions by characterization methods and indexing calculations.

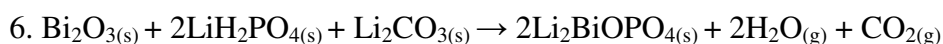
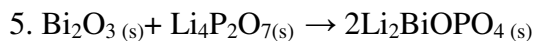
In this work, we report the new bismuth oxyphosphate materials which been synthesized are characterized by the powder XRD, SEM, IR spectroscopy analysis. Comparison of all bismuth oxy phosphates reactions and lithium oxy phosphate reactions written in below are provided.

2.1. Reactions

Na₂BiOPO₄ Synthesize Reactions:

1. $\text{Bi}_2\text{O}_3\text{(s)} + \text{Na}_4\text{P}_2\text{O}_7\text{(s)} \rightarrow 2\text{Na}_2\text{BiOPO}_4\text{(s)}$
2. $\text{Bi}_2\text{O}_3\text{(s)} + 2\text{Na}_2\text{HPO}_4\text{(s)} \rightarrow 2\text{Na}_2\text{BiOPO}_4\text{(s)} + \text{H}_2\text{O(g)}$
3. $\text{Bi}_2\text{O}_3\text{(s)} + 2\text{NH}_4\text{H}_2\text{PO}_4\text{(s)} + 2\text{Na}_2\text{CO}_3\text{(s)} \rightarrow 2\text{Na}_2\text{BiOPO}_4\text{(s)} + 2\text{NH}_3 + 3\text{H}_2\text{O(g)} + 2\text{CO}_2\text{(g)}$

Li₂BiOPO₄ Synthesize Reactions:



We have mainly followed the procedure after performing reactions at different temperatures for each solid-state reaction chemical processes are done,

- Determine the weight loss percentages for each reaction temperatures of each synthesize.
- Characterization of the compounds by XRD, IR, SEM, EDX.
- Specify any phases on XRD Pattern according to ICDD and COD References.
- And then, calculate unit cell parameters with indexing on XRD Pattern.
- Examine the crystal structures by related softwares and comparing of X-Ray diffraction results.
- Making Rietveld Refinement process. Draw on refinement pattern. Then identify the new compounds M_2BiOPO_4 M=Na, Li.

3. MATERIALS AND METHODS

3.1. Chemicals

The chemicals shown below are used in the synthesis of the oxyphosphates:

Bi₂O₃: Bismuth(III) oxide, typically 99.99% metal basis (Alfa Aesar),

Na₄P₂O₇: Sodium pyrophosphate (Sigma Aldrich),

LiH₂PO₄: Lithium dihydrogen phosphate 97% (Alfa Aesar),

Li₂CO₃: Lithium carbonate (Merck),

Na₂CO₃: Sodium Carbonate (Sigma Aldrich),

(NH₄)H₂PO₄: Ammonium di-hydrogen phosphate (Merck),

Na₂HPO₄: di-sodium hydrogen phosphate anhydrous (Merck)

Li₄P₂O₇: Lithium pyrophosphate (Synthesized in the laboratory).

3.2. Preparation of Samples

3.2.1. Agate Mortar and Pestle

The mixtures of reagents were powdered in an agate mortar and grinded by pestle until the powder mixture has been homogenized. After that, the powder mixture and crucible weighed with an analytical balance before and after located in the furnace and recorded amounts to calculate weight loss.

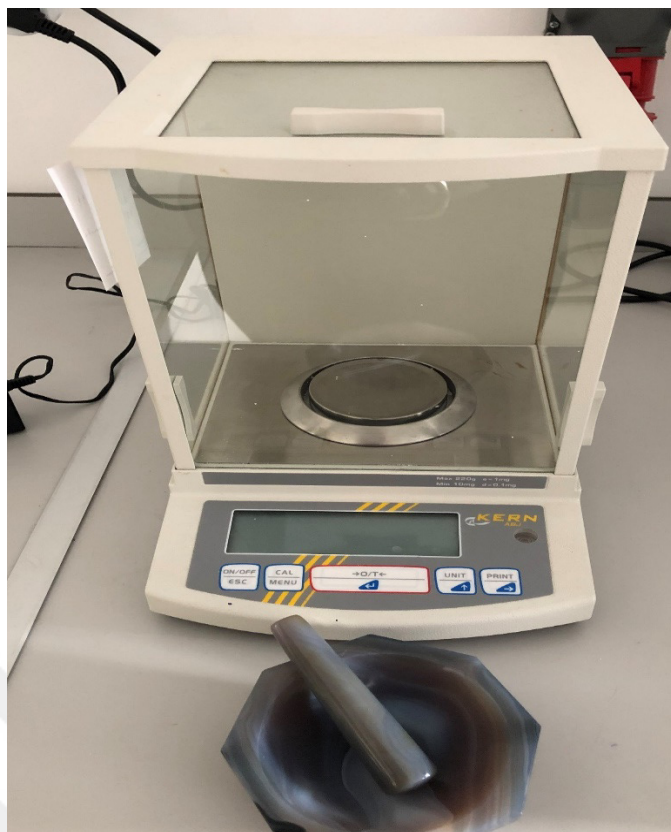


Figure 3.1. KERN Analytical balance ABS-N/ABJ-NM

3.2.2. Chamber Furnace

After the pulverizing process, the mixture located in a chamber furnace. Noticed that when the reaction was started (350 °C) once in a mono phase furnace located in the right, and the reaction was followed in the same mono phase furnace (800 °C) to avoid experimental standard deviation as much as possible. Different temperatures and different exposure time are used during the experiments.

Tri-phase furnace (leftward on the figure) cover a range from 1400°C to 1600°C.

Mono-phase furnace (rightward on the figure) cover a range from 1100°C to 1300°C.



Figure 3.2. The Protherm Chamber Furnace-PLF Series (150/5)

3.3. Experimental Procedure

All the reactions were done mainly in three steps;

1. Specify reaction temperatures,
2. Characterization of the new compounds by XRD, IR and SEM/EDS methods,
3. Rietveld refinement of X-Ray diffraction patterns and record the XRD data.

In all reactions, the amount of Bi_2O_3 was taken as 2.00g and the amounts of other reactants were calculated accordingly and stoichiometrically.

3.3.1. Solid-State Reaction of Bi_2O_3 (s) + $\text{Na}_4\text{P}_2\text{O}_7$ (s)

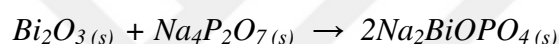
Each reagent was weighed; 2.00 grams from Bi_2O_3 and 1.47g from $\text{Na}_4\text{P}_2\text{O}_7$ with an analytical balance and the reagents were powdered in an agate mortar and pestled homogeneously. Weights of before the reaction products were transferred

into the porcelain crucible and putting into the furnace for each time (pre-post heating).

The starting temperature was 350°C (6h), and then temperatures and heating times followed respectively; 500°C (6h), 600°C (6h), 700°C (6h), 800°C (6h), and for the make sure reaction was done after checked the X-Ray results, the mixture was heated for the second time at 800°C (6h).

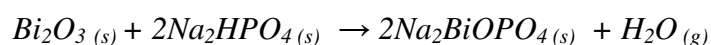
After each heating processes, the crucible was cooled in the desiccator. And the crucible with the sample was weighed after heating for the calculation of weight loss. Then, the reaction mixtures were subjected to instrumentations analysis.

The expected reaction after all heating period was done:



3.3.2. Solid-State Reaction of $Bi_2O_{3(s)} + 2Na_2HPO_{4(s)}$

The reactants were prepared by weighing with the stoichiometrical amounts of precursors in 1:2 ratio. And then the mixture was processed by heating after the reaction mixture was grinded in an agate mortar. After that, each reaction mixtures were transferred into a porcelain crucible. The reactants heated at reaction temperatures respectively 350°C (6h), 500°C (6h), 600°C (6h), 700°C (6h), 800°C (6h), and for the second time at 800°C (6h) in the Chamber Furnace. The expected reaction was:

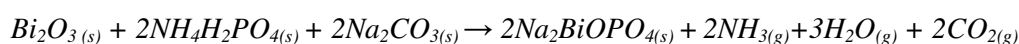


Samples were weighed after cooling process in a desiccator. And a few amounts of reacting mixtures were taken from each of reaction mixture to instrumentation process by XRD, IR, SEM after each sintering process.

3.3.3. Solid-State Reaction of Bi_2O_3 (s) + $2\text{NH}_4\text{H}_2\text{PO}_4$ (s) + $2\text{Na}_2\text{CO}_3$ (s)

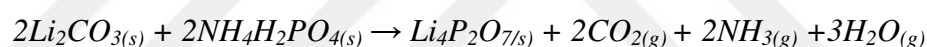
The precursors were weighed, grinded in a mortar and pestled, and all other processes were followed in sections above. Then reaction mixtures were put into the Chamber Furnace for heating at 350°C (6h) in order to expel gases, 500°C (6h), 600°C (6h), 700°C (6h), two times heated at 800°C (12h).

After the weight losses of the reaction mixtures were determined according to the following reaction:



3.3.4. Synthesis of $\text{Li}_4\text{P}_2\text{O}_7$ (s)

The compound of polycrystalline, $\text{Li}_4\text{P}_2\text{O}_7$ (s) was synthesized in our laboratory according to Zaafouri's study (Zaafouri, Megdiche, and Gargouri, 2015).



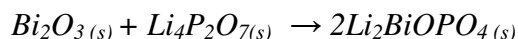
The raw materials of this solid-state reaction were Li_2CO_3 and $\text{NH}_4\text{H}_2\text{PO}_4$ were mixed with stoichiometric amounts of reagents and the mixture was pestled. Then the reaction mixture was heated in a porcelain crucible at 300°C (8h) to expel CO_2 , NH_3 , and H_2O , then 500°C (8h), and finally at 750°C (8h). After the heating process, the mixtures were cooled in desiccator than mixtures were determined by XRD, IR, and SEM.

3.3.5. Solid-State Reactions of Bi_2O_3 (s) + $\text{Li}_4\text{P}_2\text{O}_7$ (s)

The reagent of Bi_2O_3 , and $\text{Li}_4\text{P}_2\text{O}_7$ which was synthesized in the laboratory, according to 3.3.4. section, were mixed in 1:1 ratio stoichiometrically and the mixture was crushed in an agate mortar. Weights of pre-heating, post-heating of the mixtures were recorded after each heating reaction mixtures. The mixture was first

heated to 350°C (6h), then 500°C (6h), 600°C (6h), 700°C (6h), and the resultant powder mixture was grinded and heated for three times at 800°C (20h) respectively.

The expected reaction after all these main processes were done:

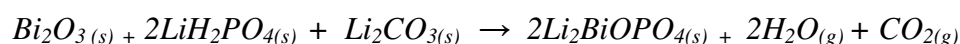


3.3.6. Solid-State Reaction of $Bi_2O_3(s) + 2LiH_2PO_4(s) + Li_2CO_3(s)$

The followed bismuth-oxyphosphate reactions were synthesized with the Lithium compounds instead of Sodium compounds.

The precursors were grinded in an agate mortar and pestled then mixed to yield Li_2BiOPO_4 compound with a 1:2:1 ratio of Bi_2O_3 , $2LiH_2PO_4$, Li_2CO_3 . Then the mixture was transferred to the porcelain crucible. And then the reaction mixture was first heated at 350°C (6h), *then 500°C (6h), 600°C (6h), 700°C (6h), 800°C (6h) respectively and for the reason of unexpected X-Ray results, the reaction was continued to heat for the four times at 800°C (24h totally) and the final temperature was 850°C (6h). After 850°C (6h) heating, the reaction mixture has adhered to porcelain crucible. Then the mixture expunged from the crucible.

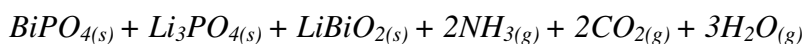
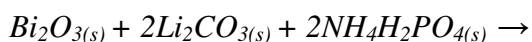
The expected reaction after final heating was:



3.3.7. Solid-State Reaction of $Bi_2O_3(s) + 2Li_2CO_3(s) + 2NH_4H_2PO_4(s)$

The reactants were weighed separately with the stoichiometric amounts of reagents according to 2.00 grams of Bi_2O_3 . Then pre-ignition weight of crucible including the mixture was recorded. After that, the reaction mixture was heated at 350°C (6h), 500°C (6h), 600°C (6h), 700°C (6h), four times heated at 800°C (24h). According to XRD and IR results, some unwanted phases have occurred and the reaction was continued at a higher temperature to solve this problem. Hence, the

reaction mixture two times heated at 850°C (12h). But there was still phase diffractions.



3.3.8. Solid-State Reaction of Bi_2O_3 (s) + $2(NH_4)_2HPO_4$ (s) + $2Li_2CO_3$ (s)

The reactants were treated in same chemical processes with other solid-state reactions above. Reaction temperatures of this solid-state reaction were 350°C (6h), 500°C (6h), 600°C (6h), 700°C (6h), three times heated at 800°C (30h) and 850°C (6h) respectively. The expected reaction was followed:



But also in this reaction, phase separation and undefined phases were observed and the reaction was not proceed properly.

3.4. Characterization

3.4.1. X-Ray Powder Diffraction

X-Ray diffraction techniques are used for the identification of crystalline phases of various materials and the quantitative phase analysis subsequent to the identification. X-Rays are high-energy electromagnetic waves with a wavelength between 10^{-3} and 10^1 nm. X-Ray diffractometers originate in three foundation parts; X-Ray detector, X-Ray tube, and a sample holder. In a cathode ray tube, X-Rays are generated by heating tungsten filament vacuum which is accelerated to produce electrons, through a high potential field, accelerating the electrons by applying a voltage toward a target and bombarding the target material with electrons. When

electrons have enough energy to dislodge inner shell electrons of the target material, characteristic X-Ray spectras are produced (Iwashita, 2016), (Epp, 2016).

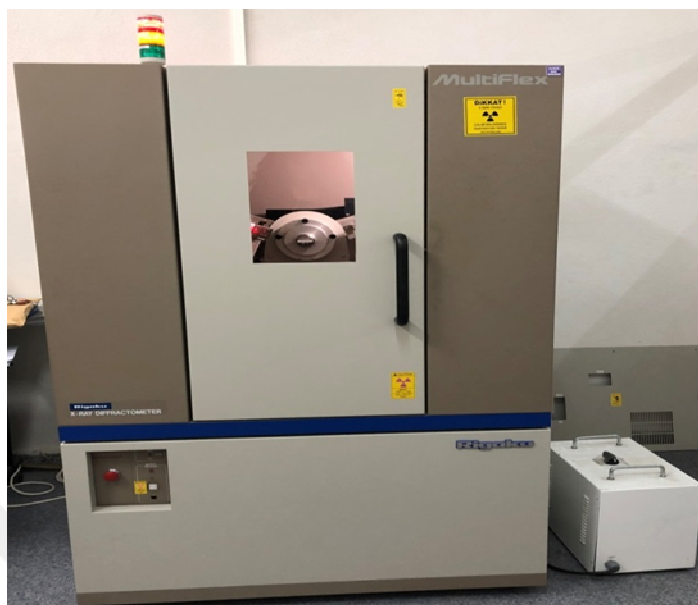


Figure 3.3. Rigaku MultiFlex X-Ray Diffractometer

X-Ray powder diffraction patterns were taken by using Rigaku Diffractometer diffracted beam monochromator with 2kW CuK_α radiation source (30-40 kV, 30 mA, $\lambda = 1.5406 \text{ \AA}$). Rec Slit: 0.15mm, Scan Speed: 5deg/min.

3.4.2. Fourier Transform Infrared (FTIR) Spectroscopy

FTIR spectrometer mainly composes of a detector, a source, an interferometer, sample compartment, A/D converter, amplifier, and a computer. The source produces radiation that passes the sample through the interferometer, and then reaches to the detector. After that, the signal is stabilized and converted to a digital signal by the amplifier and Analog to Digital converter, respectively. Finally, the signal is transferred to a computer in that Fourier transform is carried out (Birkner, 2011).

The spectral range for infrared absorption spectroscopy is $4000\text{-}400 \text{ cm}^{-1}$ commonly in the case of the absorption radiation of most organic compounds and inorganic ions are within this region.



Figure 3.4. PerkinElmer Spectrum Two FT-IR Spectroscopy

Detector Type: LiTaO₃

Operating Range: 5-45 °C

Wave Length Range: 8300-350 cm⁻¹

3.4.3. Scanning Electron Microscopy (SEM) and Energy Dispersive X-Ray (EDX) Analysis

A scanning electron microscope consist of a focused beam of electrons bring out the detailed surface characteristics of a specimen and supply relating information to its three-dimensional structure. SEM produces electronic and digitized images and so they are suitable for computer manipulations. Image analysis is used to have quantitative data obtained directly from the images. When a fine beam of electrons is focused on to the surface of a specimen, different interactions occur including the emission of secondary and backscattered primary electrons. The electron beam is scanned in a raster pattern repeatedly across the specimen which is synchronized with the scan of a cathode ray tube and the image is introduced in a digitized form which built upon a monitor (Yoshida, Kaburagi, and Hishiyama, 2016).



Figure 3.5. Jeol model-JSM 6390 LV Scanning Electron Microscope

Objective lens: Super conical lens

Objective lens apertures: Three positions, controllable in X/Y directions

Resolution : 3.0 nm(30kV)

These novel type of synthesized bismuth oxyphosphate materials were indexed through the instrument of related softwares. SpectraGryph is optical spectroscopy software was used to analyze Infrared results in the spectral range of $4000-400\text{ cm}^{-1}$. Match3! Software (Putz n.d.) for phase identification from powder diffraction data was used to analyze and indexing of XRD pattern. Jana2006 Software was used to make refinement and interpretation of structure, also fitting profiles of products drawn on with it. OriginPro software was used for data analysis and graphing

3.5. Calculations

3.5.1. Weight Loss Calculation

The loss on heating of the dry mass of a powder sample expressed in percentage calculated from the equation;

$$wv = \frac{(mb - mc)}{(mb - ma)} \times 100\%$$

wv is the loss on heating of the dry mass of a solid sample, in % ;

ma is the mass of the empty crucible, in grams;

mb is the mass of the crucible which is containing the dry mass, in grams;

mc is the mass of the crucible containing the heated dry mass, in grams.

$$wr = 100 - wv$$

wr is the residue on heating of the dry mass of a solid sample, in percentage.

Table 3.1. a) Weight Loss results of the last temperature of each reaction product were charted.

| SAMPLE ID | LAST REACTION T. (°C) | CRUCIBLE WEIGHT (ma) | BEFORE HEATING WEIGHT (mb-ma) | BEFORE HEATING + CRUCIBLE (mb) | AFTER HEATING WEIGHT (mc) | M % |
|-----------|-----------------------|-------------------------------|--|---|------------------------------------|-------|
| 1.RXN | 800°C(12h heating) | 29.7432 g | 0.8426 g | 30.5860 g | 30.5230 g | 7.47% |
| 2.RXN | 800°C(12h heating) | 26.9332 g | 0.8047 g | 27.7379 g | 27.6972 g | 5.06% |
| 3.RXN | 800°C(12h heating) | 25.4982 g | 1.5420 g | 27.0402 g | 27.0112 g | 1.88% |
| 4.RXN | 800°C(26h heating) | 20.3515 g | 1.0703 g | 21.4218 g | 21.4059 g | 1.49% |
| 5.RXN | 850°C(6h heating) | 11.6927 g | 0.7751 g | 12.4678 g | 12.4591 g | 1.12% |

1. Rxn: $\text{Bi}_2\text{O}_3(\text{s}) + \text{Na}_4\text{P}_2\text{O}_7(\text{s})$

2. Rxn: $\text{Bi}_2\text{O}_3(\text{s}) + 2\text{Na}_2\text{HPO}_4(\text{s})$

3. Rxn: $\text{Bi}_2\text{O}_3(\text{s}) + 2\text{NH}_4\text{H}_2\text{PO}_4(\text{s}) + 2\text{Na}_2\text{CO}_3(\text{s})$

4. Rxn: $\text{Bi}_2\text{O}_3(\text{s}) + \text{Li}_4\text{P}_2\text{O}_7(\text{s})$

5. Rxn: $\text{Bi}_2\text{O}_3(\text{s}) + 2\text{LiH}_2\text{PO}_4(\text{s}) + \text{Li}_2\text{CO}_3(\text{s})$

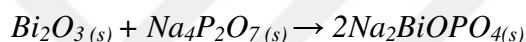
b) Weight Loss results of each reaction temperatures from starting temperature to ending temperature for each reaction were charted.

| | 1.RXN | 2. RXN | 3. RXN | 4. RXN | 5. RXN |
|-----------------------------|--------|--------|--------|--------|--------|
| 350°C (6h) | 0.11% | 5.16% | 17.35% | 0.15% | 10.29% |
| 500°C (6h) | 0.087% | 0.23% | 7.58% | 0.007% | 5.72% |
| 600°C (6h) | 1.53% | 0.006% | 1.02% | 0.39% | 1.36% |
| 700°C (6h) | 0.28% | 0.28% | 0.91% | 0.31% | 0.53% |
| 800°C | 8.06% | 7.73% | 2.0% | 2.45% | 10.45% |
| Total heating time at 800°C | 12h | 12h | 12h | 26h | 24h |

4. RESULT AND DISCUSSION

4.1. Solid State Reaction of $\text{Bi}_2\text{O}_3(s) + \text{Na}_4\text{P}_2\text{O}_7(s)$

$\text{Na}_2\text{BiOPO}_4$ compound was synthesized by mixing of the Bi_2O_3 and $\text{Na}_4\text{P}_2\text{O}_7$ reagents with a 1:1 ratio. Reaction heated at 350°C (6h), 500°C (6h), 600°C (6h), 700°C (6h), and twice at 800°C (12h). At all heating process, samples were separated for XRD, IR, and SEM studies. Weight loss was calculated at each step of the heating process shown in Table 3.1 b. And we expected to synthesize $\text{Na}_2\text{BiOPO}_4$ compound by this following solid-state reaction:



4.1.1. Infrared (IR) Studies of $\text{Bi}_2\text{O}_3(s) + \text{Na}_4\text{P}_2\text{O}_7(s)$

In the Infrared Spectra of this solid-state reaction (see Figure 4.2.) at from 350°C to 500°C, $\text{Na}_4\text{P}_2\text{O}_7$ was observed at about 700-800 cm^{-1} frequency and Bi_2O_3 at around 500 cm^{-1} frequency according to IR data of pure compounds (see Table 4.1.). At the 600-700°C, the IR absorption frequencies belong to $\text{Na}_3\text{Bi}(\text{PO}_4)_2$, Na_3PO_4 and BiPO_4 which are explained in detail on Section 4.1.2. After that, at 800°C (see Figure A.1.), the $\text{Na}_3\text{Bi}(\text{PO}_4)_2$, Na_3PO_4 and BiPO_4 frequencies were disappeared and the expected product obtained at this temperature according to IR results.

Table 4.1. The observed IR frequencies of reagents Bi_2O_3 and $\text{Na}_4\text{P}_2\text{O}_7$.

| PURE COMPOUNDS | IR FREQUENCIES (cm^{-1}) |
|-----------------------------------|---|
| Bi_2O_3 | 422, 427, 496, 536, 315, 410, 448, and 522 cm^{-1} |
| $\text{Na}_4\text{P}_2\text{O}_7$ | 424, 490, 520, 553, 615, 664, 733 , 986, 994, 1028 and 1119 cm^{-1} |

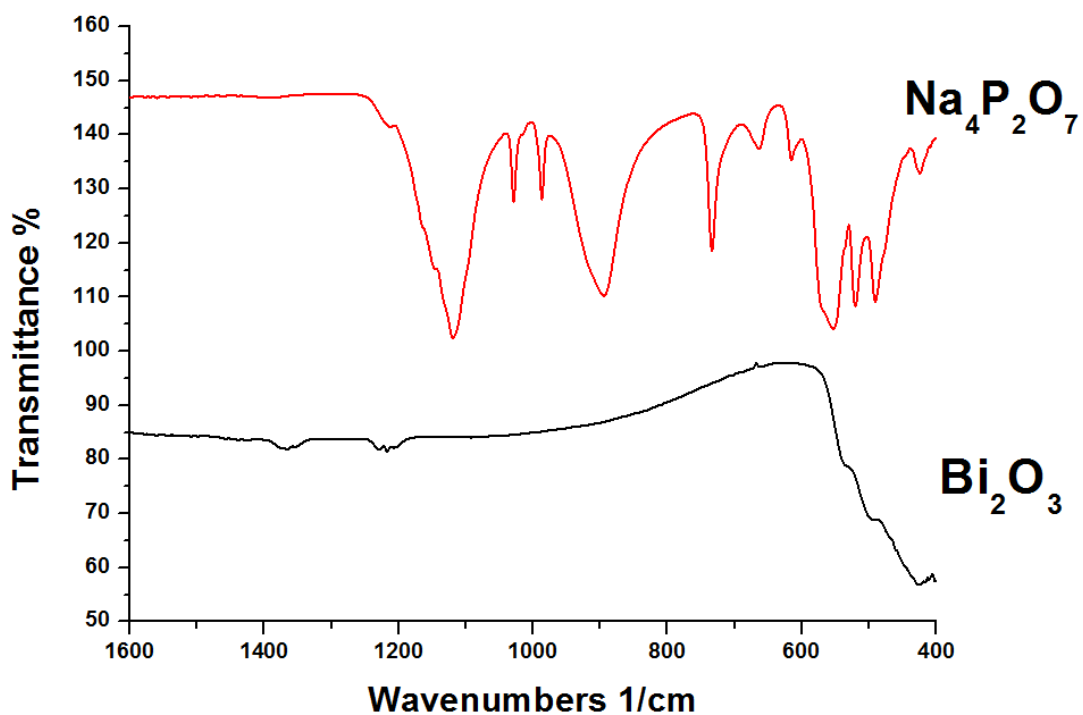


Figure 4.1. IR Spectra of the Initial Pure Compounds $\text{Na}_4\text{P}_2\text{O}_7$ and Bi_2O_3 .

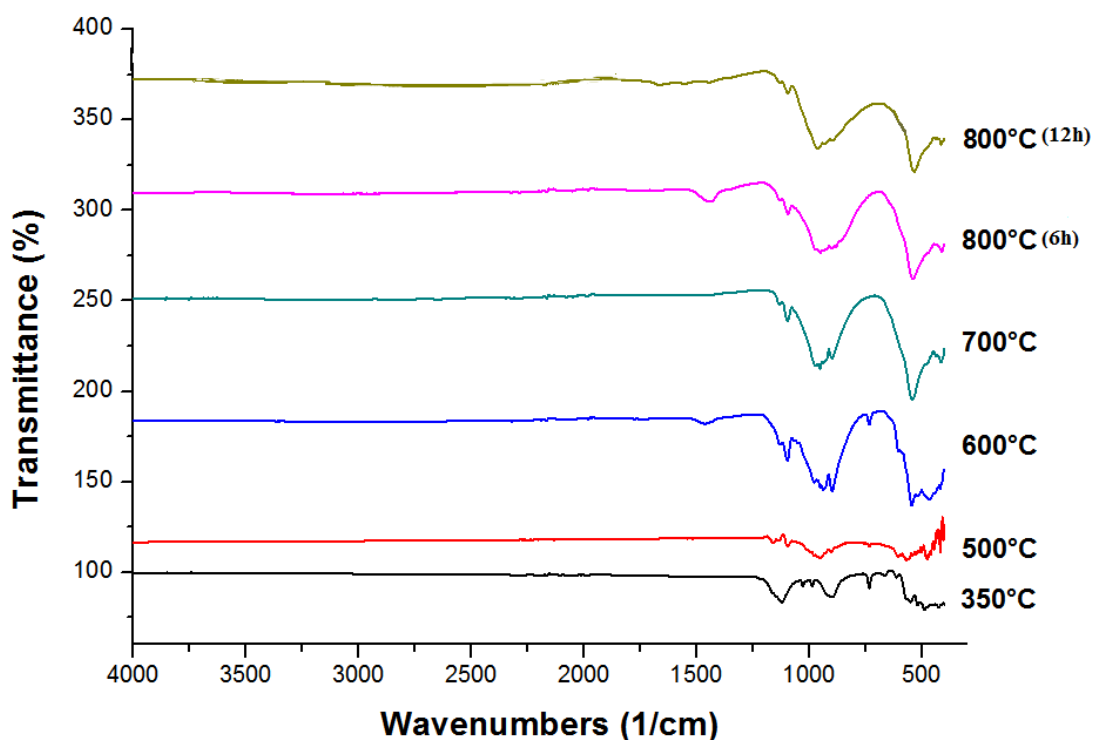


Figure 4.2. IR Spectra of the products of $\text{Bi}_2\text{O}_3(\text{s}) + \text{Na}_4\text{P}_2\text{O}_7(\text{s})$ at 350°C (6h), 500°C (6h), 600°C (6h), 700°C (6h), and twice at 800°C (12h).

For the examination of IR band locations for the product, the broadband between 1130 and 895 cm^{-1} is resolved into four peaks associated with ν_3 fundamental of the PO_4 (ν_{as} P-O-P asymmetric assigned as ν_3). These frequencies observed at 1131, 1094, 1041, 963 cm^{-1} . The ν_1 (ν_s P-O-P symmetric assign) vibration is also found in this region. And in this study, it shows at 933 and 897 cm^{-1} . The rest of the peaks in the region between 590 and 440 cm^{-1} are bound to the splitting of degenerate ν_4 and ν_2 PO_4 modes which are observed at 591, 534, 439 and 414 cm^{-1} .

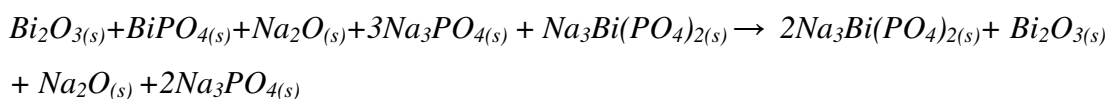
4.1.2. X-Ray Diffraction (XRD) Studies

As the reaction heated at 350°C and 500°C, there were unreacted lines of Bi_2O_3 **ICDD:** 41-1449, and $\text{Na}_4\text{P}_2\text{O}_7$ **ICDD:** 10-0187 have been seen on the XRD pattern (see Figure 4.4.).

At 600°C, there was still unreacted lines of Bi_2O_3 . Also, lines of BiPO_4 **ICDD:** 80-0209, Na_2O **ICDD:** 65-2978, Na_3PO_4 **ICDD:** 84-0195, and α - $\text{Na}_3\text{Bi}(\text{PO}_4)_2$ **ICDD:** 81-0036 were observed in that reaction temperature.



At 700°C, Na_3PO_4 , α - $\text{Na}_3\text{Bi}(\text{PO}_4)_2$, 1 mole of unreacted Bi_2O_3 and Na_2O lines were still appeared.



At 800°C, a minor amount of Bi_2O_3 , Na_2O , and α - $\text{Na}_3\text{Bi}(\text{PO}_4)_2$ peaks were detected. And other compounds were disappeared. After second heating at 800°C, a negligible amount of peak of α - $\text{Na}_3\text{Bi}(\text{PO}_4)_2$ was detected but finally, oxyphosphate peaks were observed and orthorhombic compounds of $\text{Na}_2\text{BiOPO}_4$ were obtained. It

was concluded that the derived product in this work resembles to orthorhombic $\text{Na}_2\text{GdOPO}_4$ presented by Gönen et al (Gonen and Kizilyalli, 2000).

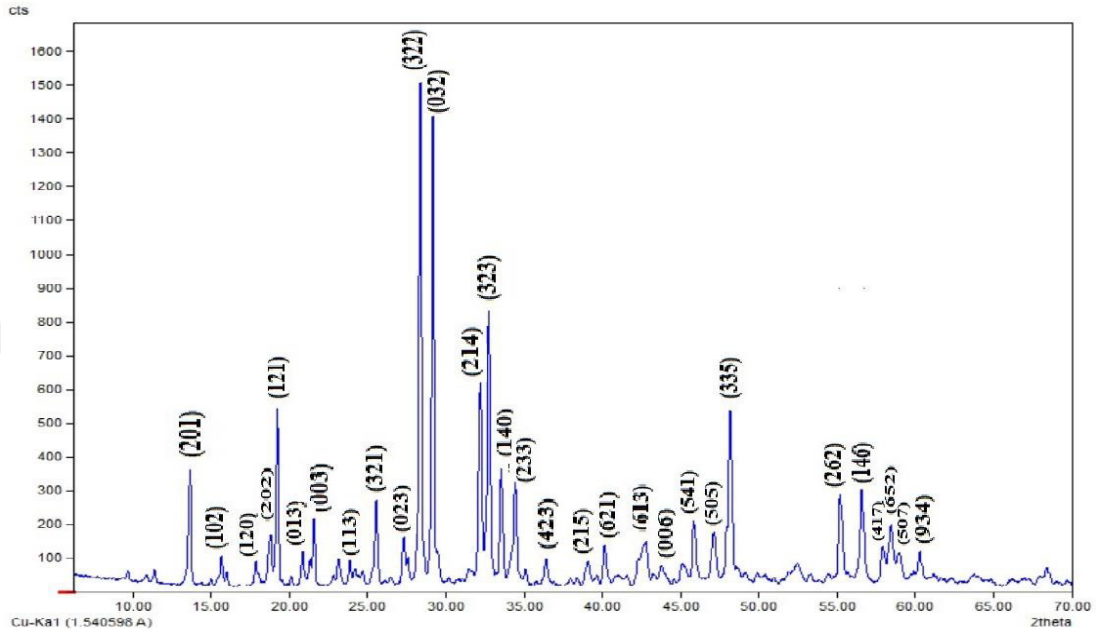
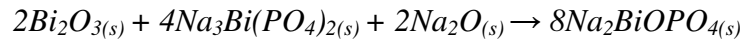


Figure 4.3. X-Ray Powder Diffraction Pattern of $\text{Bi}_2\text{O}_3(s) + \text{Na}_4\text{P}_2\text{O}_7(s)$ at 800°C (12h)

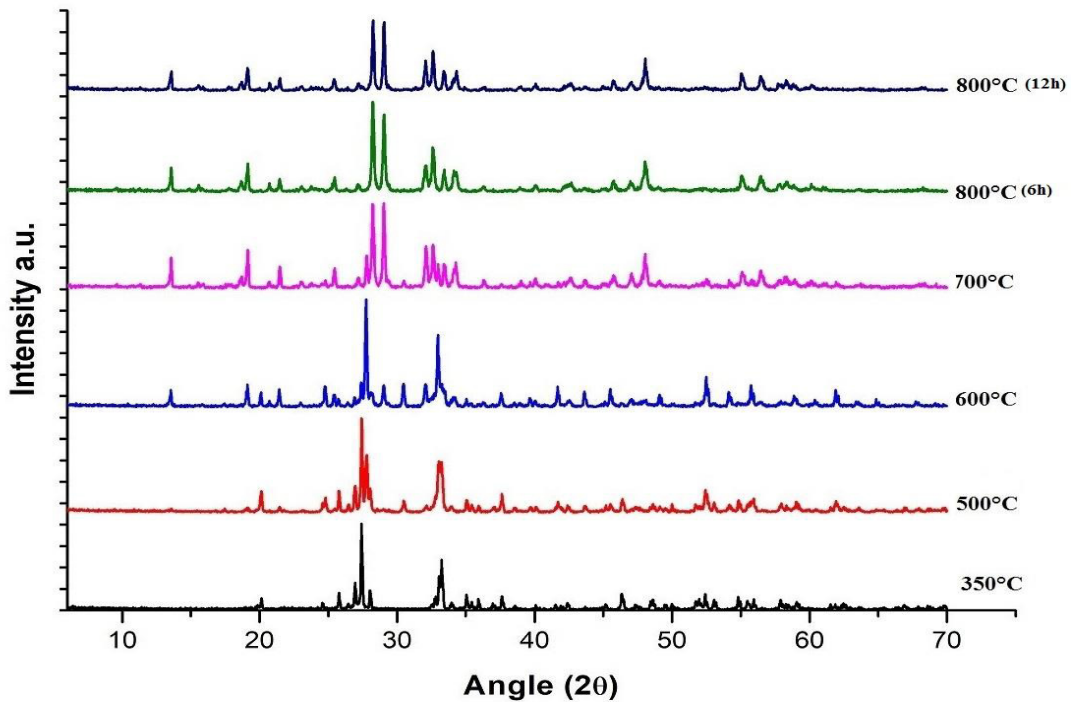


Figure 4.4. X-Ray Powder Diffraction Pattern of $\text{Bi}_2\text{O}_3(s) + \text{Na}_4\text{P}_2\text{O}_7(s)$ at 350°C (6h), 500°C (6h), 600°C (6h), 700°C (6h) and two times at 800°C (6h).

The new product compound was found to be an orthorhombic structure with the refined cell parameters which is given on the table are $a=15.4658$, $b=10.8601$, $c=12.6592$ Å, and most probable space group determined as Pmm_2 . This refining process was done with Jana2006 software. The Graph of fixed data was drawn and recorded with the following refinement data from software (see Figure 4.5.). The orthorhombic compound fit close enough to Rietveld refined plot and that agreement factors are shown in Table 4.2.

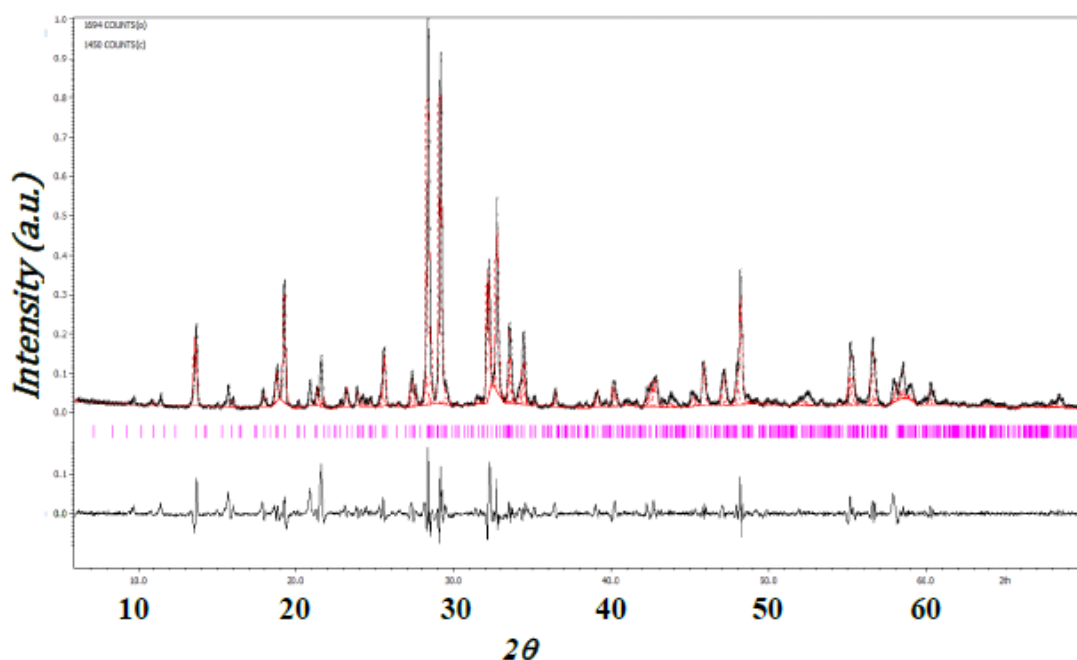


Figure 4.5. Jana2006 refinement pattern for Bi_2O_3 and $\text{Na}_4\text{P}_2\text{O}_7$.

Table 4.2. Refinement and structural parameters of product recorded from Jana2006

| | |
|---|--|
| Reaction Sample | 1. $\text{Bi}_2\text{O}_3(s) + \text{Na}_4\text{P}_2\text{O}_7(s)$ |
| Sample | Powder Crystal |
| Symmetry | Orthorhombic |
| Space Group | Pmm_2 (No:25) |
| a(Å) | 15.4658 |
| b(Å) | 10.8601 |
| c(Å) | 12.6592 |
| α° degree | 90.000 |
| β° degree | 90.000 |
| δ° degree | 90.000 |
| Diffractometer | Rigaku |
| Radiation Type | Cu $K\alpha$ |
| Monochromator | Graphite |
| Wavelength (Å) | 1.5405 |
| Refined profile range (2θ) | 6.00-70.00 |
| GOF | 1.67 |
| R_p | 13.89 |
| R_{wp} | 19.76 |
| V | 2126.2 |

Table 4.3. X-Ray powder diffraction data of orthorhombic Na_2BiOPO_4 from the reaction of $Bi_2O_3(s) + Na_4P_2O_7(s)$ with refined cell parameters (see Table 4.2).

| I/I_0 | hkl | $Sin^2(\theta)_{calc}$ | $Sin^2(\theta)_{obs}$ | d_{cal} | d_{obs} |
|---------|-------|------------------------|-----------------------|-----------|-----------|
| 17 | 2 0 1 | 0.01396 | 0.01355 | 6.517 | 6.616 |
| 9 | 1 0 2 | 0.01774 | 0.01781 | 5.783 | 5.771 |
| 6 | 1 2 0 | 0.02326 | 0.02314 | 5.050 | 5.063 |
| 13 | 2 0 2 | 0.02536 | 0.02567 | 4.836 | 4.807 |
| 21 | 1 2 1 | 0.02706 | 0.02707 | 4.682 | 4.681 |
| 10 | 0 0 3 | 0.03420 | 0.03399 | 4.165 | 4.177 |
| 6 | 0 1 3 | 0.03938 | 0.03937 | 3.881 | 3.881 |
| 6 | 1 1 3 | 0.04192 | 0.04164 | 3.762 | 3.774 |
| 12 | 3 2 1 | 0.04739 | 0.04773 | 3.538 | 3.525 |
| 7 | 0 2 3 | 0.05492 | 0.05450 | 3.286 | 3.299 |
| 100 | 3 2 2 | 0.05879 | 0.05873 | 3.176 | 3.178 |
| 92 | 0 3 2 | 0.06182 | 0.06197 | 3.098 | 3.094 |
| 27 | 2 1 4 | 0.07614 | 0.07560 | 2.791 | 2.801 |
| 54 | 3 2 3 | 0.07779 | 0.07797 | 2.761 | 2.758 |
| 24 | 1 4 0 | 0.08297 | 0.08325 | 2.674 | 2.669 |
| 22 | 2 3 3 | 0.08852 | 0.08764 | 2.588 | 2.601 |
| 7 | 4 2 3 | 0.09559 | 0.09606 | 2.491 | 2.485 |
| 5 | 2 1 5 | 0.11034 | 0.11039 | 2.318 | 2.318 |
| 8 | 6 2 1 | 0.11603 | 0.11648 | 2.261 | 2.257 |
| 12 | 6 1 3 | 0.13089 | 0.13119 | 2.129 | 2.126 |
| 5 | 0 0 6 | 0.13680 | 0.13689 | 2.082 | 2.081 |
| 15 | 5 4 1 | 0.15023 | 0.14974 | 1.987 | 1.990 |
| 12 | 5 0 5 | 0.15855 | 0.15831 | 1.934 | 1.936 |
| 43 | 3 3 5 | 0.16449 | 0.16434 | 1.899 | 1.900 |
| 22 | 2 6 2 | 0.21184 | 0.21237 | 1.673 | 1.671 |
| 23 | 1 4 6 | 0.22222 | 0.22215 | 1.634 | 1.634 |
| 10 | 4 1 7 | 0.23205 | 0.23186 | 1.599 | 1.599 |
| 14 | 6 5 2 | 0.23621 | 0.23630 | 1.584 | 1.584 |
| 10 | 5 0 7 | 0.24975 | 0.24964 | 1.541 | 1.541 |
| 6 | 9 3 4 | 0.31332 | 0.31348 | 1.376 | 1.375 |

4.1.3. Scanning Electron Microscopy (SEM) and (EDX) Studies

The morphology and the structural features of Na_2BiOPO_4 were investigated using SEM-EDX which showed in Figure 4.6 (10 μ m and 5 μ m magnifications respectively). SEM images showed that the compound uniformity exists between the specimens of the sample shape and particle size and have an irregularly grained powder. The compound showed rod and laminated plates shapes. And the EDX spectrum shows the presence of Na, O, P and Bi without any other unwanted extra elemental peak contribution (see Figure 4.7.).

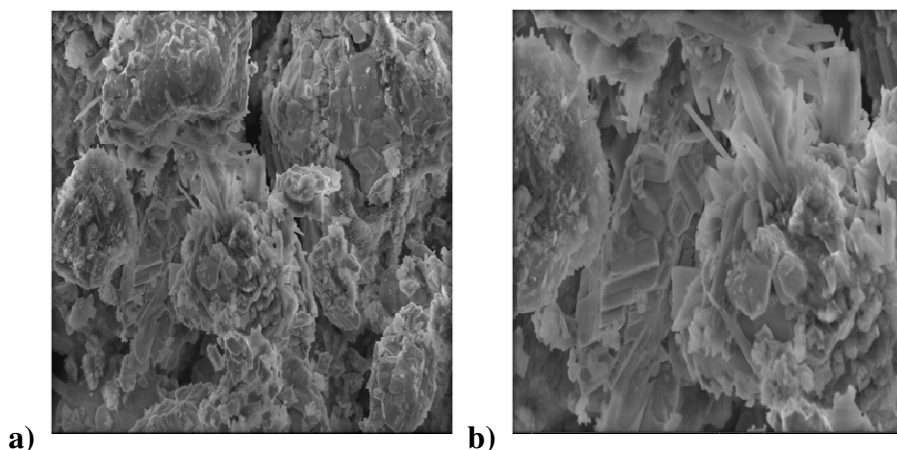
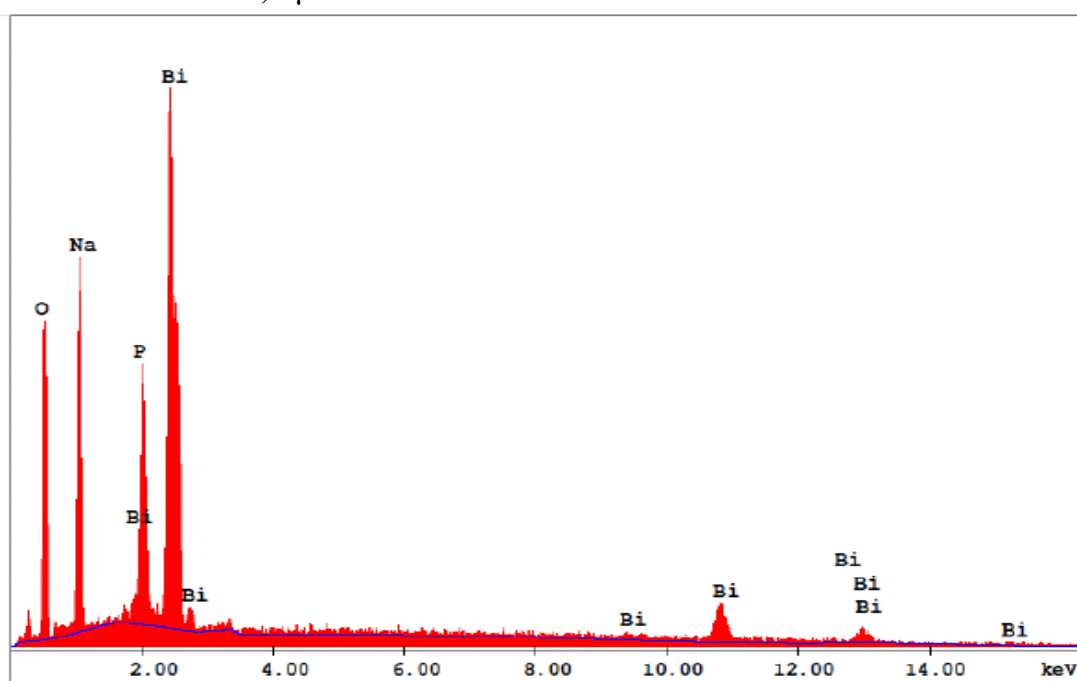


Figure 4.6. SEM images of $Bi_2O_{3(s)} + Na_4P_2O_{7(s)}$ reaction at 800°C a) 10 μm
b) 5 μm .



EDAX ZAF Quantification (Standardless)
Element Normalized
SEC Table : Default

| Element | Wt % | At % | K-Ratio | Z | A | F |
|---------|--------|--------|---------|--------|--------|--------|
| O K | 21.19 | 51.35 | 0.0528 | 1.1675 | 0.2134 | 1.0003 |
| NaK | 16.80 | 28.34 | 0.0556 | 1.0912 | 0.3032 | 1.0004 |
| P K | 8.26 | 10.34 | 0.0605 | 1.1045 | 0.6633 | 1.0000 |
| BiM | 53.75 | 9.97 | 0.4431 | 0.7954 | 1.0366 | 1.0000 |
| Total | 100.00 | 100.00 | | | | |

| Element | Net Inte. | Bkgd Inte. | Inte. Error | F/B |
|---------|-----------|------------|-------------|-------|
| O K | 129.02 | 3.63 | 1.69 | 35.54 |
| NaK | 179.68 | 9.11 | 1.46 | 19.72 |
| P K | 164.54 | 17.49 | 1.60 | 9.41 |
| BiM | 350.03 | 14.52 | 1.04 | 24.10 |

Figure 4.7 EDS Spectrum of the Products obtained from the $Bi_2O_{3(s)} + Na_4P_2O_{7(s)}$ reaction at 800°C(12h).

In this part of this work, the decomposition temperature of product compound was detected by this solid state reaction of $Bi_2O_{3(s)} + Na_4P_2O_{7(s)}$ at $900^\circ C$ (5h). The instrumentation results were proved that the Na_2BiOPO_4 compound decomposes to γ - $Na_3Bi(PO_4)_2$ **ICDD: 41-0178**. As shown in Figure 4.8, the broad bands at 700 - 750 cm^{-1} were attributed to condense phosphates. These vibrational bands were assigned as the modes of γ - $Na_3Bi(PO_4)_2$. And in XRD pattern (see Figure 4.9), beside γ - $Na_3Bi(PO_4)_2$, also minor amounts of Na_3PO_4 , Na_2O , and Bi_3PO_7 peaks were detected. And this data showed that the Na_2BiOPO_4 compound starts to decompose at $900^\circ C$ due to the following reaction;

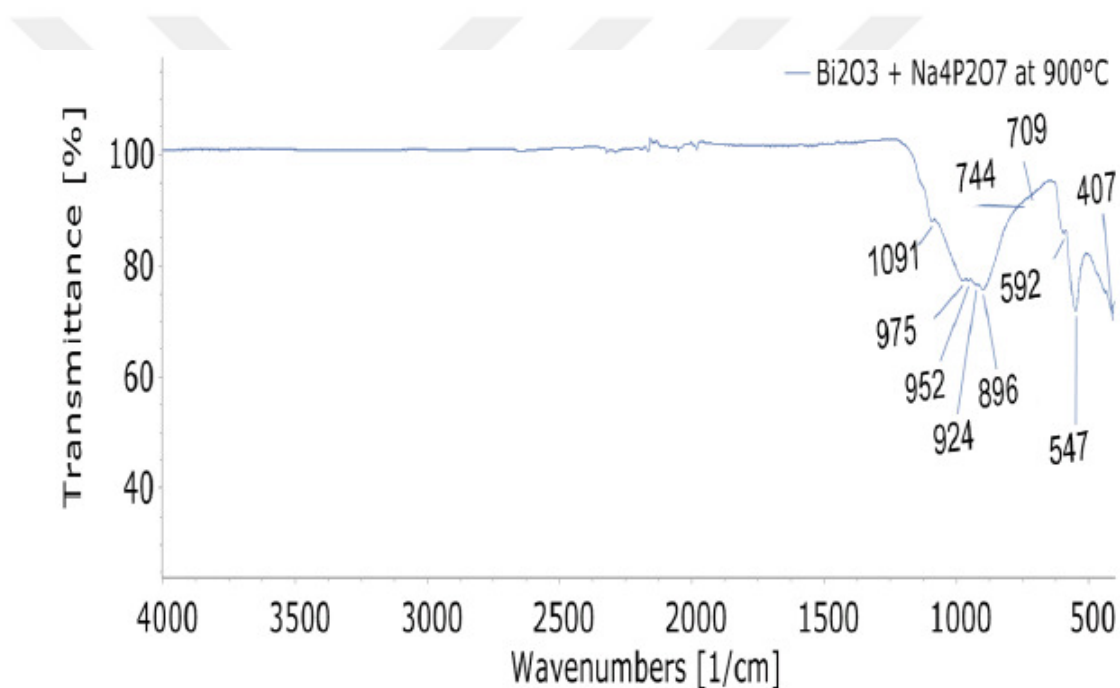
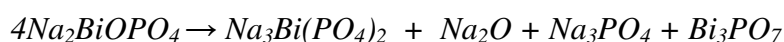


Figure 4.8. The IR Spectrum of the decomposed Na_2BiOPO_4 compound to γ - $Na_3Bi(PO_4)_2$ from the reaction of $Bi_2O_{3(s)} + Na_4P_2O_{7(s)}$ at $900^\circ C$.

The following data of Figure 4.9. b) was to establish the presence of a principal amount of γ - $Na_3Bi(PO_4)_2$ at $900^\circ C$.

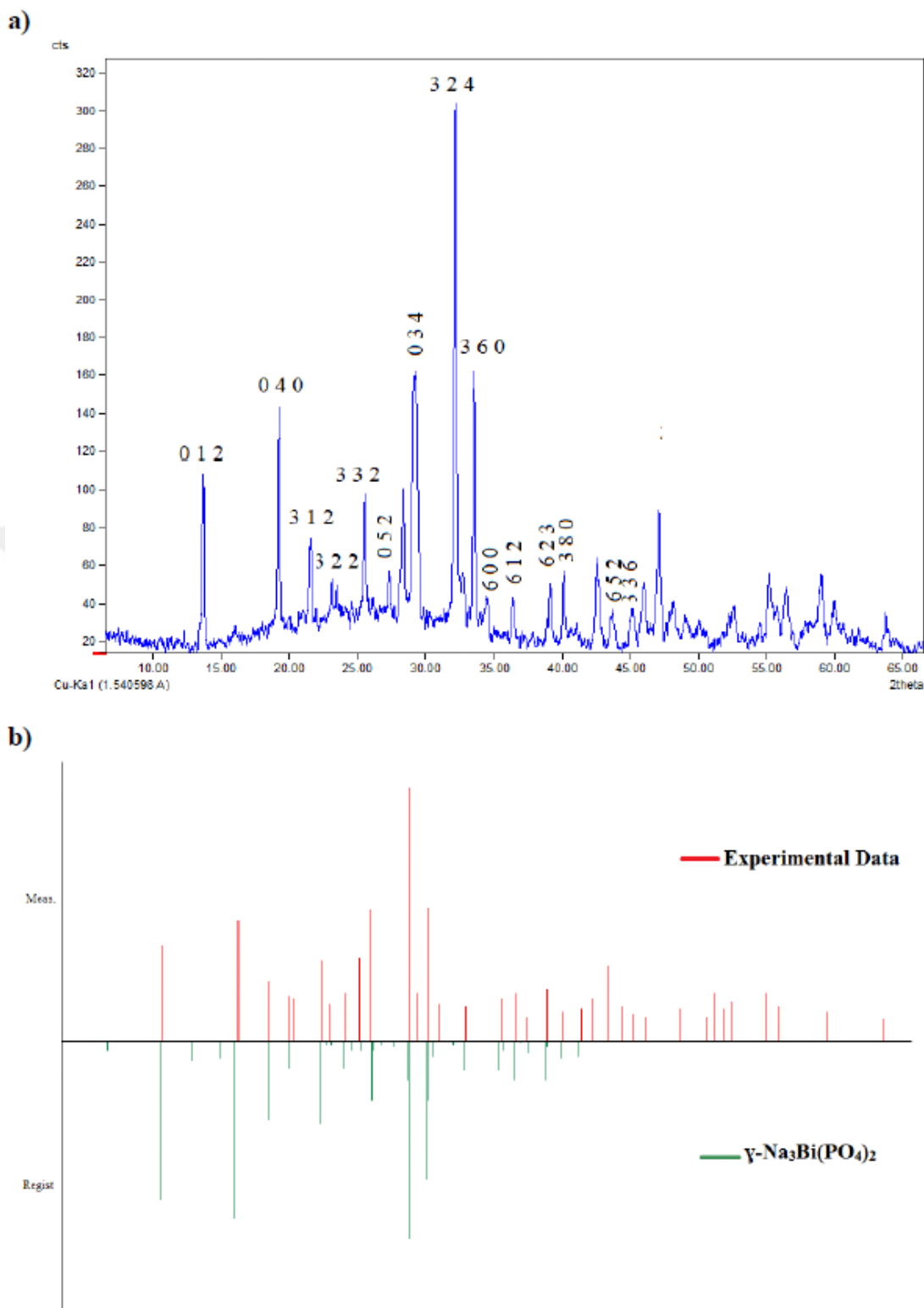
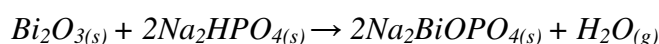


Figure 4.9 a) X-Ray Powder Diffraction Pattern of the decomposed $\text{Na}_2\text{BiOPO}_4$ compound to $\gamma\text{-Na}_3\text{Bi}(\text{PO}_4)_2$ from the reaction of $\text{Bi}_2\text{O}_3(s) + \text{Na}_4\text{P}_2\text{O}_7(s)$ at 900°C **b)** Shows the simplified quantitative analysis of difference plot of the reaction product and $\gamma\text{-Na}_3\text{Bi}(\text{PO}_4)_2$ **ICDD: 41-0178.**

4.2. Solid State Reaction of $\text{Bi}_2\text{O}_{3(s)} + 2\text{Na}_2\text{HPO}_{4(s)}$

This reaction was synthesized by mixing 1 mole of $\text{Bi}_2\text{O}_{3(s)}$ and 2 moles of $\text{Na}_2\text{HPO}_{4(s)}$. The reaction mixture was heated at $350^\circ\text{C}(6\text{h})$, $500^\circ\text{C}(6\text{h})$, $600^\circ\text{C}(6\text{h})$, $700^\circ\text{C}(6\text{h})$, and twice at $800^\circ\text{C}(12\text{h})$. After each heating process of the reaction mixture in a porcelain crucible, samples were taken for XRD, IR and SEM analysis which are examined in details as follows below sections. The expected reaction after all processes is:



4.2.1. Infrared (IR) Studies of $\text{Bi}_2\text{O}_{3(s)} + 2\text{Na}_2\text{HPO}_{4(s)}$

The Infrared Spectra of this solid-state reaction (see Figure 4.10.) at from 350°C to 600°C showed that the observed $\text{Na}_4\text{P}_2\text{O}_7$, and P-O-P bond at about $700\text{--}800\text{ cm}^{-1}$ frequency and Bi_2O_3 and Bi(II) bonds at around 550 cm^{-1} frequency. At the $600\text{--}700^\circ\text{C}$, the IR absorption frequencies belong to $\text{Na}_3\text{Bi}(\text{PO}_4)_2$ at around $400\text{--}450\text{ cm}^{-1}$ frequency, Na_3PO_4 , Na_2O were observed at $450\text{--}500\text{ cm}^{-1}$ frequency. After that, at 800°C (see Figure A.2.), Na_3PO_4 and Na_2O and other compounds were disappeared and the expected product obtained at 800°C (12h). And oxyphosphate peaks were detected at 1132 , 1092 , 1035 and 952 cm^{-1} .

The IR band locations for the product from $\text{Bi}_2\text{O}_{3(s)} + 2\text{Na}_2\text{HPO}_{4(s)}$ reaction at $800^\circ\text{C}(12\text{h})$, ν_3 bands were observed between 1132 and 952 cm^{-1} is resolved into four peaks associated with ν_3 fundamental of the PO_4 . These frequencies observed at 1132 , 1092 , 1035 , 952 cm^{-1} . The ν_1 vibration is also found in this region due to stretching modes which we observed at band 920 cm^{-1} . The remainder of the peaks in the region between 533 and 438 cm^{-1} are attributed to the bound to the splitting of degenerate ν_4 and ν_2 (O-P-P) PO_4 modes which are observed at 533 , 438 and 410 cm^{-1} .

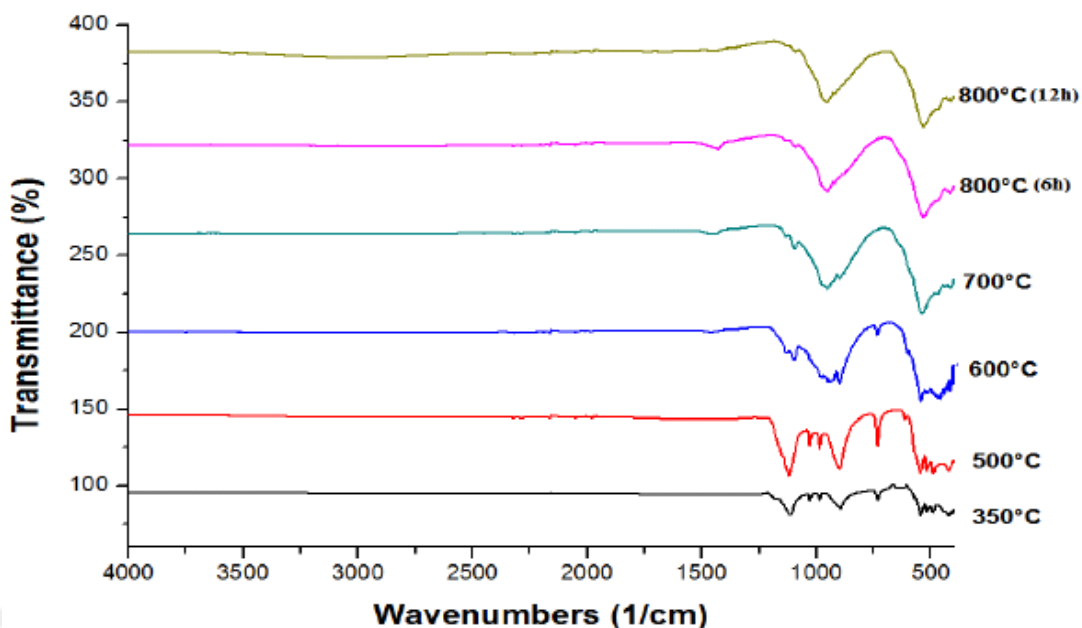
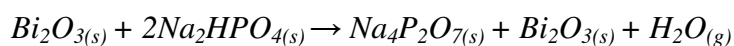


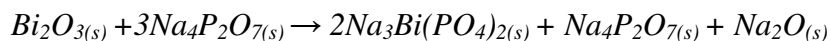
Figure 4.10. IR Spectra of the products of $Bi_2O_{3(s)} + 2Na_2HPO_{4(s)}$ reaction at 350°C (6h), 500°C (6h), 600°C (6h), 700°C (6h) and twice at 800°C (12h).

4.2.2. X-Ray Diffraction (XRD) Studies

When the reaction processed at 350°C and 500°C, there were unreacted lines of Bi_2O_3 **ICDD:** 41-1449 and $Na_4P_2O_7$ **COD:** 96-152-2371 appear on XRD Pattern (see Figure 4.11.).

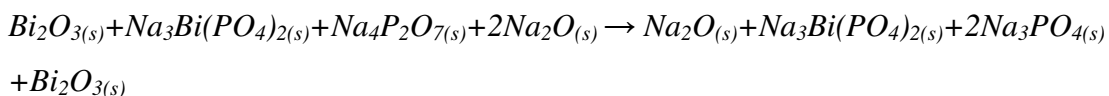


When the heating process was followed at 600°C, lines of α - $Na_3Bi(PO_4)_2$ **ICDD:** 81-0036, $Na_4P_2O_7$, negligible amount of Na_2O lines **ICDD:**06-0500 were exist.

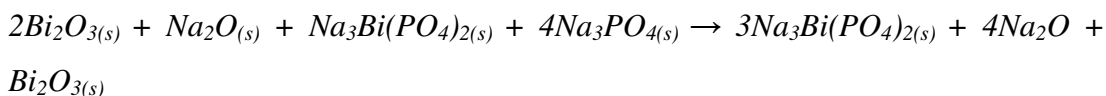


Also, there was 1 mole of unreacted Bi_2O_3 line at 700°C but it is insignificant. And there were Na_2O , Na_3PO_4 **COD:** 96-722-2420 and α - $Na_3Bi(PO_4)_2$ lines appeared at this reaction temperature.

The following reaction was assumed according to the peak search and analyzing results.



At 800°C, there were still lines of α - $Na_3Bi(PO_4)_2$ and still unreacted Bi_2O_3 lines were observed in the X-Ray powder diffraction pattern.



Finally, at second heating of 800°C (12h) no other lines of compounds were observed. And the expected final reaction of orthorhombic compound was obtained by the following solid-state reaction:

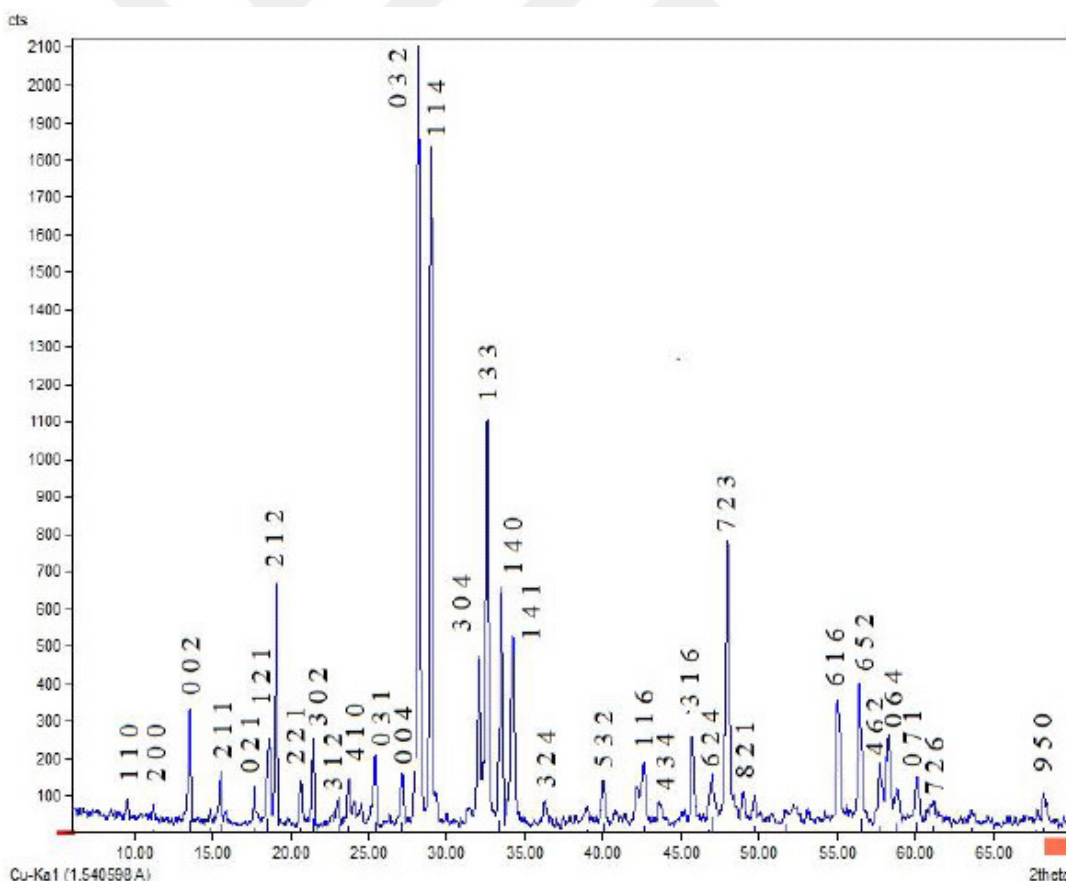
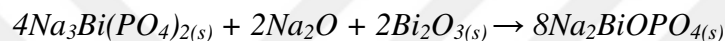


Figure 4.11. X-Ray Powder Diffraction Pattern of $Bi_2O_{3(s)} + 2Na_2HPO_{4(s)}$ at 800°C (12h).

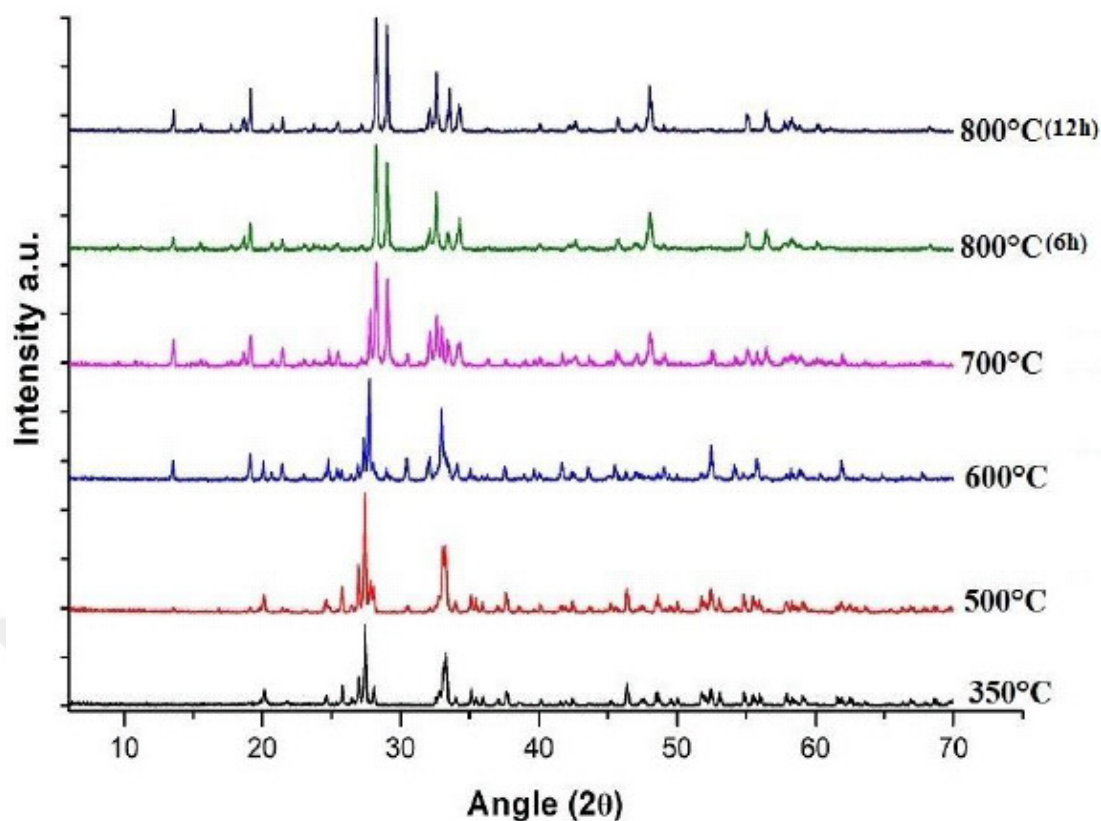


Figure 4.12. X-Ray Powder Diffraction Pattern of $Bi_2O_3(s) + 2Na_2HPO_4(s)$ at 350°C(6h), 500°C(6h), 600°C(6h), 700°C(6h), and two times at 800°C(12h).

The crystal symmetry of this new compound from $Bi_2O_3(s) + 2Na_2HPO_4(s)$ solid-state reaction was found to be an orthorhombic structure with the refined cell parameters which are given in Table 4.4. with other agreement parameters are $a=15.932$, $b=10.913$, $c=13.128$ Å and space group determined as Pmm_2 number: 25.

The Graph of fixed data (see Figure 4.13) was shown with the following refinement data from the software. The orthorhombic Na_2BiOPO_4 compound fit closely the Rietveld refined plot which is the continuous curve in the main graph (represents in red color). Their difference is shown by the continuous curve in the smaller-sized graph. The vertical bars are the calculated peak positions (represents in pink color).

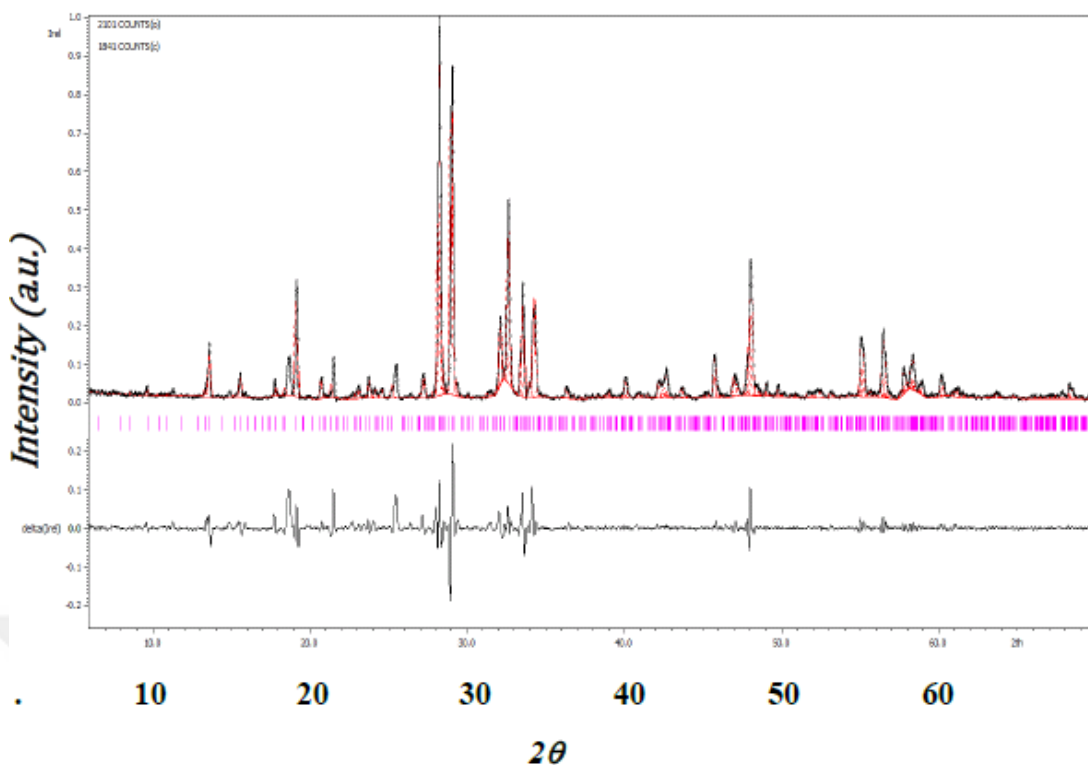


Figure 4.13. Jana2006 refinement XRD pattern of product.

Table 4.4. Refinement and structural parameters of product recorded from Jana2006.

| | |
|------------------------------------|--|
| Reaction Sample | 2. Bi ₂ O ₃ + 2Na ₂ HPO ₄ |
| Sample | Powder Crystal |
| Symmetry | Orthorhombic |
| Space Group | Pmm ₂ |
| a(Å) | 15.9320 |
| b(Å) | 10.9136 |
| c(Å) | 13.1287 |
| α° degree | 90.000 |
| β° degree | 90.000 |
| δ° degree | 90.000 |
| Diffractometer | Rigaku |
| Radiation Type | Cu Kα |
| Monochromator | Graphite |
| Wavelength (Å) | 1.5405 |
| Refined profile range (°2θ) | 6.00-70.00 |
| GOF | 2.13 |
| R_p | 15.57 |
| R_{WP} | 23.60 |
| V | 2282.8 |

Table 4.5. X-Ray powder diffraction data of orthorhombic Na_2BiOPO_4 from the reaction of $Bi_2O_3 (s) + 2Na_2HPO_4 (s)$ with the refined cell parameters (see Table 4.4).

| I/I_0 | hkl | $Sin^2(\theta)_{calc}$ | $Sin^2(\theta)_{obs}$ | d_{cal} | d_{obs} |
|---------|-------|------------------------|-----------------------|-----------|-----------|
| 4 | 0 0 1 | 0.00347 | 0.00416 | 13.076 | 11.936 |
| 5 | 1 1 0 | 0.00738 | 0.00703 | 8.966 | 9.186 |
| 4 | 2 0 0 | 0.00928 | 0.00962 | 7.996 | 7.851 |
| 17 | 0 0 2 | 0.01388 | 0.01397 | 6.538 | 6.515 |
| 4 | 1 0 2 | 0.01620 | 0.01672 | 6.052 | 5.956 |
| 9 | 2 1 1 | 0.01781 | 0.01832 | 5.772 | 5.690 |
| 7 | 0 2 1 | 0.02371 | 0.02377 | 5.002 | 4.995 |
| 12 | 1 2 1 | 0.02603 | 0.02639 | 4.774 | 4.741 |
| 34 | 2 1 2 | 0.02811 | 0.02769 | 4.594 | 4.628 |
| 7 | 2 2 1 | 0.03299 | 0.03240 | 4.241 | 4.279 |
| 13 | 3 0 2 | 0.03476 | 0.03479 | 4.131 | 4.129 |
| 5 | 3 1 2 | 0.03982 | 0.04009 | 3.860 | 3.847 |
| 8 | 4 1 0 | 0.04218 | 0.04231 | 3.750 | 3.744 |
| 4 | 2 2 2 | 0.04340 | 0.04358 | 3.697 | 3.689 |
| 4 | 0 3 0 | 0.04554 | 0.04531 | 3.609 | 3.618 |
| 10 | 0 3 1 | 0.04901 | 0.04855 | 3.479 | 3.495 |
| 3 | 3 0 3 | 0.05211 | 0.05207 | 3.374 | 3.375 |
| 8 | 0 0 4 | 0.05552 | 0.05529 | 3.269 | 3.275 |
| 100 | 0 3 2 | 0.05942 | 0.05951 | 3.160 | 3.157 |
| 89 | 1 1 4 | 0.06290 | 0.06286 | 3.071 | 3.072 |
| 3 | 5 1 1 | 0.06653 | 0.06707 | 2.986 | 2.974 |
| 4 | 4 1 3 | 0.07341 | 0.07359 | 2.843 | 2.839 |
| 22 | 3 0 4 | 0.07640 | 0.07644 | 2.786 | 2.786 |
| 53 | 1 3 3 | 0.07909 | 0.07887 | 2.739 | 2.742 |
| 34 | 1 4 0 | 0.08328 | 0.08325 | 2.669 | 2.669 |
| 26 | 1 4 1 | 0.08675 | 0.08685 | 2.615 | 2.613 |
| 5 | 3 2 4 | 0.09664 | 0.09683 | 2.477 | 2.475 |
| 2 | 0 3 4 | 0.10106 | 0.10100 | 2.423 | 2.423 |
| 3 | 1 3 4 | 0.10338 | 0.10343 | 2.395 | 2.395 |
| 3 | 3 4 1 | 0.10531 | 0.10567 | 2.373 | 2.369 |
| 3 | 3 0 5 | 0.10763 | 0.10761 | 2.347 | 2.348 |
| 7 | 5 3 2 | 0.11742 | 0.11732 | 2.247 | 2.248 |
| 3 | 4 4 1 | 0.12155 | 0.12174 | 2.209 | 2.207 |
| 3 | 0 0 6 | 0.12492 | 0.12541 | 2.179 | 2.175 |
| 9 | 1 1 6 | 0.13230 | 0.13230 | 2.117 | 2.117 |
| 5 | 4 3 4 | 0.13818 | 0.13815 | 2.072 | 2.072 |
| 3 | 8 0 0 | 0.14848 | 0.14819 | 1.999 | 2.001 |
| 13 | 3 1 6 | 0.15086 | 0.15092 | 1.983 | 1.982 |
| 8 | 6 2 4 | 0.15928 | 0.15926 | 1.930 | 1.930 |
| 38 | 7 2 3 | 0.16515 | 0.16556 | 1.895 | 1.893 |
| 6 | 8 2 1 | 0.17219 | 0.17223 | 1.856 | 1.856 |
| 5 | 2 4 5 | 0.17699 | 0.17700 | 1.830 | 1.830 |
| 3 | 1 5 4 | 0.18434 | 0.18413 | 1.794 | 1.795 |
| 3 | 0 2 7 | 0.19027 | 0.19012 | 1.765 | 1.766 |
| 4 | 8 3 0 | 0.19402 | 0.19423 | 1.748 | 1.747 |
| 4 | 8 2 3 | 0.19995 | 0.19994 | 1.722 | 1.722 |
| 3 | 4 3 6 | 0.20758 | 0.20767 | 1.690 | 1.690 |
| 18 | 6 1 6 | 0.21350 | 0.21365 | 1.667 | 1.666 |
| 20 | 6 5 2 | 0.22390 | 0.22360 | 1.627 | 1.629 |
| 10 | 4 6 2 | 0.23316 | 0.23326 | 1.595 | 1.594 |
| 13 | 0 6 4 | 0.23768 | 0.23756 | 1.580 | 1.580 |
| 6 | 6 5 3 | 0.24125 | 0.24174 | 1.568 | 1.566 |
| 8 | 0 7 1 | 0.25141 | 0.25136 | 1.536 | 1.536 |
| 5 | 7 2 6 | 0.25884 | 0.25899 | 1.514 | 1.513 |
| 6 | 9 5 0 | 0.31442 | 0.31480 | 1.373 | 1.372 |

4.2.3. Scanning Electron Microscopy (SEM) and (EDX) Studies

The morphology and the structural features of Na_2BiOPO_4 were investigated by SEM-EDX as shown in Figure 4.14. Micrograph images of this orthorhombic compound showed that the uniformity exists between the specimens of the sample. The shapes were interpreted as agglomerate aspect. The granular structure was seen in that micrographs. And the elemental composition of all samples was provided by the EDX analysis. EDX spectrum showed the presence of Na, O, P and Bi and no other peak was seen (see Figure 4.15.).

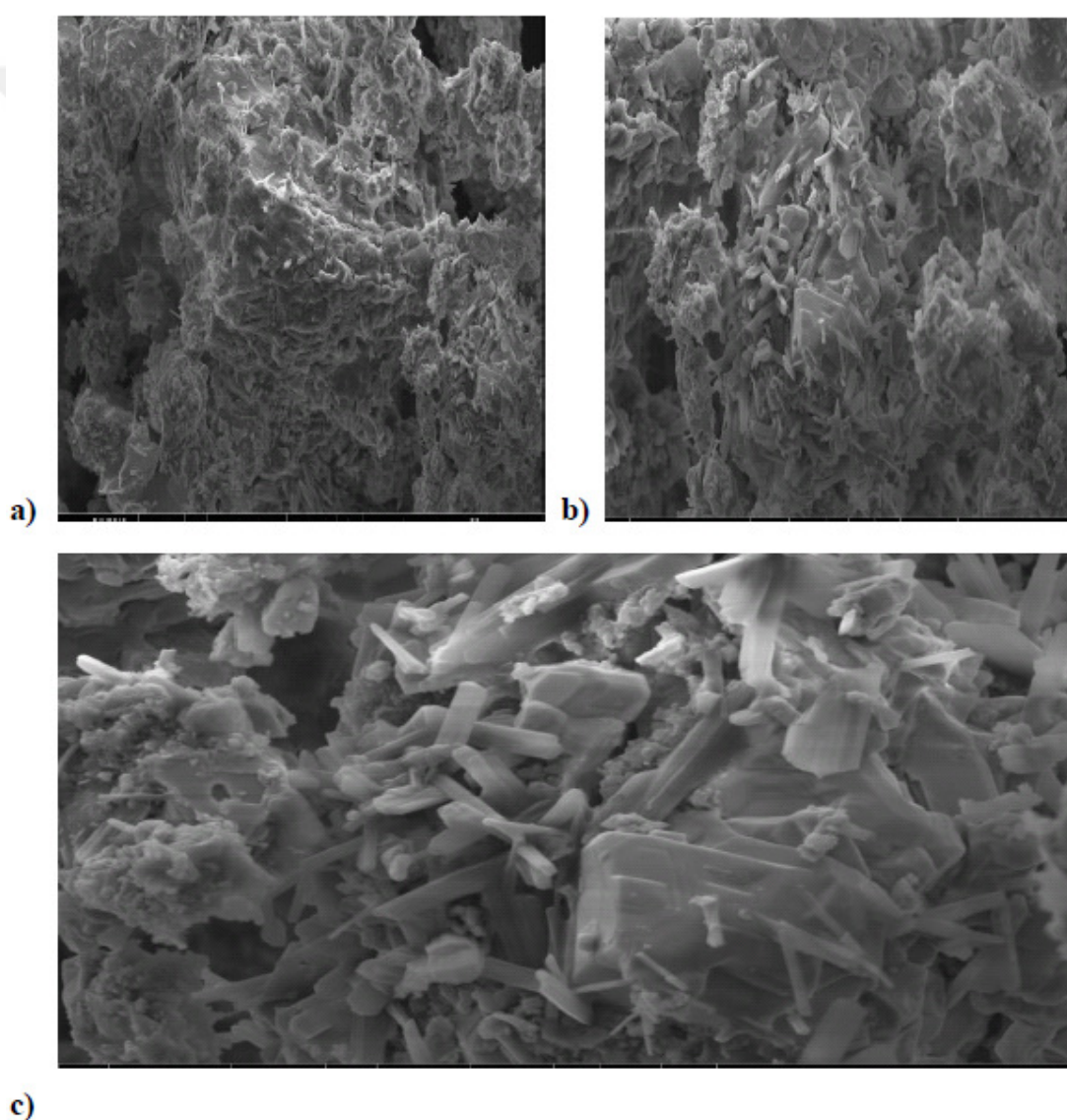
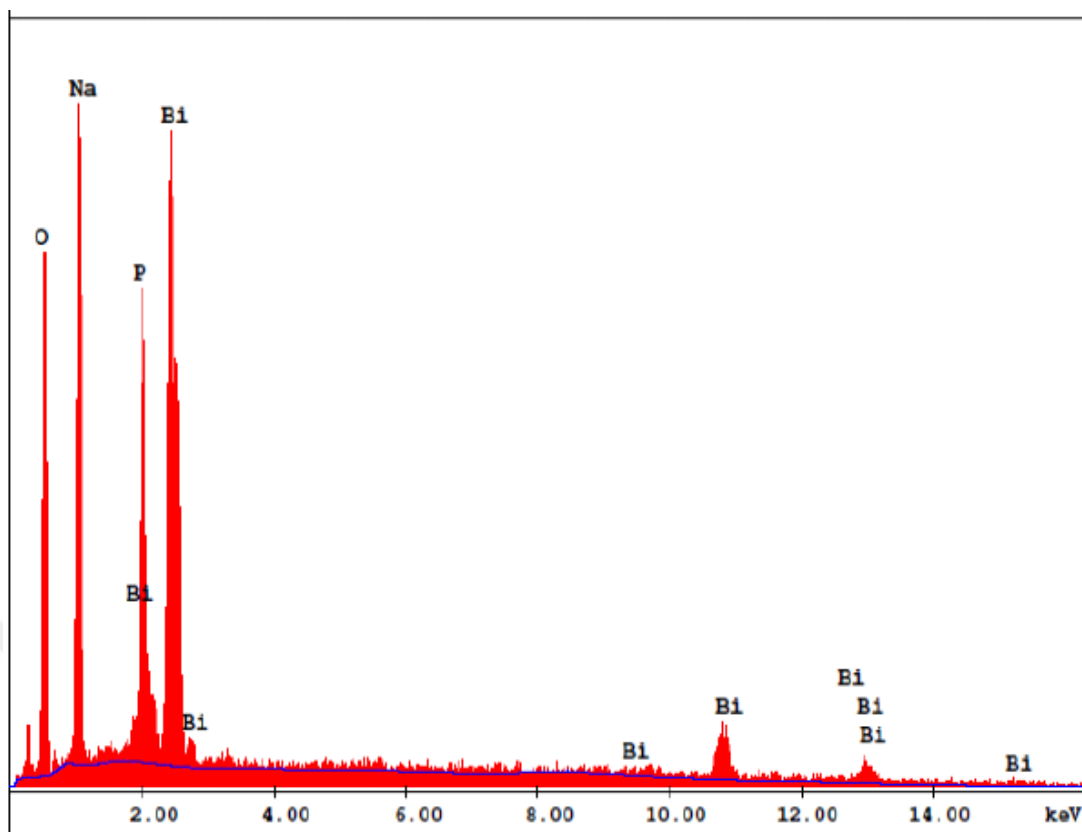


Figure 4.14. SEM images of $Bi_2O_3(s) + 2Na_2HPO_4(s)$ reaction at $800^\circ C$ a) $20\ \mu m$ b) $10\ \mu m$ c) $5\ \mu m$



EDAX ZAF Quantification (Standardless)
 Element Normalized
 SEC Table : Default

| Element | Wt % | At % | K-Ratio | Z | A | F |
|---------|--------|--------|---------|--------|--------|--------|
| O K | 24.36 | 51.92 | 0.0638 | 1.1426 | 0.2291 | 1.0004 |
| NaK | 20.05 | 29.73 | 0.0687 | 1.0682 | 0.3205 | 1.0005 |
| P K | 9.89 | 10.88 | 0.0714 | 1.0762 | 0.6715 | 1.0000 |
| BiM | 45.71 | 7.46 | 0.3655 | 0.7731 | 1.0343 | 1.0000 |
| Total | 100.00 | 100.00 | | | | |

| Element | Net Inte. | Bkqd Inte. | Inte. Error | P/B |
|---------|-----------|------------|-------------|-------|
| O K | 94.11 | 2.38 | 1.83 | 39.54 |
| NaK | 134.00 | 5.90 | 1.56 | 22.69 |
| P K | 117.35 | 8.19 | 1.71 | 14.32 |
| BiM | 174.33 | 7.17 | 1.37 | 24.32 |

Figure 4.15. EDS Spectrum of the Product obtained from the $Bi_2O_{3(s)} + 2Na_2HPO_{4(s)}$ reaction at $800^\circ C$ (12h).

4.3. Solid State Reaction of $Bi_2O_{3(s)} + 2NH_4H_2PO_{4(s)} + 2Na_2CO_{3(s)}$

In this examination of this solid-state reaction, Na_2BiOPO_4 compound was synthesized by mixing of 1 mole Bi_2O_3 , 2 moles $NH_4H_2PO_4$ and 2 moles Na_2CO_3

reagents. The reaction was processed at 350°C, 500°C, 600°C, 700°C and two times at 800°C (12h). The following reaction was expected:



4.3.1. Infrared (IR) Studies of $\text{Bi}_2\text{O}_3(s) + 2\text{NH}_4\text{H}_2\text{PO}_4(s) + 2\text{Na}_2\text{CO}_3(s)$

Infrared Spectra of this solid-state reaction at 350 and 500°C, C-O bond has been seen around 430 cm^{-1} and Na_2CO_3 was formed at 1428, 1138, 879 cm^{-1} frequencies (see Table 4.6. and see Figure 4.16.), also (Bi)-O-P bond observed at 460 cm^{-1} and at 730 cm^{-1} frequency N-O bond was seen. And these observations were taken and recorded from SpectraGryph spectroscopy software. At the 600-700°C (see Figure 4.17.), the IR absorption frequencies belong to $\text{Na}_3\text{Bi}(\text{PO}_4)_2$ at around $450\text{--}470\text{ cm}^{-1}$ frequency. And there was still Na_2CO_3 was seen at 600°C. Then at 800°C (see Figure A.3.), other compounds were disappeared and oxyphosphates were observed at 1131, 1092, 1030 and 951 cm^{-1} hence the expected product obtained at 800°C (12h).

Table 4.6. The observed IR frequencies of reagents Na_2CO_3 and $\text{NH}_4\text{H}_2\text{PO}_4$.

| PURE COMPOUNDS | IR FREQUENCIES (cm^{-1}) |
|------------------------------------|--|
| Na_2CO_3 | 1651, 1422, 1231, 1048, 1033, 877, 836, 694, 670, 451, 434, 418 cm^{-1} |
| $\text{NH}_4\text{H}_2\text{PO}_4$ | 1436, 1402, 1266, 1231, 1071, 540, 402 cm^{-1} |

The IR Frequencies of Bi_2O_3 was shown in Table 4.1.

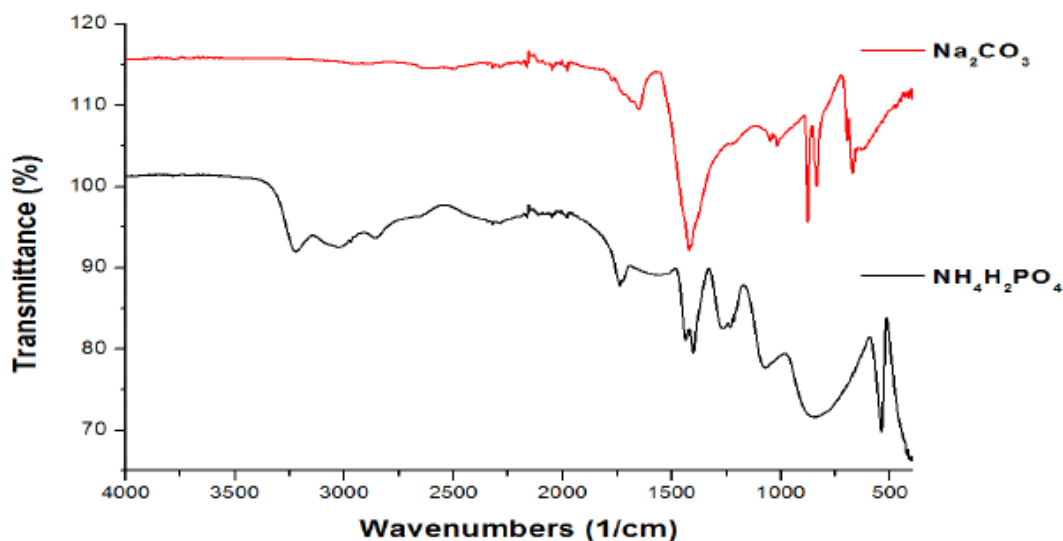


Figure 4.16. IR Spectra of the Initial Pure Compounds Na_2CO_3 and $\text{NH}_4\text{H}_2\text{PO}_4$.

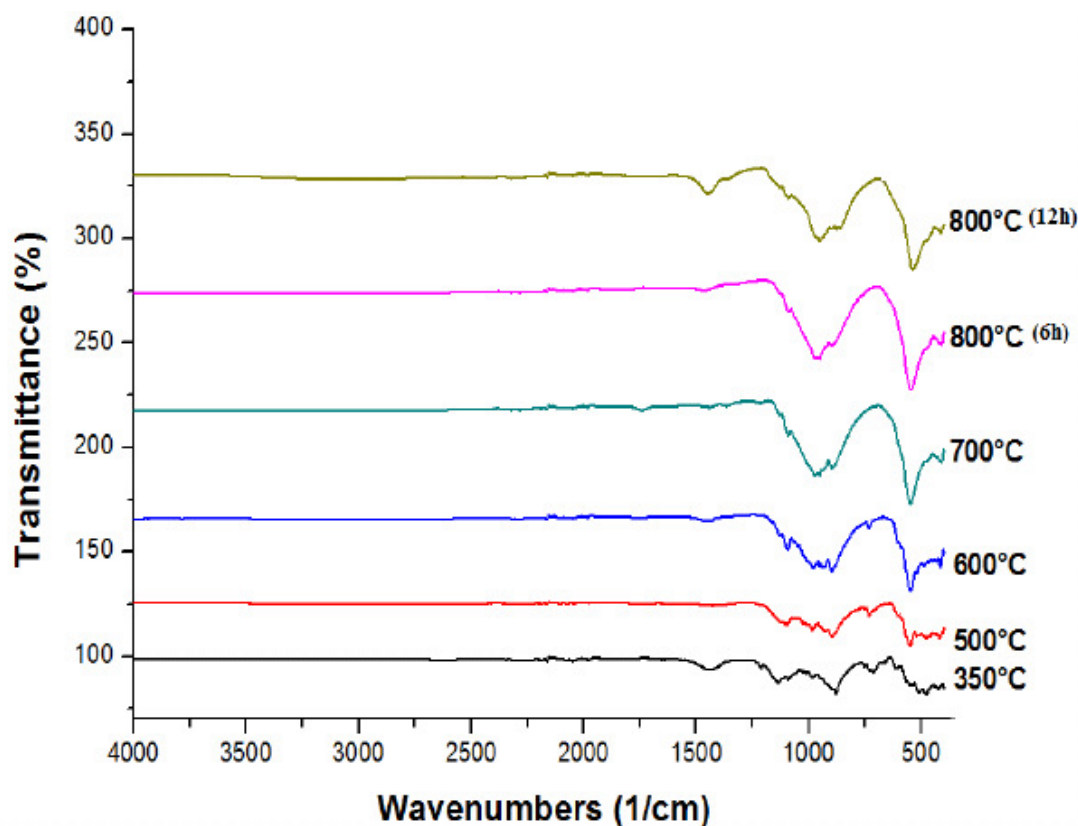


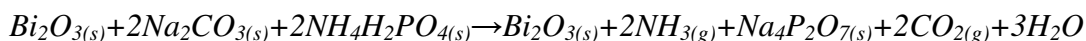
Figure 4.17. IR Spectra of the products of $\text{Bi}_2\text{O}_3 (s) + 2\text{NH}_4\text{H}_2\text{PO}_4(s) + 2\text{Na}_2\text{CO}_3(s)$ reaction at 350°C (6h), 500°C (6h), 600°C (6h), 700°C (6h) and twice at 800°C (6h).

The absence of bands in the $900\text{-}700\text{ cm}^{-1}$ region originated from the P-O-P bridging bands while the strongest bands are generally centered near 1050 cm^{-1} .

The IR band locations for the orthorhombic product from the reaction of $\text{Bi}_2\text{O}_3(s) + 2\text{NH}_4\text{H}_2\text{PO}_4(s) + 2\text{Na}_2\text{CO}_3(s)$ at $800^\circ\text{C}(12\text{h})$ (Figure A.3.), the ν_3 bands were observed between 1132 and 951 cm^{-1} is resolved into four peaks associated with ν_3 fundamental of the PO_4 . These frequencies observed at $1131, 1092, 1030, 951\text{ cm}^{-1}$. And the ν_1 vibration is also found in this region due to stretching modes which we observed bands at $901, 879$ and 863 cm^{-1} . The remainder of the frequencies at 538 and 439 cm^{-1} are attributed to the bound to the splitting of deformation modes ν_4 and ν_2 (O-P-P) PO_4 modes which are observed at $538, 439$ and 411 cm^{-1} .

4.3.2. X-Ray (XRD) Studies

When the product examined on the XRD Pattern at 350°C, lines of α - Bi_2O_3 **ICDD: 71-0465** $\text{Na}_4\text{P}_2\text{O}_7$ **ICDD: 10-0187** and some lines of NH_3 were observed. Hence, the following reaction was proposed;



At 500°C, Na_2CO_3 **ICDD: 19-1130**, and a minor amount of $\text{Na}_4\text{P}_2\text{O}_7$ were detected. At 600°C XRD peaks showed the presence of $\text{Na}_3\text{Bi}(\text{PO}_4)_2$ **ICDD: 81-0036** unreacted Bi_2O_3 and Na_3PO_4 **ICDD: 84-0195** also lines of Na_2O were observed. At 700°C, $\text{Na}_3\text{Bi}(\text{PO}_4)_2$ and Na_3PO_4 lines were still there. At 800°C (12h), all the other compounds were disappeared and an orthorhombic compound of $\text{Na}_2\text{BiOPO}_4$ was obtained according to the following estimated reaction;

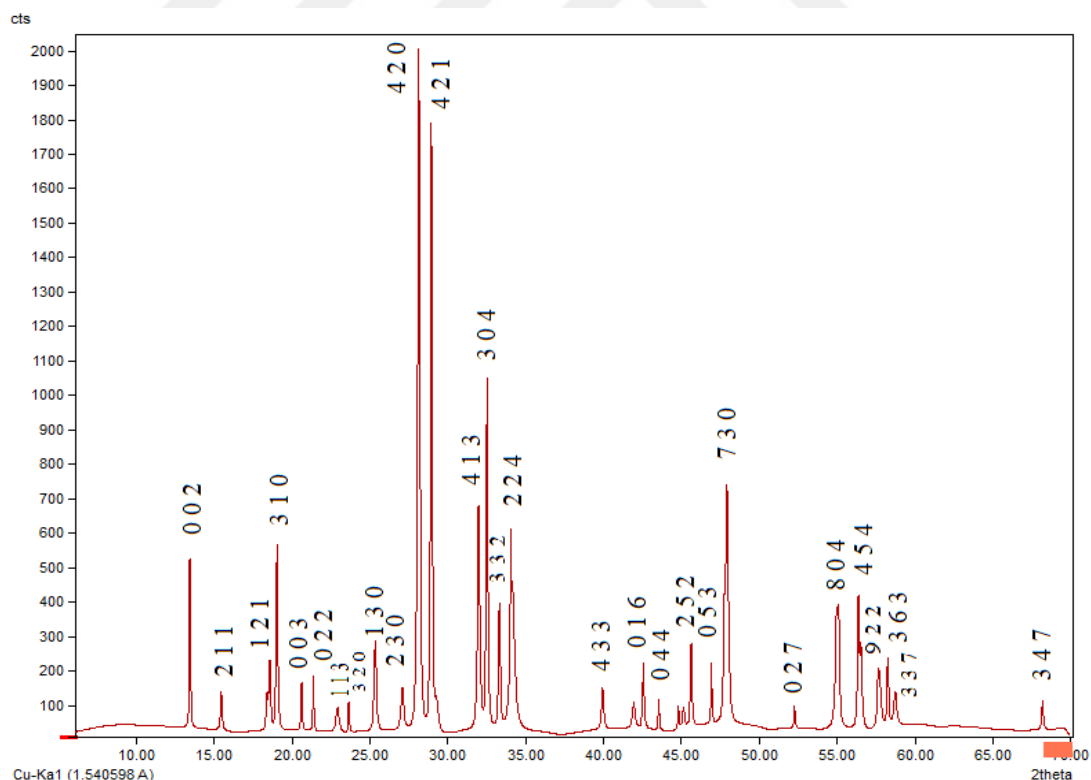


Figure 4.18. X-Ray Powder Diffraction Pattern of $\text{Bi}_2\text{O}_{3(s)} + 2\text{NH}_4\text{H}_2\text{PO}_{4(s)} + 2\text{Na}_2\text{CO}_{3(s)}$ solid-state reaction at 800°C (12h).

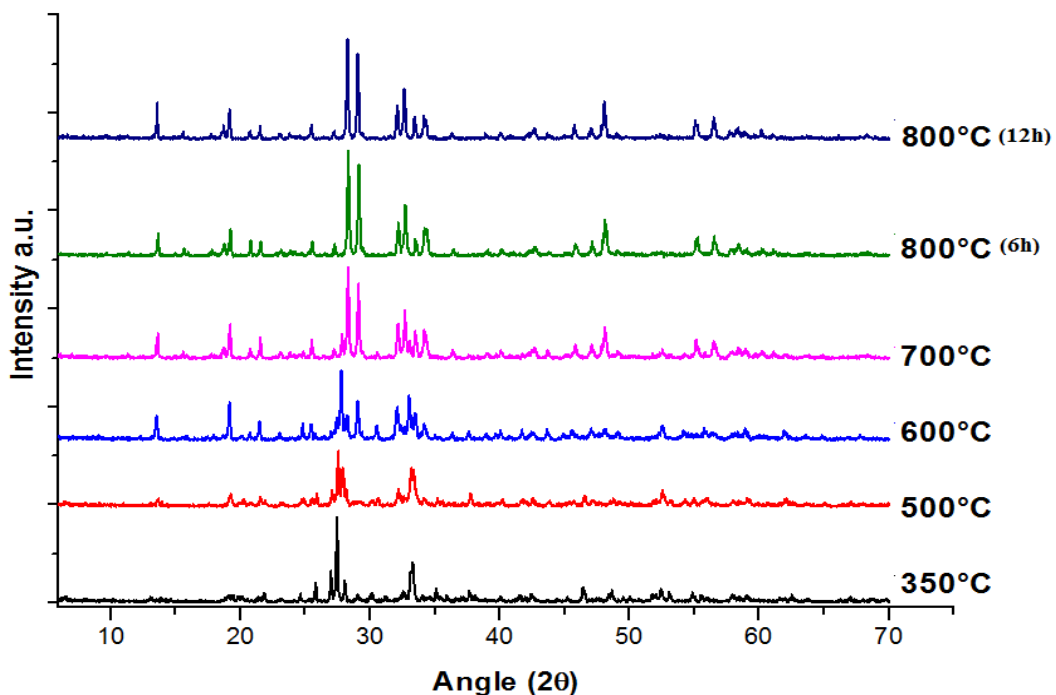


Figure 4.19. X-Ray Powder Diffraction Pattern of $Bi_2O_{3(s)}+2NH_4H_2PO_{4(s)}+2Na_2CO_{3(s)}$ at $350^\circ C(6h)$, $500^\circ C(6h)$, $600^\circ C(6h)$, $700^\circ C(6h)$ and two times at $800^\circ C(12h)$.

The crystal symmetry of this new compound from $Bi_2O_{3(s)}+2NH_4H_2PO_{4(s)}+2Na_2CO_{3(s)}$ solid-state reaction was found to be an orthorhombic structure with the refined cell parameters which is given in Table 4.7. with other parameters are $a=15.3244$, $b=10.7467$, $c=13.0113$ Å and the possible space group determined as *Pnma* number: 62. The Graph of fixed data was shown with the following figure of refinement pattern from the software.

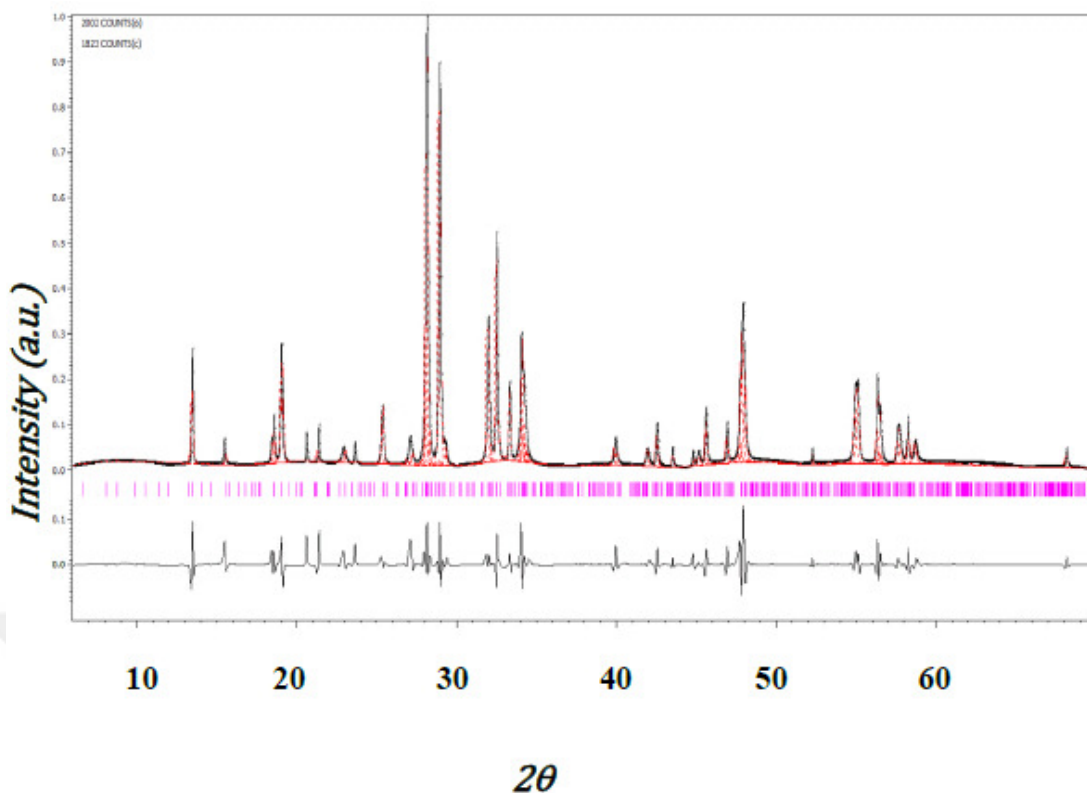


Figure 4.20. Jana2006 refinement pattern for $\text{Bi}_2\text{O}_3 + \text{Na}_2\text{CO}_3 + \text{NH}_4\text{H}_2\text{PO}_4$.

Table 4.7. Refinement and structural parameters of product recorded from Jana2006

| Reaction Sample | 3. $\text{Bi}_2\text{O}_3(\text{s}) + 2\text{NH}_4\text{H}_2\text{PO}_4(\text{s}) + 2\text{Na}_2\text{CO}_3(\text{s})$ |
|--|--|
| Sample | Powder Crystal |
| Symmetry | Orthorhombic |
| Space Group | Pnma |
| $a(\text{Å})$ | 15.3244 |
| $b(\text{Å})$ | 10.7467 |
| $c(\text{Å})$ | 13.0113 |
| α° degree | 90.000 |
| β° degree | 90.000 |
| δ° degree | 90.000 |
| Diffractometer | Rigaku |
| Radiation Type | Cu K α |
| Monochromator | Graphite |
| Wavelength (Å) | 1.5405 |
| Refined profile range ($^\circ 2\theta$) | 6.00-70.00 |
| GOF | 1.53 |
| R_p | 12.15 |
| R_{wp} | 18.87 |
| V | 2142.8 |

Table 4.8. X-Ray powder diffraction data of orthorhombic Na_2BiOPO_4 from reaction of $Bi_2O_3(s) + 2NH_4H_2PO_4(s) + 2Na_2CO_3(s)$ with the refined cell parameters (see Table 4.7.).

| I/I_0 | hkl | $Sin^2(\theta)_{calc}$ | $Sin^2(\theta)_{obs}$ | d_{cal} | d_{obs} |
|---------|-------|------------------------|-----------------------|-----------|-----------|
| 32 | 0 0 2 | 0.01420 | 0.01393 | 6.464 | 6.524 |
| 8 | 2 1 1 | 0.01845 | 0.01837 | 5.671 | 5.682 |
| 14 | 1 2 1 | 0.02640 | 0.02639 | 4.740 | 4.741 |
| 32 | 3 1 0 | 0.02715 | 0.02769 | 4.674 | 4.628 |
| 10 | 0 0 3 | 0.03195 | 0.03240 | 4.309 | 4.279 |
| 12 | 0 2 2 | 0.03460 | 0.03479 | 4.141 | 4.129 |
| 6 | 1 1 3 | 0.03950 | 0.03981 | 3.875 | 3.860 |
| 7 | 3 2 0 | 0.04245 | 0.04238 | 3.738 | 3.741 |
| 16 | 1 3 0 | 0.04835 | 0.04855 | 3.503 | 3.495 |
| 9 | 2 3 0 | 0.05570 | 0.05545 | 3.263 | 3.271 |
| 100 | 4 2 0 | 0.05960 | 0.05959 | 3.155 | 3.155 |
| 91 | 4 2 1 | 0.06315 | 0.06294 | 3.065 | 3.070 |
| 37 | 4 1 3 | 0.07625 | 0.07644 | 2.789 | 2.786 |
| 56 | 3 0 4 | 0.07885 | 0.07896 | 2.743 | 2.741 |
| 19 | 3 3 2 | 0.08215 | 0.08267 | 2.687 | 2.679 |
| 24 | 2 2 4 | 0.08700 | 0.08685 | 2.611 | 2.613 |
| 9 | 4 3 3 | 0.11705 | 0.11732 | 2.251 | 2.248 |
| 12 | 0 1 6 | 0.13290 | 0.13243 | 2.112 | 2.116 |
| 6 | 0 4 4 | 0.13840 | 0.13827 | 2.070 | 2.071 |
| 16 | 2 5 2 | 0.15150 | 0.15116 | 1.979 | 1.981 |
| 13 | 0 5 3 | 0.15945 | 0.15939 | 1.929 | 1.929 |
| 41 | 7 3 0 | 0.16595 | 0.16570 | 1.890 | 1.892 |
| 6 | 0 2 7 | 0.19435 | 0.19479 | 1.747 | 1.745 |
| 20 | 8 0 4 | 0.21360 | 0.21365 | 1.666 | 1.666 |
| 23 | 4 5 4 | 0.22350 | 0.22390 | 1.629 | 1.627 |
| 9 | 9 2 2 | 0.23305 | 0.23297 | 1.595 | 1.595 |
| 14 | 3 6 3 | 0.23760 | 0.23786 | 1.580 | 1.579 |
| 8 | 3 3 7 | 0.24190 | 0.24174 | 1.566 | 1.566 |
| 5 | 3 4 7 | 0.27760 | 0.27817 | 1.462 | 1.460 |

4.3.3. Scanning Electron Microscopy (SEM) and (EDX) Studies

The morphology and the structural features of Na_2BiOPO_4 reaction compound were investigated using SEM-EDX as given in figures below. SEM images showed that the orthorhombic compound uniformity exists between the specimens of the sample shape and particle size and have an irregularly grained powder. The shape of images seen as flaky or disc shapes in the micrographs. And the EDX spectrum shows the presence of Na, O, P and Bi (see Figure 4.22).

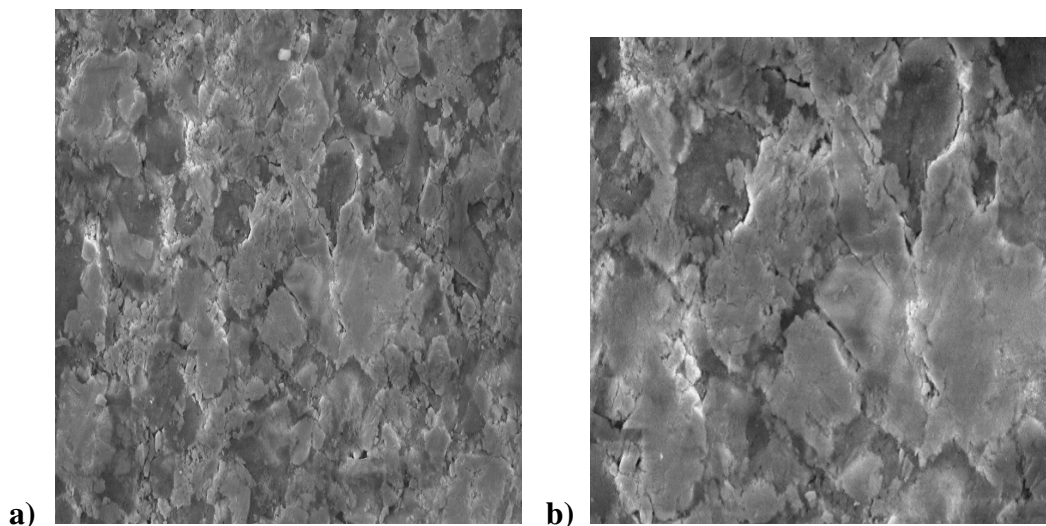
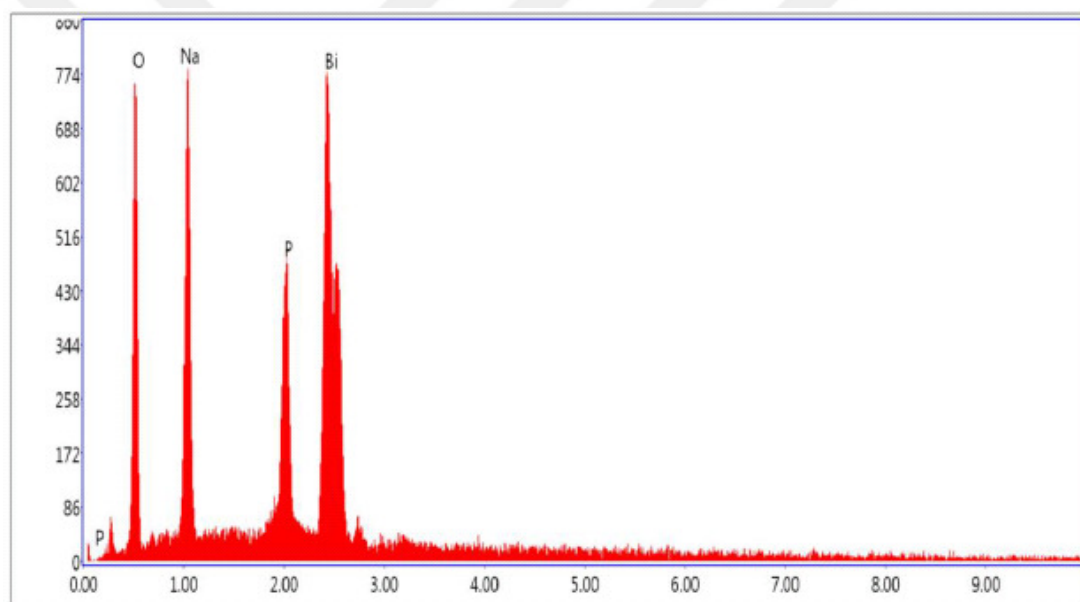


Figure 4.21. SEM images of $Bi_2O_3(s) + 2NH_4H_2PO_4(s) + 2Na_2CO_3(s)$ reaction at 800°C a) 10 µm b) 5 µm.



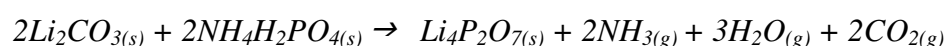
Lsec: 28.50 Cnts 0.000 keV Det: Octane Pro Det

| <i>Element</i> | <i>Weight %</i> | <i>Atomic %</i> | <i>Net Int.</i> | <i>Error %</i> | <i>K ratio</i> | <i>Z</i> | <i>R</i> | <i>A</i> | <i>F</i> |
|-------------------|-----------------|-----------------|-----------------|----------------|----------------|----------|----------|----------|----------|
| <i>OK</i> | 25.60 | 51.74 | 130.01 | 9.63 | 0.11 | 1.27 | 0.86 | 0.34 | 1 |
| <i>NaK</i> | 21.40 | 30.10 | 162.42 | 8.42 | 0.11 | 1.16 | 0.9 | 0.46 | 1 |
| <i>PK</i> | 11.21 | 11.70 | 127.71 | 6.05 | 0.10 | 1.12 | 0.93 | 0.78 | 1 |
| <i>BiM</i> | 41.79 | 6.47 | 193.79 | 5.27 | 0.33 | 0.72 | 1.28 | 1.06 | 1.03 |

Figure 4.22. EDS Spectrum of the Product obtained from the $Bi_2O_3(s) + NH_4H_2PO_4(s) + 2Na_2CO_3(s)$ reaction at 800°C (12h).

4.4. Synthesize of Li₄P₂O₇

The Li₄PO₇ compound was synthesized in this work with solid-state reaction method according to Zaafour work (Zaafour, Megdiche, and Gargouri, 2015) to use this compound as a precursor for synthesizing of Li₂BiOPO₄ compound. The reaction processed by mixing 2 moles of Li₂CO₃ and 2 moles of NH₄H₂PO₄ stoichiometrically. And progressively heated at 300°C (8h), 500°C (8h), 750°C (8h). And the following reaction was expected:



4.4.1. Infrared (IR) Studies

At 300°C, the IR spectrum showed that the presence of Li₂CO₃ at 742, and 784 cm⁻¹ also NH₄H₂PO₄ was observed at 538 cm⁻¹ (see Figure 4.24). At 500°C, there was still Li₂CO₃ frequency at 742 cm⁻¹ and NH₄H₂PO₄ at 537 cm⁻¹ (referenced by Table 4.9.), and also P₂O₇ (P-O-P) bonds were started to exist at 500°C. And finally, at 750°C, these frequencies of precursors disappeared, and there were no other side products. Therefore, oxyphosphate frequencies were observed at 1196, 1113, 1035, 1018, and 934 cm⁻¹. The IR result of observed Li₄P₂O₇ compound was figured which was shown in Figure A.5.

Table 4.9. The observed IR frequencies of reagents Li₂CO₃ and NH₄H₂PO₄.

| PURE COMPOUNDS | IR FREQUENCIES (cm ⁻¹) |
|--|--|
| Li ₂ CO ₃ | 1471, 1413, 1230, 1217, 1087, 858, 740, 476 cm ⁻¹ |
| NH ₄ H ₂ PO ₄ | 1436, 1402, 1266, 1231, 1071, 540, 402 cm ⁻¹ |

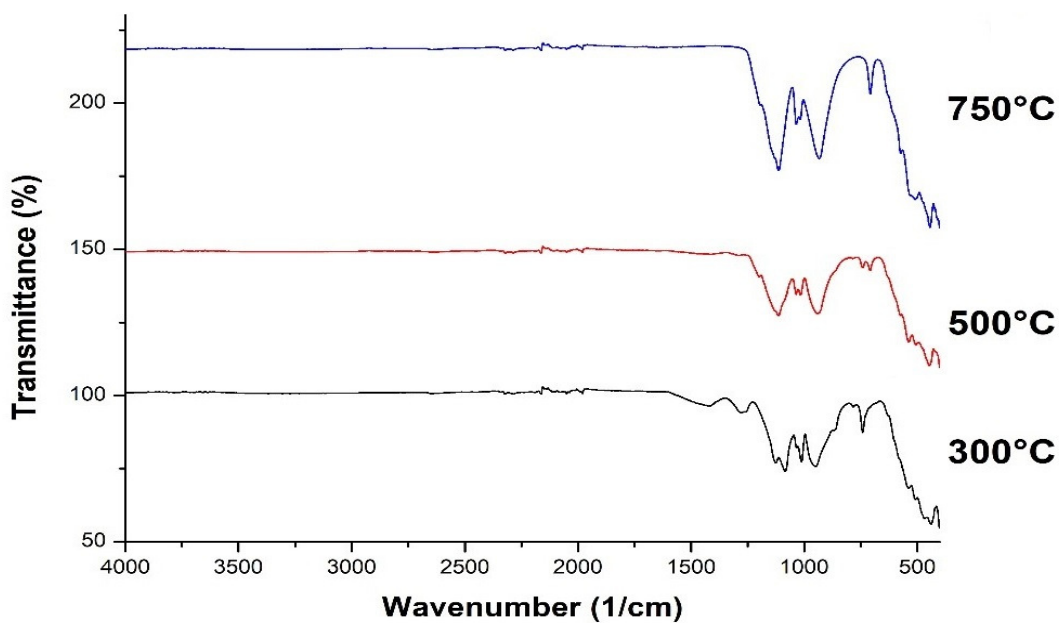


Figure 4.23 IR Spectra of the Initial Pure Compounds Li_2CO_3 and $\text{NH}_4\text{H}_2\text{PO}_4$.

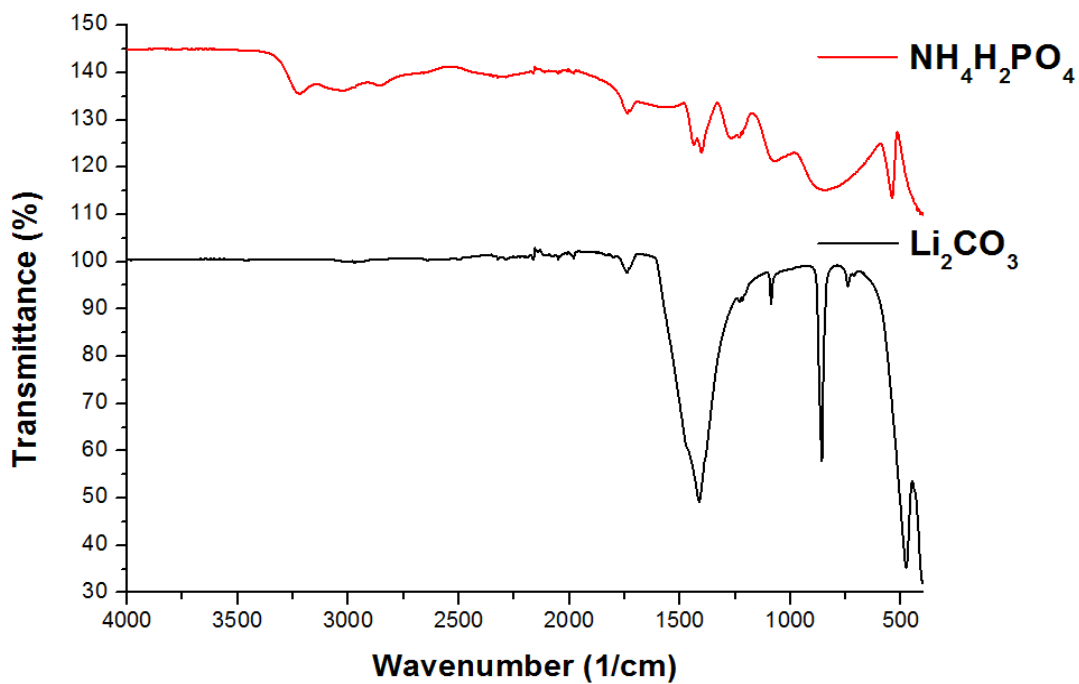
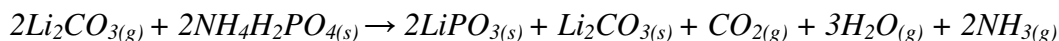


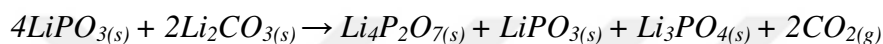
Figure 4.24. IR Spectra of the reaction $\text{Li}_2\text{CO}_3 + \text{NH}_4\text{H}_2\text{PO}_4$ at 300°C (8h), 500°C (8h), and 750°C (8h).

4.4.2. X-Ray (XRD) Studies

When each reaction mixtures were examined on the XRD Pattern, in the first heating at 300°C (8h), there were unreacted lines of Li_2CO_3 **ICDD:** 87-0728 and also lines of LiPO_3 was observed **ICDD:** 26-1177 (see Figure 4.26).



At 500°C (8h), additional to the lines of LiPO_3 , d spacings of Li_3PO_4 were observed **ICDD:** 15-0760. And $\text{Li}_4\text{P}_2\text{O}_7$ peaks were started to appear at this temperature.



At 750°C (8h), 2 moles of $\text{Li}_4\text{P}_2\text{O}_7$ occurred and the reaction compound matched with the reference compound of triclinic $\text{Li}_4\text{P}_2\text{O}_7$ with 81.7% ratio **ICDD:** 87-0409.

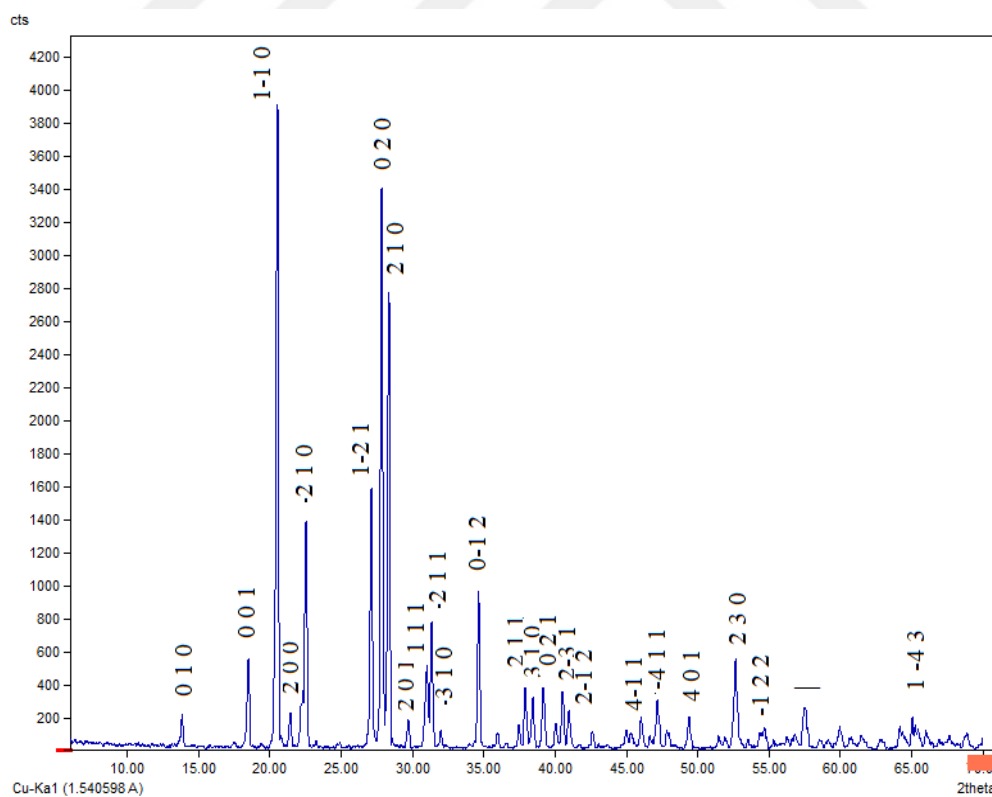


Figure 4.25. X-Ray Powder Diffraction Pattern of $\text{Li}_4\text{P}_2\text{O}_{7(s)}$ at 750°C (8h).

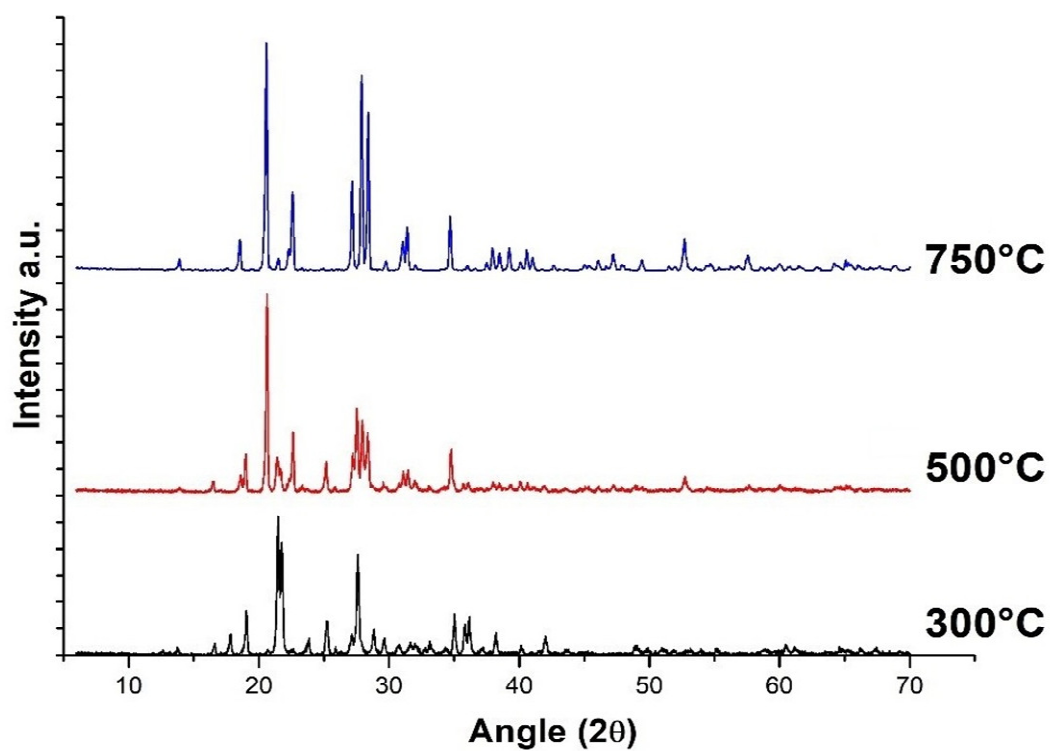


Figure 4.26. X-Ray Powder Diffraction Pattern of $Li_4P_2O_7(s)$ at 300°C(8h), 500°C(8h), and 750°C(8h).

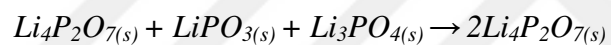


Table 4.10. X-Ray Powder Data for Triclinic $\text{Li}_4\text{P}_2\text{O}_7$ compound by the $2\text{Li}_2\text{CO}_3(\text{g}) + 2\text{NH}_4\text{H}_2\text{PO}_4(\text{s})$ solid-state reaction at $750^\circ\text{C}(8\text{h})$ from Rietveld Calculation.

| I/I_o | hkl | $2\theta(^{\circ})_{\text{calc}}$ | d_{obs} | d_{cal} | Matched Reference |
|---------|--------|-----------------------------------|------------------|------------------|-----------------------------------|
| 6 | 0 1 0 | 13.81 | 6.365 | 6.407 | $\text{Li}_4\text{P}_2\text{O}_7$ |
| 14 | 0 0 1 | 18.45 | 4.781 | 4.804 | $\text{Li}_4\text{P}_2\text{O}_7$ |
| 100 | 1-1 0 | 20.49 | 4.312 | 4.330 | $\text{Li}_4\text{P}_2\text{O}_7$ |
| 6 | 2 0 0 | 21.41 | 4.129 | 4.147 | $\text{Li}_4\text{P}_2\text{O}_7$ |
| 10 | 1 0 1 | 22.20 | 4.000 | 4.000 | $\text{Li}_4\text{P}_2\text{O}_7$ |
| 35 | -2 1 0 | 22.50 | 3.931 | 3.948 | $\text{Li}_4\text{P}_2\text{O}_7$ |
| 40 | 1-2 1 | 23.08 | 3.280 | 3.290 | $\text{Li}_4\text{P}_2\text{O}_7$ |
| 87 | 0 2 0 | 27.80 | 3.197 | 3.206 | $\text{Li}_4\text{P}_2\text{O}_7$ |
| 71 | 2 1 0 | 28.31 | 3.140 | 3.149 | $\text{Li}_4\text{P}_2\text{O}_7$ |
| 5 | 2 0 1 | 29.67 | 2.999 | 3.008 | $\text{Li}_4\text{P}_2\text{O}_7$ |
| 13 | 1 1 1 | 30.97 | 2.876 | 2.885 | $\text{Li}_4\text{P}_2\text{O}_7$ |
| 20 | -2 1 1 | 31.29 | 2.848 | 2.856 | $\text{Li}_4\text{P}_2\text{O}_7$ |
| 4 | -3 1 0 | 31.93 | 2.791 | 2.800 | $\text{Li}_4\text{P}_2\text{O}_7$ |
| 25 | 0-1 2 | 34.59 | 2.584 | 2.590 | $\text{Li}_4\text{P}_2\text{O}_7$ |
| 3 | -3 0 1 | 35.92 | 2.492 | 2.498 | $\text{Li}_4\text{P}_2\text{O}_7$ |
| 4 | 0-2 2 | 37.40 | 2.396 | 2.402 | $\text{Li}_4\text{P}_2\text{O}_7$ |
| 10 | 2 1 1 | 37.85 | 2.370 | 2.375 | $\text{Li}_4\text{P}_2\text{O}_7$ |
| 9 | 3 1 0 | 38.38 | 2.337 | 2.343 | $\text{Li}_4\text{P}_2\text{O}_7$ |
| 11 | 0 2 1 | 39.12 | 2.295 | 2.300 | $\text{Li}_4\text{P}_2\text{O}_7$ |
| 5 | 1 0 2 | 40.00 | 2.246 | 2.252 | $\text{Li}_4\text{P}_2\text{O}_7$ |
| 10 | 2-3 1 | 40.46 | 2.222 | 2.227 | $\text{Li}_4\text{P}_2\text{O}_7$ |
| 7 | 2-1 2 | 40.92 | 2.198 | 2.203 | $\text{Li}_4\text{P}_2\text{O}_7$ |
| 3 | 0 1 2 | 44.94 | 2.117 | 2.015 | $\text{Li}_4\text{P}_2\text{O}_7$ |
| 4 | -2-2 2 | 45.26 | 2.011 | 2.002 | $\text{Li}_4\text{P}_2\text{O}_7$ |
| 5 | 4-1 1 | 45.98 | 1.969 | 1.972 | $\text{Li}_4\text{P}_2\text{O}_7$ |
| 3 | 3 1 1 | 46.57 | 1.944 | 1.948 | $\text{Li}_4\text{P}_2\text{O}_7$ |
| 9 | -4 1 1 | 47.12 | 1.923 | 1.927 | $\text{Li}_4\text{P}_2\text{O}_7$ |
| 4 | -1-3 2 | 47.94 | 1.898 | 1.896 | $\text{Li}_4\text{P}_2\text{O}_7$ |
| 6 | 4 0 1 | 49.34 | 1.842 | 1.845 | $\text{Li}_4\text{P}_2\text{O}_7$ |
| 3 | -1 3 1 | 51.41 | 1.773 | 1.776 | $\text{Li}_4\text{P}_2\text{O}_7$ |
| 14 | 2 3 0 | 52.60 | 1.734 | 1.738 | $\text{Li}_4\text{P}_2\text{O}_7$ |
| 4 | -1 2 2 | 54.76 | 1.676 | 1.675 | $\text{Li}_4\text{P}_2\text{O}_7$ |
| 7 | — | 57.64 | 1.598 | 1.597 | Undefined |
| 4 | -2 0 3 | 59.91 | 1.540 | 1.542 | $\text{Li}_4\text{P}_2\text{O}_7$ |
| 3 | 2 0 3 | 64.11 | 1.507 | 1.451 | $\text{Li}_4\text{P}_2\text{O}_7$ |
| 4 | 1 -4 3 | 64.29 | 1.449 | 1.447 | $\text{Li}_4\text{P}_2\text{O}_7$ |
| 6 | -5 0 2 | 65.19 | 1.431 | 1.430 | $\text{Li}_4\text{P}_2\text{O}_7$ |
| 3 | -6 1 0 | 65.39 | 1.413 | 1.426 | $\text{Li}_4\text{P}_2\text{O}_7$ |

While in that work of Zaafour which is about $\text{Li}_4\text{P}_2\text{O}_7$ synthesise, the unit cell parameters have been defined as $a=6.3373(4)$, $b=12.8997(5)$, $c=8.0158(6)$ Å, and $\beta=90.8329(12)^\circ$ and the system is monoclinic with the space group (P_2 No:2). But in this our study, the unit cell parameters are $a=7.099$, $b=5.179$, $c=8.549$ Å and the system is found to be triclinic; $\alpha=89.841$, $\beta=103.180$, $\gamma=111.342^\circ$.

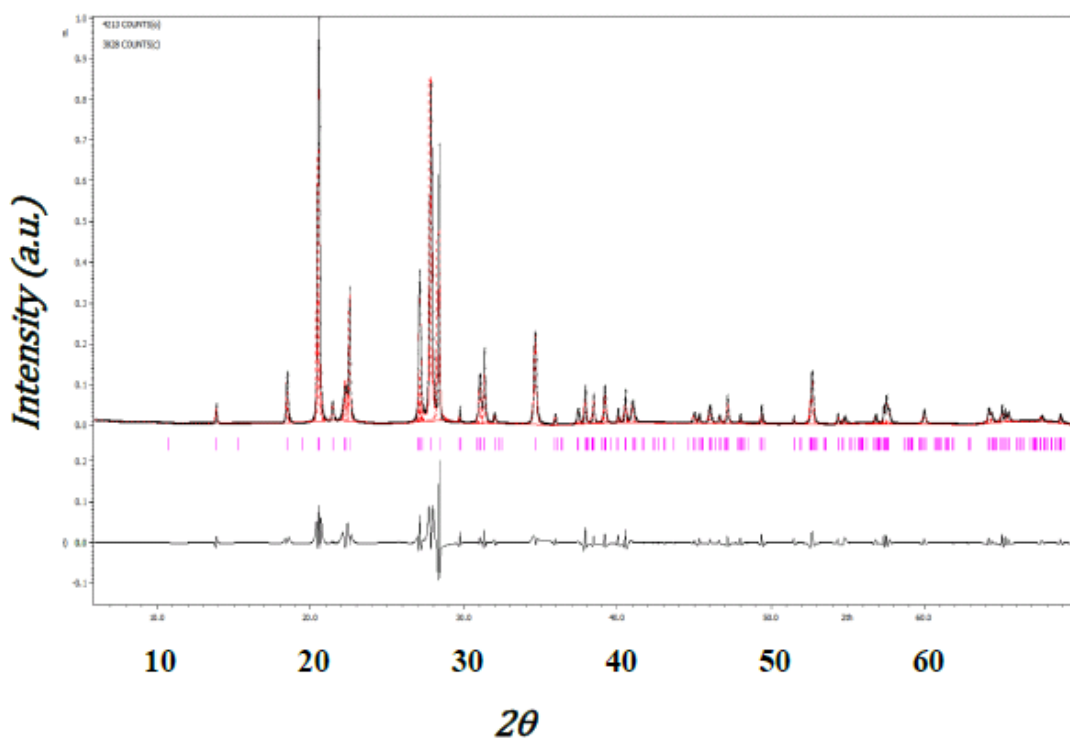


Figure 4.27. Jana2006 refinement pattern of synthesized $\text{Li}_4\text{P}_2\text{O}_7$.

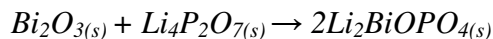
Table 4.11. Refinement and structural parameters of product recorded from Jana2006

| Sample | 4. $\text{Li}_4\text{P}_2\text{O}_7$ |
|--|--------------------------------------|
| Sample | Powder Crystal |
| Symmetry | Triclinic |
| Space Group | P_1 (No: 2) |
| a (Å) | 7.099 |
| b (Å) | 5.179 |
| c (Å) | 8.549 |
| α° degree | 89.841 |
| β° degree | 103.180 |
| δ° degree | 111.342 |
| Diffractometer | Rigaku |
| Radiation Type | Cu $K\alpha$ |
| Monochromator | Graphite |
| Wavelength (Å) | 1.5405 |
| Refined profile range ($^\circ 2\theta$) | 6.00-70.00 |
| GOF | 1.76 |
| R_p | 12.85 |
| R_{wp} | 19.35 |
| V | 284.0 |

4.5. Solid-State Reaction of $\text{Bi}_2\text{O}_3(s) + \text{Li}_4\text{P}_2\text{O}_7(s)$

In this work about bismuth containing a novel type of oxyphosphate, we were also processed to synthesize a new compound of $\text{Li}_2\text{BiOPO}_4$. In this solid-state reaction, 2.00 grams of Bi_2O_3 and 0.866 gram of $\text{Li}_4\text{P}_2\text{O}_7$ were mixed

stoichiometrically in 1:1 ratio to yield $\text{Li}_2\text{BiOPO}_4$ compound. The white reaction mixture formed from these precursors and crystal structure of lithium bismuth oxyphosphate reported which detected by Match!3 Software. And the expected reaction was:



4.5.1. Infrared (IR) Studies

In the Infrared Spectra of this solid-state reaction at from 350°C to 500°C (figure 4.28.), $\text{Li}_4\text{P}_2\text{O}_7$ was observed at about 1198, 1113, 1035, 1019, 707, 575, 443 cm^{-1} frequency (referenced by the Table 4.12.). At the 600°C, there was still $\text{Li}_4\text{P}_2\text{O}_7$ at 1198, 1016 and 708 cm^{-1} . And at 700°C, the IR absorption frequencies belong to side products at 959, 718, 586, 508, 494, and 454 cm^{-1} . Finally, at 800°C (20h) the product occurred at 1158, 1134, 1096, 977 and 946 cm^{-1} and other compounds were disappeared (see Figure A.4.).

Table 4.12. The observed IR frequencies of reagents Bi_2O_3 and $\text{Li}_4\text{P}_2\text{O}_7$.

| PURE COMPOUNDS | IR FREQUENCIES (cm^{-1}) |
|-----------------------------------|--|
| Bi_2O_3 | 422, 427, 496, 536, 315, 410, 448, and 522 cm^{-1} |
| $\text{Li}_4\text{P}_2\text{O}_7$ | 443, 511, 535, 573, 707, 934, 1018, 1035, 1113 and 1196 cm^{-1} |

The IR Spectrum of this new monoclinic compound from the reaction mixture of $\text{Bi}_2\text{O}_{3(s)} + \text{Li}_4\text{P}_2\text{O}_{7(s)}$ at third heating of 800°C (totally 20h) shown in Figure A.4. on Appendices section of this work.

The broadband between 1158 and 977 cm^{-1} is resolved into four peaks associated with ν_3 fundamental of the PO_4 . These frequencies observed at 1158, 1134, 1096, 977 cm^{-1} . The ν_l vibration is also found in this region which we observed at 946 and 881 cm^{-1} . The rest of the peaks in the region between 578 and 455 cm^{-1} are bound to the splitting of degenerate ν_4 and ν_2 PO_4 modes which are observed at 578, 536, 510, 494, and 455 cm^{-1} .

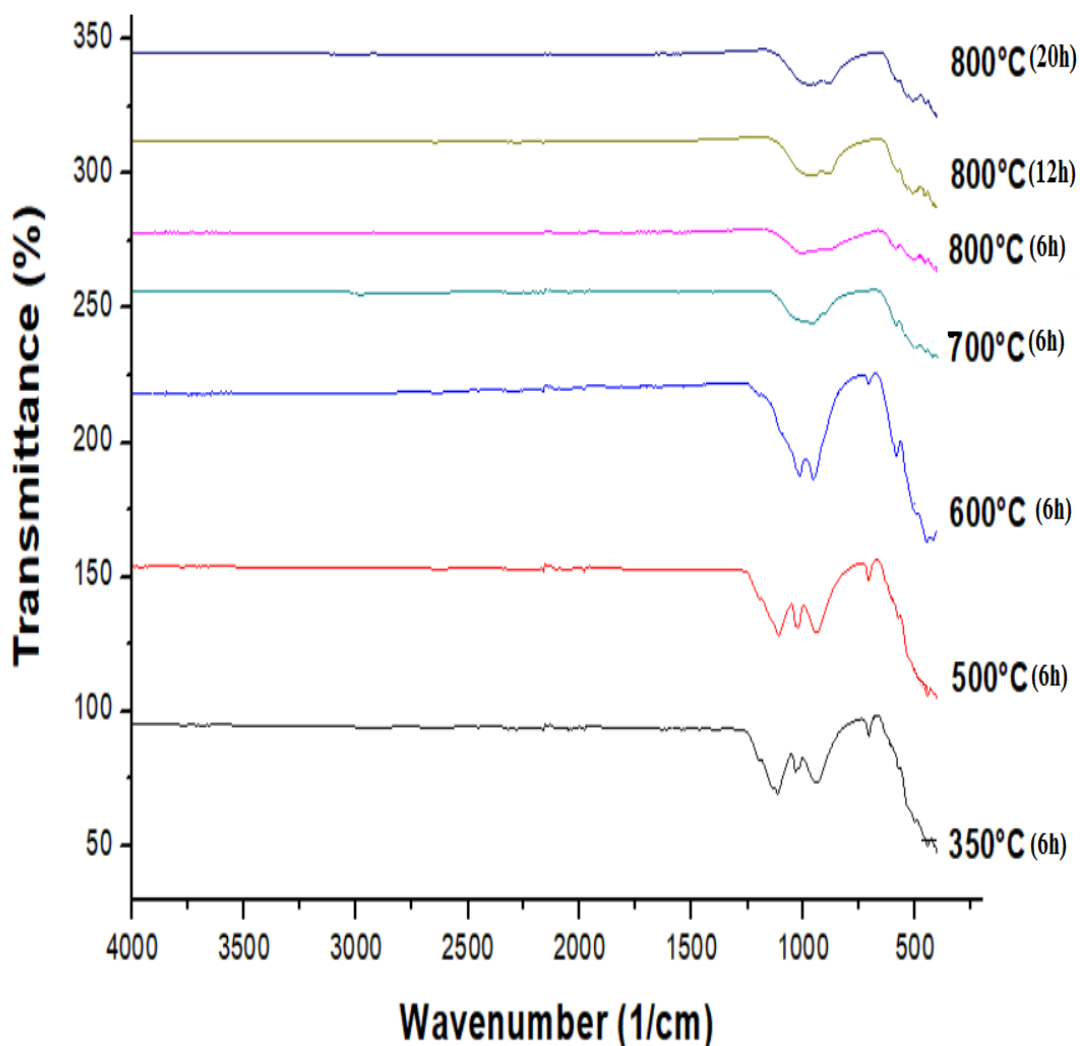


Figure 4.28. IR Spectra of the products of $Bi_2O_{3(s)} + Li_4P_2O_{7(s)}$ reaction at 350°C (6h), 500°C (6h), 600°C (6h), 700°C (6h), and three times at 800°C (20h).

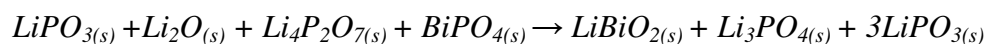
4.5.2. X-Ray Diffraction (XRD) Studies

At 350°C and 500°C, lines of Bi_2O_3 **ICDD:** 41-1449, $Li_4P_2O_7$ **ICDD:** 27-1221 and Li_2O **COD:** 96-151-4099 were detected (see Figure 4.30).

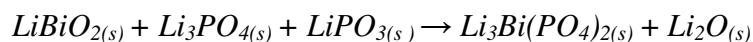
At 600°C, $LiPO_3$ **ICDD:** 26-1177, Li_2O , $Li_4P_2O_7$, and $BiPO_4$ lines were observed in XRD Pattern. The following reaction was proposed:



At 700°C, LiBiO₂ **ICDD:** 27-1221, LiPO₃, γ-Li₃PO₄ **ICDD:** 72-1963 and also a negligible amount of BiPO₄ lines were detected and the following reaction occurred:



At 800°C (12h), lines of Li₃Bi(PO₄)₂, and Li₂O were detected and the following reaction was expected;



When the reaction followed at 800°C (20h), this obtained compound processed Rietveld refinement on Match! Software. The results showed this new material, Li₂BiOPO₄ had similar XRD pattern data with reported LiBi_{7.37}O₇(PO₄)₃ in the literature (Muktha, Darriet, and Guru Row, 2008). These two works matched in 90.3% ratio **COD:** 96-201-6221 Arumugam, Lynch, and Steinfink (2007) (see Table 4.13.). The programme was compared the diffraction pattern of the synthesized compound to a database containing reference patterns of known phases and made quantitative analysis using Rietveld refinement.

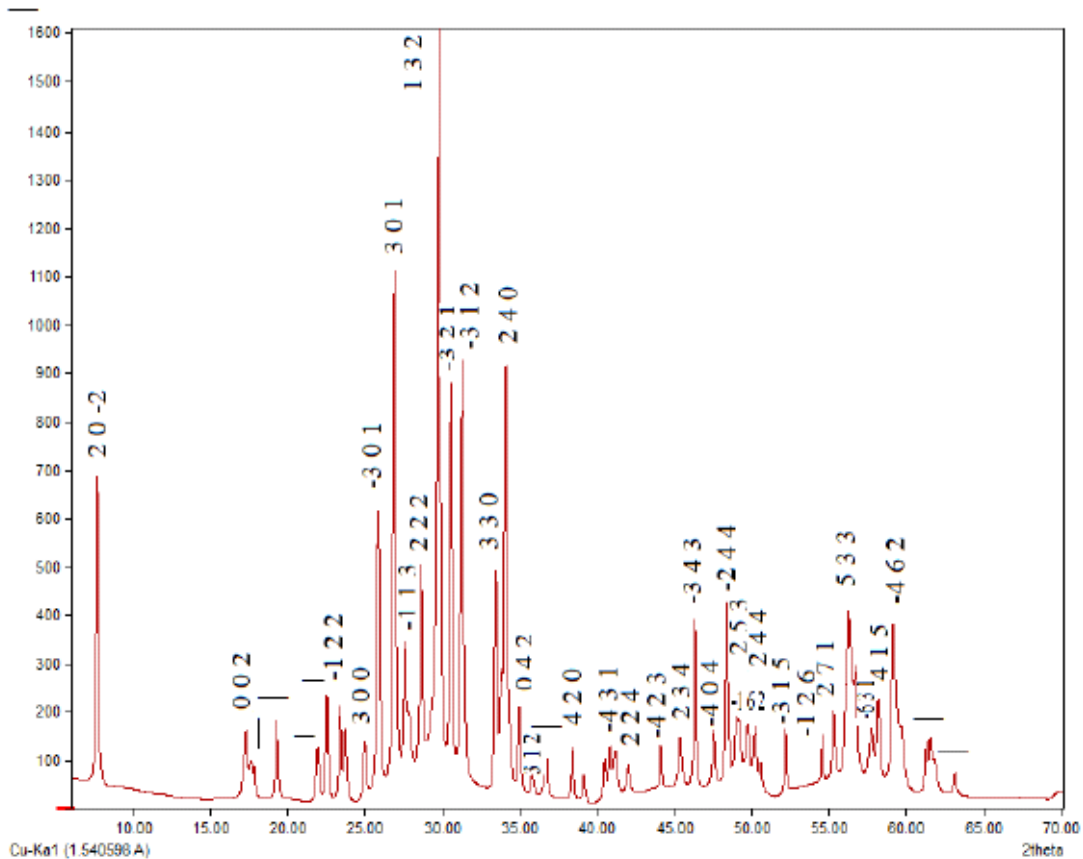


Figure 4.29. X-Ray Powder Diffraction Pattern of $\text{Bi}_2\text{O}_3(\text{s}) + \text{Li}_4\text{P}_2\text{O}_7(\text{s})$ at 800°C (20h).

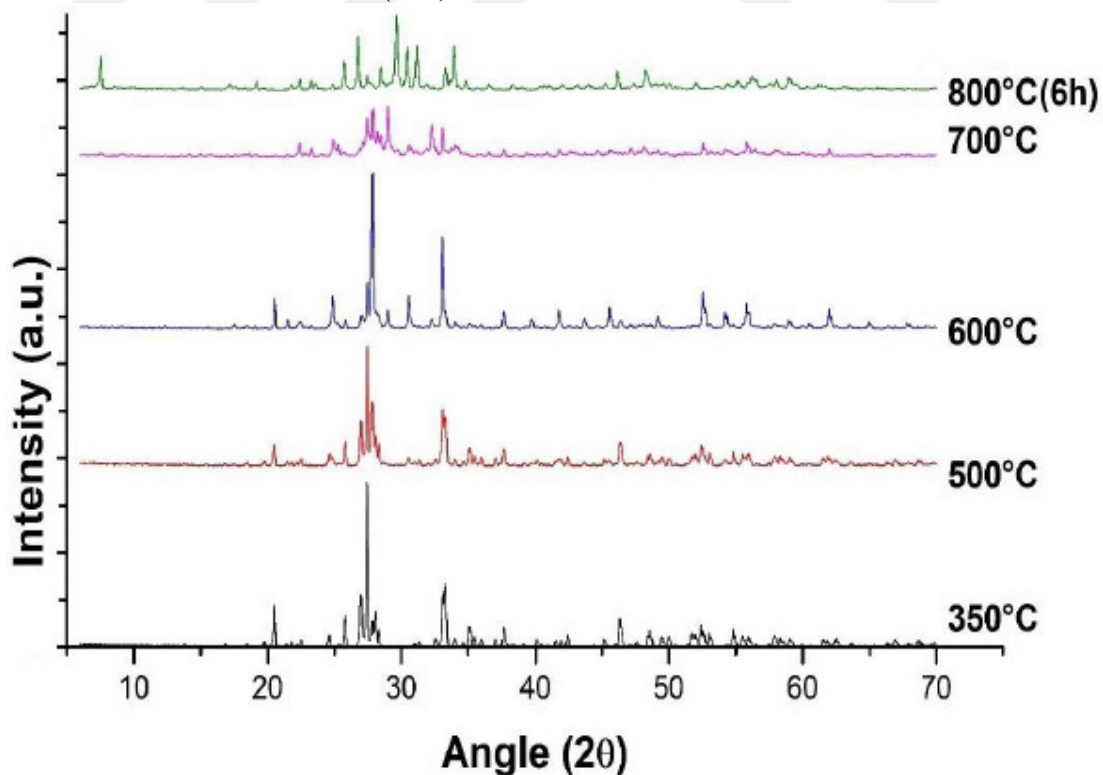


Figure 4.30. X-Ray Powder Diffraction Pattern of $\text{Bi}_2\text{O}_3(\text{s}) + \text{Li}_4\text{P}_2\text{O}_7(\text{s})$ at 350°C (6h), 500°C (6h), 600°C (6h), 700°C (6h), and first heating at 800°C .

Table 4.13. X-Ray Powder Data for Monoclinic compound by the solid-state reaction of $\text{Bi}_2\text{O}_3(\text{s}) + \text{Li}_4\text{P}_2\text{O}_7(\text{s})$ at 800°C (20h) from Rietveld Calculation.

| I/I_0 | hkl | $2\theta(^{\circ})_{\text{obs}}$ | $2\theta(^{\circ})_{\text{calc}}$ | d_{obs} | d_{calc} | Matched Reference |
|---------|--------|----------------------------------|-----------------------------------|------------------|-------------------|---|
| 46 | 2 0 -2 | 7.70 | 7.57 | 11.472 | 11.725 | $\text{LiBi}_{7.37}\text{O}_7(\text{PO}_4)_3$ |
| 8 | 0 0 2 | 17.36 | 17.24 | 5.104 | 5.151 | $\text{LiBi}_{7.37}\text{O}_7(\text{PO}_4)_3$ |
| 5 | — | 18.44 | — | 4.807 | — | Undefined |
| 12 | — | 19.28 | — | 4.599 | — | Undefined |
| 8 | — | 21.94 | — | 4.047 | — | Undefined |
| 9 | — | 22.56 | — | 3.938 | — | Undefined |
| 10 | — | 23.36 | — | 3.804 | — | Undefined |
| 12 | -1 2 2 | 23.70 | 23.59 | 3.751 | 3.775 | $\text{LiBi}_{7.37}\text{O}_7(\text{PO}_4)_3$ |
| 6 | 3 0 0 | 25.00 | 24.81 | 3.558 | 3.592 | $\text{LiBi}_{7.37}\text{O}_7(\text{PO}_4)_3$ |
| 38 | -3 0 1 | 25.86 | 25.77 | 3.442 | 3.461 | $\text{LiBi}_{7.37}\text{O}_7(\text{PO}_4)_3$ |
| 71 | 3 0 1 | 26.90 | 26.77 | 3.311 | 3.333 | $\text{LiBi}_{7.37}\text{O}_7(\text{PO}_4)_3$ |
| 23 | -1 1 3 | 27.58 | 27.47 | 3.231 | 3.250 | $\text{LiBi}_{7.37}\text{O}_7(\text{PO}_4)_3$ |
| 47 | 2 2 2 | 28.62 | 28.51 | 3.116 | 3.133 | $\text{LiBi}_{7.37}\text{O}_7(\text{PO}_4)_3$ |
| 100 | 1 3 2 | 29.78 | 29.23 | 2.997 | 3.057 | $\text{LiBi}_{7.37}\text{O}_7(\text{PO}_4)_3$ |
| 60 | -3 2 1 | 30.56 | 29.67 | 2.922 | 3.013 | $\text{LiBi}_{7.37}\text{O}_7(\text{PO}_4)_3$ |
| 69 | -3 1 2 | 31.26 | 30.43 | 2.859 | 2.940 | $\text{LiBi}_{7.37}\text{O}_7(\text{PO}_4)_3$ |
| 12 | 1 2 3 | 32.02 | 31.15 | 2.792 | 2.873 | $\text{LiBi}_{7.37}\text{O}_7(\text{PO}_4)_3$ |
| 4 | 3 1 2 | 32.64 | 31.92 | 2.741 | 2.805 | $\text{LiBi}_{7.37}\text{O}_7(\text{PO}_4)_3$ |
| 33 | 3 3 0 | 33.42 | 33.31 | 2.679 | 2.692 | $\text{LiBi}_{7.37}\text{O}_7(\text{PO}_4)_3$ |
| 66 | 2 4 0 | 34.10 | 33.66 | 2.627 | 2.664 | $\text{LiBi}_{7.37}\text{O}_7(\text{PO}_4)_3$ |
| 13 | 0 4 2 | 34.98 | 33.98 | 2.563 | 2.640 | $\text{LiBi}_{7.37}\text{O}_7(\text{PO}_4)_3$ |
| 5 | -4 1 1 | 35.76 | 34.88 | 2.508 | 2.574 | $\text{LiBi}_{7.37}\text{O}_7(\text{PO}_4)_3$ |
| 5 | — | 36.74 | — | 2.444 | — | Undefined |
| 8 | 4 2 0 | 38.40 | 36.62 | 2.342 | 2.456 | $\text{LiBi}_{7.37}\text{O}_7(\text{PO}_4)_3$ |
| 4 | -2 1 4 | 39.08 | 38.32 | 2.303 | 2.350 | $\text{LiBi}_{7.37}\text{O}_7(\text{PO}_4)_3$ |
| 7 | -4 3 1 | 40.96 | 40.72 | 2.201 | 2.217 | $\text{LiBi}_{7.37}\text{O}_7(\text{PO}_4)_3$ |
| 8 | 2 2 4 | 42.14 | 42.01 | 2.142 | 2.152 | $\text{LiBi}_{7.37}\text{O}_7(\text{PO}_4)_3$ |
| 8 | -5 1 1 | 43.34 | 43.22 | 2.086 | 2.094 | $\text{LiBi}_{7.37}\text{O}_7(\text{PO}_4)_3$ |
| 9 | -4 2 3 | 44.08 | 44.00 | 2.052 | 2.059 | $\text{LiBi}_{7.37}\text{O}_7(\text{PO}_4)_3$ |
| 12 | 2 3 4 | 45.48 | 45.35 | 1.992 | 2.001 | $\text{LiBi}_{7.37}\text{O}_7(\text{PO}_4)_3$ |
| 26 | -3 4 3 | 46.30 | 46.22 | 1.959 | 1.965 | $\text{LiBi}_{7.37}\text{O}_7(\text{PO}_4)_3$ |
| 12 | -4 0 4 | 47.44 | 47.34 | 1.914 | 1.921 | $\text{LiBi}_{7.37}\text{O}_7(\text{PO}_4)_3$ |
| 35 | -2 4 4 | 48.38 | 48.26 | 1.879 | 1.887 | $\text{LiBi}_{7.37}\text{O}_7(\text{PO}_4)_3$ |
| 9 | -1 6 2 | 49.26 | 48.42 | 1.848 | 1.881 | $\text{LiBi}_{7.37}\text{O}_7(\text{PO}_4)_3$ |
| 11 | 2 5 3 | 49.68 | 49.05 | 1.833 | 1.858 | $\text{LiBi}_{7.37}\text{O}_7(\text{PO}_4)_3$ |
| 10 | 2 4 4 | 50.18 | 49.61 | 1.816 | 1.838 | $\text{LiBi}_{7.37}\text{O}_7(\text{PO}_4)_3$ |
| 11 | -3 1 5 | 52.18 | 50.07 | 1.751 | 1.823 | $\text{LiBi}_{7.37}\text{O}_7(\text{PO}_4)_3$ |
| 5 | -3 6 1 | 53.12 | 52.05 | 1.722 | 1.758 | Undefined |
| 8 | -1 2 6 | 54.60 | 55.24 | 1.679 | 1.664 | Undefined |
| 12 | 2 7 1 | 54.96 | 56.07 | 1.669 | 1.641 | Undefined |
| 18 | 5 3 3 | 56.56 | 56.26 | 1.625 | 1.636 | Undefined |
| 11 | -6 3 1 | 57.64 | 56.44 | 1.597 | 1.631 | Undefined |
| 14 | 4 1 5 | 58.18 | 58.08 | 1.584 | 1.589 | Undefined |
| 19 | -4 6 2 | 59.08 | 58.96 | 1.562 | 1.567 | Undefined |
| 11 | 3 6 3 | 59.60 | 59.14 | 1.549 | 1.563 | Undefined |
| 9 | — | 61.54 | — | 1.505 | — | Undefined |
| 8 | — | 63.32 | — | 1.467 | — | Undefined |

In that $\text{LiBi}_{7.37}\text{O}_7(\text{PO}_4)_3$ work (Muktha, Darriet, and Guru Row, 2008), that compound has been synthesized with single crystal solid-state method for the first time with the reagents of Bi_2O_3 , Li_2CO_3 and $(\text{NH}_4)_2\text{HPO}_4$. But there are some differences between this work and that study about synthesise of $\text{LiBi}_{7.37}\text{O}_7(\text{PO}_4)_3$

which are unit cell parameters, space groups, products, production temperature, and precursors. In $\text{LiBi}_{7.37}\text{O}_7(\text{PO}_4)_3$ work, the unit cell parameters are $a=30.8524(3)$, $b=5.2688(2)$, $c=24.5719(3)$ Å and the system is monoclinic $\beta=122.852(2)^\circ$, space group $C_{2/c}$ (No:15).

In this $\text{Li}_2\text{BiOPO}_4$ work, this compound was synthesized by the solid-state method for the first time with the precursors of Bi_2O_3 and $\text{Li}_4\text{P}_2\text{O}_7$ in 1:1 ratio. And with using the Match software, the calculated and refined unit cell parameters detected; $a=10.7380$, $b=12.2486$, $c=10.4148$ Å and concluded that it crystallizes in the monoclinic system, $\beta=93.088$. The probable space group is $P2_1$ (No:4). The refined pattern from this calculated data shown in Figure 4.31. And the refined list is shown in Table 4.14.

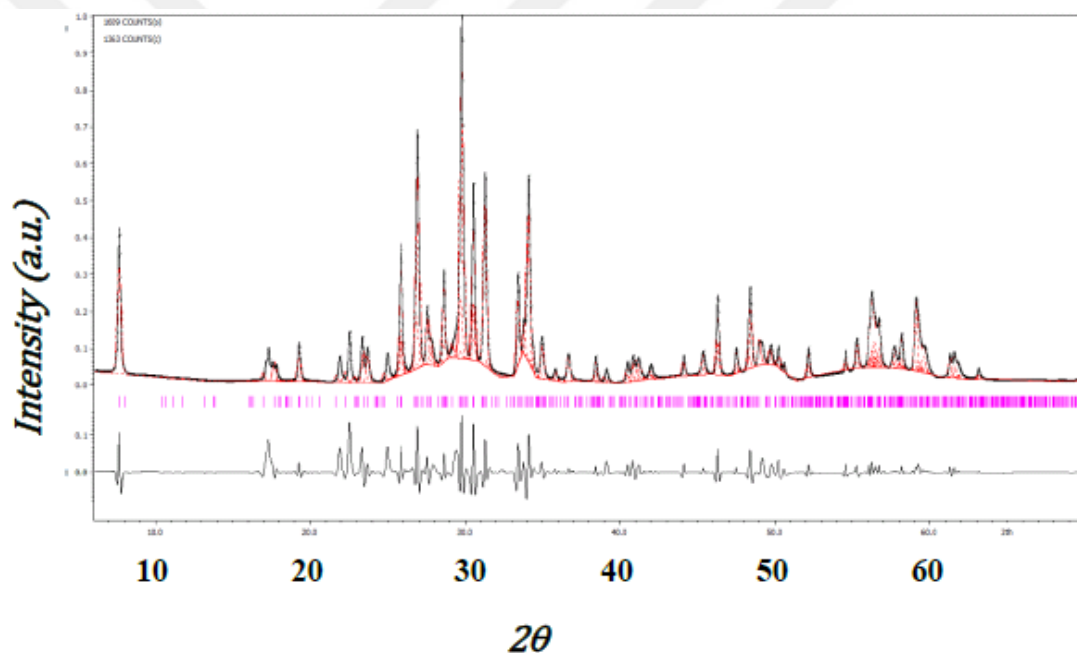


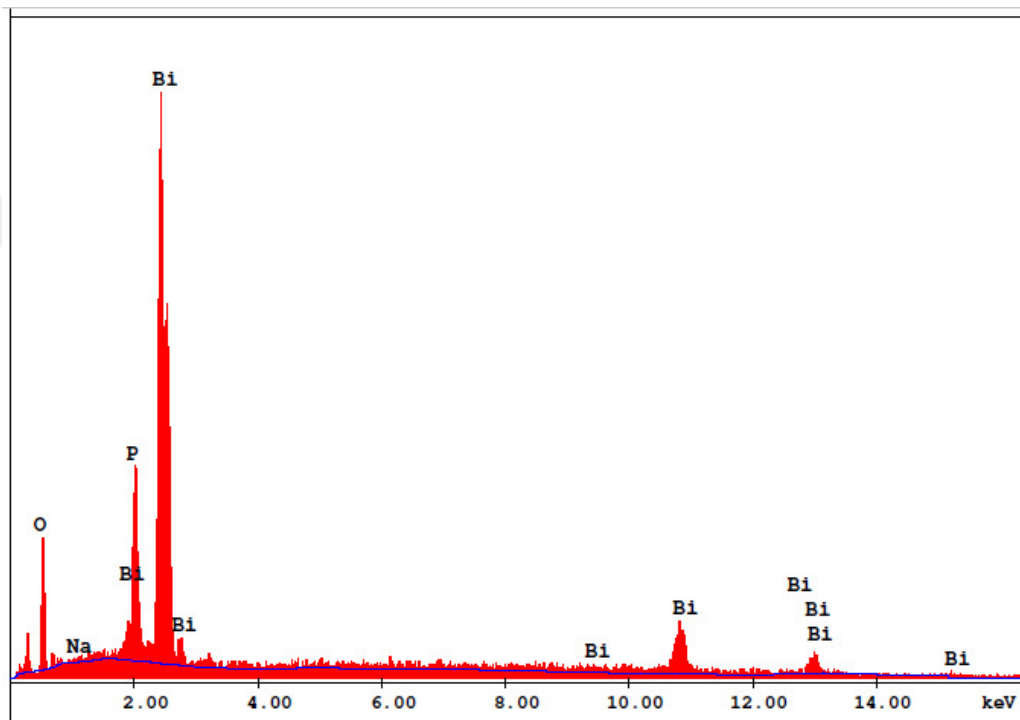
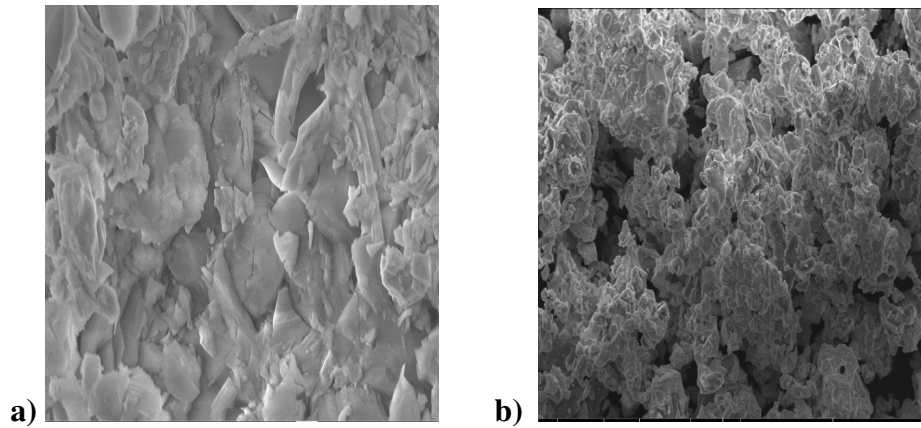
Figure 4.31. Jana2006 refinement pattern for $\text{Bi}_2\text{O}_{3(s)} + \text{Li}_4\text{P}_2\text{O}_{7(s)}$.

Table 4.14. Refinement and structural parameters of product recorded from Jana2006.

| Reaction Sample | 5. $\text{Bi}_2\text{O}_{3(s)} + \text{Li}_4\text{P}_2\text{O}_{7(s)}$ |
|--|--|
| Sample | Powder Crystal |
| Symmetry | Monoclinic |
| Space Group | $P2_1$ |
| $a(\text{\AA})$ | 10.7380 |
| $b(\text{\AA})$ | 12.2486 |
| $c(\text{\AA})$ | 10.4148 |
| α° degree | 90.000 |
| β° degree | 93.088 |
| δ° degree | 90.000 |
| Diffractometer | Rigaku |
| Radiation Type | Cu $K\alpha$ |
| Monochromator | Graphite |
| Wavelength (\AA) | 1.5405 |
| Refined profile range ($^\circ 2\theta$) | 6.00-70.00 |
| GOF | 1.87 |
| R_p | 12.54 |
| R_{wp} | 19.35 |
| V | 1367.8 |

4.5.3. Scanning Electron Microscopy (SEM) and (EDX) Study

The morphology and the structural features of $\text{Li}_2\text{BiOPO}_4$ were investigated using SEM-EDX as given in Figure 4.32. SEM images of this monoclinic compound showed that the compound uniformity exists between the specimens of the sample. Micrographs showed flat and disc shape with a layered structure and spread homogeneously, also the morphologies seem to be fibular. EDX Spectrum (see Figure 4.32.c)), showed the presence of Na, Bi, O, and P. But Li could not see on EDX. The reason maybe the atomic weight of Lithium is very low, hence the characteristic peak of Li is very weak. It can be detected with designed low energy resolution detectors.



EDAX ZAF Quantification (Standardless)
 Element Normalized
 SEC Table : Default

| Element | Wt % | At % | K-Ratio | Z | A | F |
|---------|--------|--------|---------|--------|--------|--------|
| O K | 14.75 | 58.39 | 0.0319 | 1.2533 | 0.1722 | 1.0000 |
| NaK | 0.25 | 0.68 | 0.0007 | 1.1702 | 0.2520 | 1.0004 |
| P K | 8.72 | 17.82 | 0.0688 | 1.2019 | 0.6568 | 1.0000 |
| BiM | 76.28 | 23.11 | 0.6787 | 0.8724 | 1.0199 | 1.0000 |
| Total | 100.00 | 100.00 | | | | |

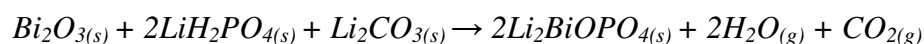
| Element | Net Inte. | Bkgd Inte. | Inte. Error | P/B |
|---------|-----------|------------|-------------|-------|
| O K | 51.91 | 4.33 | 3.49 | 11.98 |
| NaK | 1.57 | 9.86 | 68.36 | 0.16 |
| P K | 124.80 | 14.14 | 2.31 | 8.83 |
| BiM | 357.55 | 11.97 | 1.27 | 29.86 |

c)

Figure 4.32. SEM images of $\text{Bi}_2\text{O}_3(\text{s}) + \text{Li}_4\text{P}_2\text{O}_7(\text{s})$ reaction at 800°C (20h) a) 5 μm b) 10 μm c) EDX Spectrum.

4.6. Solid-State Reaction of $\text{Bi}_2\text{O}_3(\text{s}) + 2\text{LiH}_2\text{PO}_4(\text{s}) + \text{Li}_2\text{CO}_3(\text{s})$

Also in this work, $\text{Li}_2\text{BiOPO}_4$ was synthesized with another solid-state reaction by mixing of the 1 mole Bi_2O_3 , 2 moles of LiH_2PO_4 and 1 mole of Li_2CO_3 precursors stoichiometrically. Reaction heated at $350^\circ\text{C}(6\text{h})$, $500^\circ\text{C}(6\text{h})$, $600^\circ\text{C}(6\text{h})$, $700^\circ\text{C}(6\text{h})$, $800^\circ\text{C}(24\text{h})$ and $850^\circ\text{C}(6\text{h})$ in a porcelain crucible. And the expected reaction was:



Characterization of the new reaction compound was performed by FTIR and XRD instruments. In the IR Spectra of the reaction at $850^\circ\text{C}(6\text{h})$, the oxyphosphate peaks were seen at 1152, 1014, 971 and 947 cm^{-1} (see Figure A.6). The broadband between 1158 and 977 cm^{-1} is resolved into four peaks associated with ν_3 fundamental of the PO_4 . These frequencies observed at 1152, 1014, 971 and 947 cm^{-1} . The ν_1 vibration is seen at 947 and 904 cm^{-1} . The rest of the peaks in the region between 588 and 455 cm^{-1} are bound to the splitting of degenerate ν_4 and ν_2 PO_4 modes which are observed at 588, 510, 455 and 419 cm^{-1} .

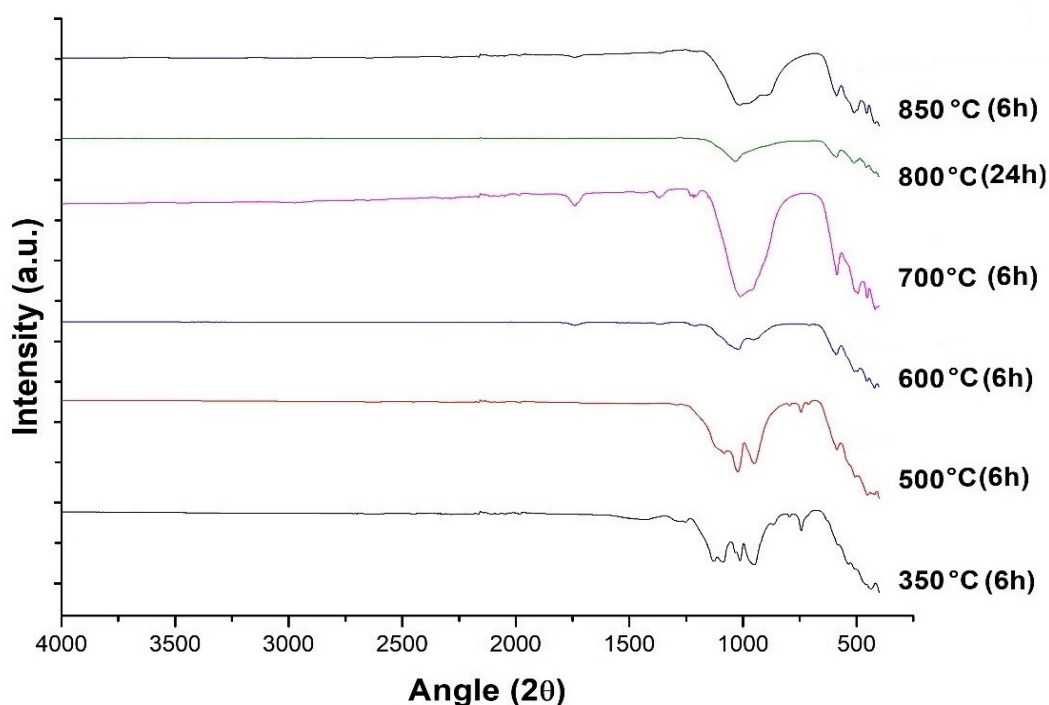


Figure 4.33. IR Spectra of the product of $\text{Bi}_2\text{O}_3(\text{s}) + 2\text{LiH}_2\text{PO}_4(\text{s}) + \text{Li}_2\text{CO}_3(\text{s})$ at $350^\circ\text{C}(6\text{h})$, $500^\circ\text{C}(6\text{h})$, $800^\circ\text{C}(24\text{h})$, $850^\circ\text{C}(6\text{h})$.

The product obtained from $\text{Bi}_2\text{O}_{3(s)} + 2\text{LiH}_2\text{PO}_{4(s)} + \text{Li}_2\text{CO}_{3(s)}$, also examined the XRD Pattern with Match! Software and the indexed results showed that the occurred compound was similar to the reaction of $\text{Bi}_2\text{O}_{3(s)} + \text{Li}_4\text{P}_2\text{O}_{7(s)}$ which was detailed on section 4.5. But more undefined phases were seen in this $\text{Bi}_2\text{O}_{3(s)} + 2\text{LiH}_2\text{PO}_{4(s)} + \text{Li}_2\text{CO}_{3(s)}$. The results were compared based on Muktha work (Muktha, Darriet, and Guru Row, 2008).

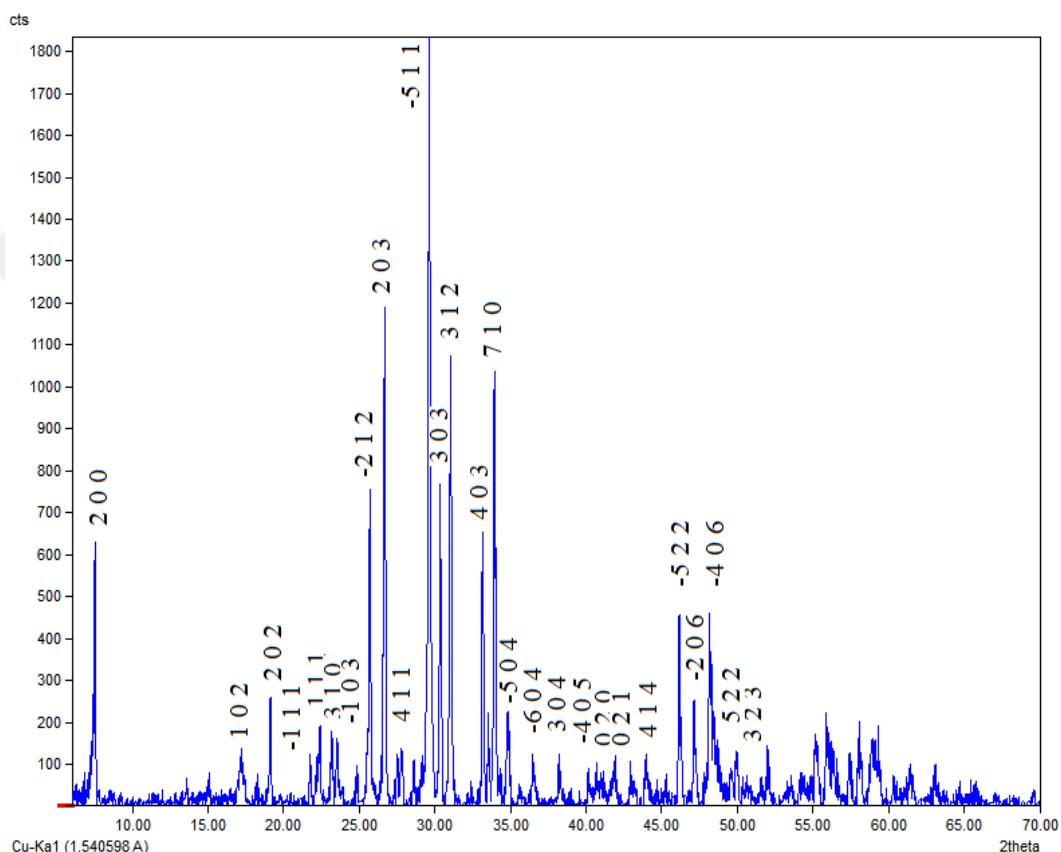


Figure 4.34. X-Ray Powder Diffraction Pattern of $\text{Bi}_2\text{O}_{3(s)} + 2\text{LiH}_2\text{PO}_{4(s)} + \text{Li}_2\text{CO}_{3(s)}$ at 850°C (6h).

According to refinement results which examined on Jana Software, the crystal symmetry of this compound from $\text{Bi}_2\text{O}_{3(s)} + 2\text{LiH}_2\text{PO}_{4(s)} + \text{Li}_2\text{CO}_{3(s)}$ reaction was found to be monoclinic structure. The unit cell parameters; $a = 24.0345$, $b = 4.3912$, $c = 11.3362$, $\beta = 101.802$. The unit cell parameters and the symmetry have been found based on the indexing process by Match! Software. And the agreement factors converged to $GOF = 2.15$, $R_p = 13.14$, $R_{wp} = 32.69$. $V = 1171$. And possible space group was determined as $P2_1$ Number: 4.

The Graph of fixed data was shown with the following refinement data from Jana Software.

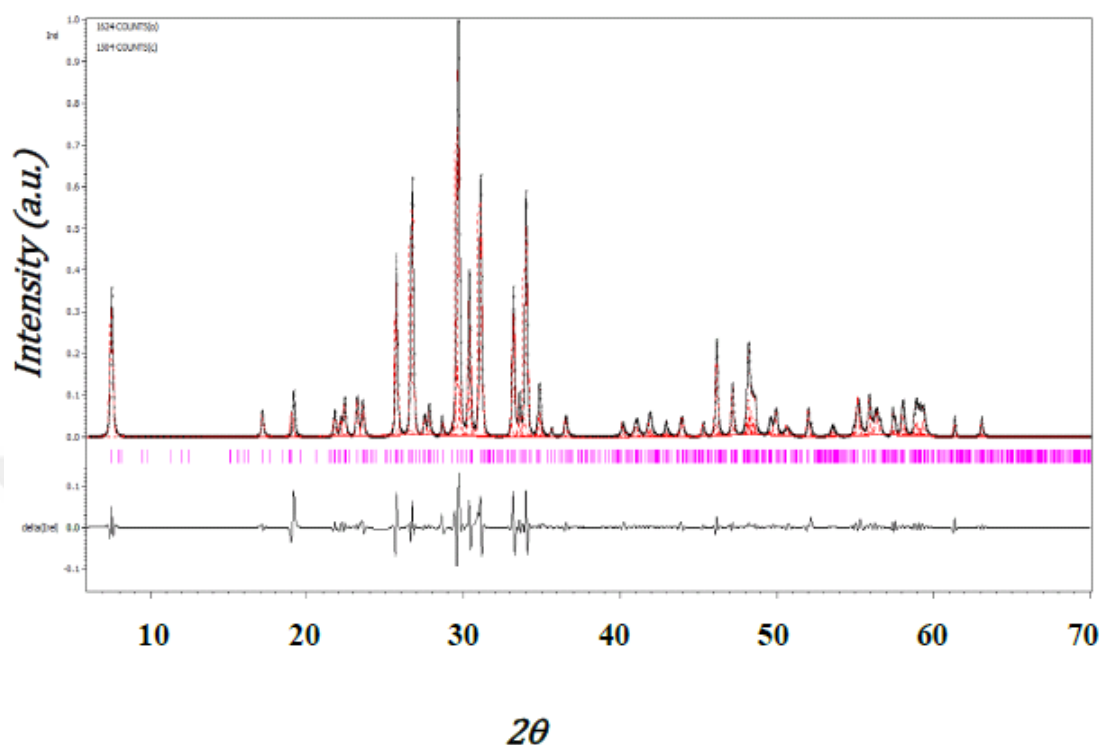


Figure 4.35. Jana2006 refinement pattern for $\text{Bi}_2\text{O}_3(\text{s}) + 2\text{LiH}_2\text{PO}_4(\text{s}) + \text{Li}_2\text{CO}_3(\text{s})$.

And according to refinement calculation results, the compound which we synthesized was matched with the refinement results of $\text{LiBi}_{7.37}\text{O}_7(\text{PO}_4)_3$ compound **COD: 96-201-6221** (Arumugam, Lynch, and Steinfink, 2007) in 57.5% ratio. The rest 42.5% ratio is marked as undefined which means and represents unwanted phases (see Table 4.15.).

Table 4.15. X-Ray Powder Data for Monoclinic compound by the solid-state reaction of $\text{Bi}_2\text{O}_{3(s)} + 2\text{LiH}_2\text{PO}_{4(s)} + \text{Li}_2\text{CO}_{3(s)}$ at 850°C (6h) from Rietveld Calculation.

| I/I_o | hkl | $2\theta(^{\circ})_{obs}$ | $2\theta(^{\circ})_{calc}$ | d_{obs} | d_{cal} | Matched Reference |
|---------|--------|---------------------------|----------------------------|-----------|-----------|---|
| 37 | 2 0 0 | 7.70 | 7.53 | 11.715 | 11.733 | $\text{LiBi}_{7.37}\text{O}_7(\text{PO}_4)_3$ |
| 8 | 1 0 2 | 15.24 | 17.15 | 5.145 | 5.166 | $\text{LiBi}_{7.37}\text{O}_7(\text{PO}_4)_3$ |
| 5 | 2 0 2 | 17.34 | 19.14 | 4.638 | 4.633 | $\text{LiBi}_{7.37}\text{O}_7(\text{PO}_4)_3$ |
| 15 | -1 1 1 | 19.26 | 21.77 | 4.080 | 4.078 | $\text{LiBi}_{7.37}\text{O}_7(\text{PO}_4)_3$ |
| 8 | -5 0 2 | 21.94 | 22.17 | 4.047 | 4.006 | $\text{LiBi}_{7.37}\text{O}_7(\text{PO}_4)_3$ |
| 11 | 1 1 1 | 22.54 | 22.39 | 3.965 | 3.967 | $\text{LiBi}_{7.37}\text{O}_7(\text{PO}_4)_3$ |
| 11 | 3 1 0 | 23.34 | 23.21 | 3.834 | 3.829 | $\text{LiBi}_{7.37}\text{O}_7(\text{PO}_4)_3$ |
| 9 | -1 0 3 | 23.68 | 23.55 | 3.773 | 3.775 | $\text{LiBi}_{7.37}\text{O}_7(\text{PO}_4)_3$ |
| 7 | -4 0 3 | 24.96 | 25.71 | 3.578 | 3.462 | $\text{LiBi}_{7.37}\text{O}_7(\text{PO}_4)_3$ |
| 42 | -2 1 2 | 25.86 | 25.98 | 3.460 | 3.426 | $\text{LiBi}_{7.37}\text{O}_7(\text{PO}_4)_3$ |
| 65 | 2 0 3 | 26.84 | 26.7 | 3.338 | 3.336 | $\text{LiBi}_{7.37}\text{O}_7(\text{PO}_4)_3$ |
| 9 | 4 1 1 | 28.00 | 27.51 | 3.213 | 3.239 | $\text{LiBi}_{7.37}\text{O}_7(\text{PO}_4)_3$ |
| 100 | -5 1 1 | 29.78 | 27.8 | 3.015 | 3.207 | $\text{LiBi}_{7.37}\text{O}_7(\text{PO}_4)_3$ |
| 43 | 3 0 3 | 30.52 | 28.62 | 2.941 | 3.116 | $\text{LiBi}_{7.37}\text{O}_7(\text{PO}_4)_3$ |
| 60 | 3 1 2 | 31.20 | 29.64 | 2.876 | 3.011 | $\text{LiBi}_{7.37}\text{O}_7(\text{PO}_4)_3$ |
| 5 | 8 0 0 | 32.54 | 30.37 | 2.761 | 2.940 | $\text{LiBi}_{7.37}\text{O}_7(\text{PO}_4)_3$ |
| 37 | 4 0 3 | 33.32 | 31.06 | 2.699 | 2.876 | $\text{LiBi}_{7.37}\text{O}_7(\text{PO}_4)_3$ |
| 14 | -7 1 1 | 33.68 | 33.19 | 2.671 | 2.697 | $\text{LiBi}_{7.37}\text{O}_7(\text{PO}_4)_3$ |
| 57 | 7 1 0 | 34.10 | 33.56 | 2.637 | 2.668 | $\text{LiBi}_{7.37}\text{O}_7(\text{PO}_4)_3$ |
| 13 | -5 0 4 | 34.98 | 33.97 | 2.570 | 2.637 | $\text{LiBi}_{7.37}\text{O}_7(\text{PO}_4)_3$ |
| 4 | -8 0 3 | 35.80 | 34.85 | 2.522 | 2.572 | $\text{LiBi}_{7.37}\text{O}_7(\text{PO}_4)_3$ |
| 7 | -6 0 4 | 36.66 | 35.59 | 2.461 | 2.520 | $\text{LiBi}_{7.37}\text{O}_7(\text{PO}_4)_3$ |
| 8 | 3 0 4 | 38.36 | 36.52 | 2.344 | 2.458 | $\text{LiBi}_{7.37}\text{O}_7(\text{PO}_4)_3$ |
| 6 | -4 0 5 | 40.32 | 40.16 | 2.242 | 2.243 | $\text{LiBi}_{7.37}\text{O}_7(\text{PO}_4)_3$ |
| 7 | 0 2 0 | 40.82 | 41.02 | 2.215 | 2.198 | $\text{LiBi}_{7.37}\text{O}_7(\text{PO}_4)_3$ |
| 8 | 0 2 1 | 41.14 | 41.9 | 2.152 | 2.154 | $\text{LiBi}_{7.37}\text{O}_7(\text{PO}_4)_3$ |
| 8 | 2 2 1 | 42.00 | 42.93 | 2.105 | 2.105 | $\text{LiBi}_{7.37}\text{O}_7(\text{PO}_4)_3$ |
| 9 | 4 1 4 | 43.08 | 43.91 | 2.057 | 2.060 | $\text{LiBi}_{7.37}\text{O}_7(\text{PO}_4)_3$ |
| 5 | 4 2 1 | 44.10 | 45.29 | 2.001 | 2.000 | $\text{LiBi}_{7.37}\text{O}_7(\text{PO}_4)_3$ |
| 7 | 9 1 2 | 45.44 | 46.17 | 1.990 | 1.964 | $\text{LiBi}_{7.37}\text{O}_7(\text{PO}_4)_3$ |
| 26 | -5 2 2 | 46.30 | 47.17 | 1.964 | 1.925 | $\text{LiBi}_{7.37}\text{O}_7(\text{PO}_4)_3$ |
| 15 | -2 0 6 | 47.30 | 48.18 | 1.928 | 1.887 | $\text{LiBi}_{7.37}\text{O}_7(\text{PO}_4)_3$ |
| 26 | -4 0 6 | 48.30 | 48.45 | 1.887 | 1.877 | $\text{LiBi}_{7.37}\text{O}_7(\text{PO}_4)_3$ |
| 8 | -1 0 6 | 49.30 | 48.54 | 1.832 | 1.871 | $\text{LiBi}_{7.37}\text{O}_7(\text{PO}_4)_3$ |
| 10 | 7 2 0 | 49.70 | 49.54 | 1.820 | 1.837 | $\text{LiBi}_{7.37}\text{O}_7(\text{PO}_4)_3$ |
| 11 | 5 2 2 | 50.06 | 49.93 | 1.821 | 1.825 | $\text{LiBi}_{7.37}\text{O}_7(\text{PO}_4)_3$ |
| 4 | 3 2 3 | 50.94 | 50.86 | 1.805 | 1.800 | $\text{LiBi}_{7.37}\text{O}_7(\text{PO}_4)_3$ |
| 4 | — | 51.00 | 52.01 | 1.791 | 1.756 | Undefined |
| 11 | — | 52.14 | 52.19 | 1.752 | 1.751 | Undefined |
| 5 | — | 53.72 | 53.57 | 1.704 | 1.709 | Undefined |
| 8 | — | 54.48 | 54.9 | 1.682 | 1.671 | Undefined |
| 15 | — | 55.28 | 55.19 | 1.660 | 1.663 | Undefined |
| 17 | — | 56.06 | 56.36 | 1.639 | 1.631 | Undefined |
| 13 | — | 56.52 | 56.61 | 1.626 | 1.624 | Undefined |
| 12 | — | 56.72 | 57.41 | 1.621 | 1.603 | Undefined |
| 13 | — | 57.56 | 57.56 | 1.587 | 1.599 | Undefined |
| 12 | — | 58.22 | 58.05 | 1.583 | 1.587 | Undefined |
| 17 | — | 59.04 | 58.93 | 1.563 | 1.566 | Undefined |
| 12 | — | 59.80 | 59.13 | 1.556 | 1.561 | Undefined |
| 8 | — | 59.50 | 59.34 | 1.533 | 1.556 | Undefined |
| 9 | — | 61.60 | 61.35 | 1.507 | 1.509 | Undefined |
| 7 | — | 63.20 | 63.08 | 1.471 | 1.472 | Undefined |

In this work, the following solid-state reactions (1 and 2) was proposed to synthesize the compound of $\text{Li}_2\text{BiOPO}_4$.

- $\text{Bi}_2\text{O}_{3(s)} + 2\text{Li}_2\text{CO}_{3(s)} + 2\text{NH}_4\text{H}_2\text{PO}_{4(s)} \rightarrow 2\text{Li}_2\text{BiOPO}_4 + 2\text{CO}_{2(g)} + 3\text{H}_2\text{O}_{(g)} + 2\text{NH}_3(g)$
- $\text{Bi}_2\text{O}_{3(s)} + 2\text{Li}_2\text{CO}_{3(s)} + 2(\text{NH}_4)_2\text{HPO}_{4(s)} \rightarrow 2\text{Li}_2\text{BiOPO}_4 + 2\text{CO}_{2(g)} + 3\text{H}_2\text{O}_{(g)} + \text{NH}_3(g)$

Reactions were heated respectively at 350°C (6h), 500°C (6h), 600°C (6h), 700°C (6h). Then for the first reaction, four times heated at 800°C (24h), and two times at 850°C (12h). For the second reaction, three times heated at 800°C (30h) and once heated at 850°C (6h). The reactions mixtures were changed color from a cream color to yellow.

According to the examination of XRD Pattern Data, hence the phase diffractions have occurred, $\text{Li}_2\text{BiOPO}_4$ was not been observed properly. It was decided that $\text{Li}_2\text{BiOPO}_4$ compounds can be obtained as a mixed phase (BiPO_4 , Li_3PO_4 , LiBiO_2) materials by these two solid-state reactions.

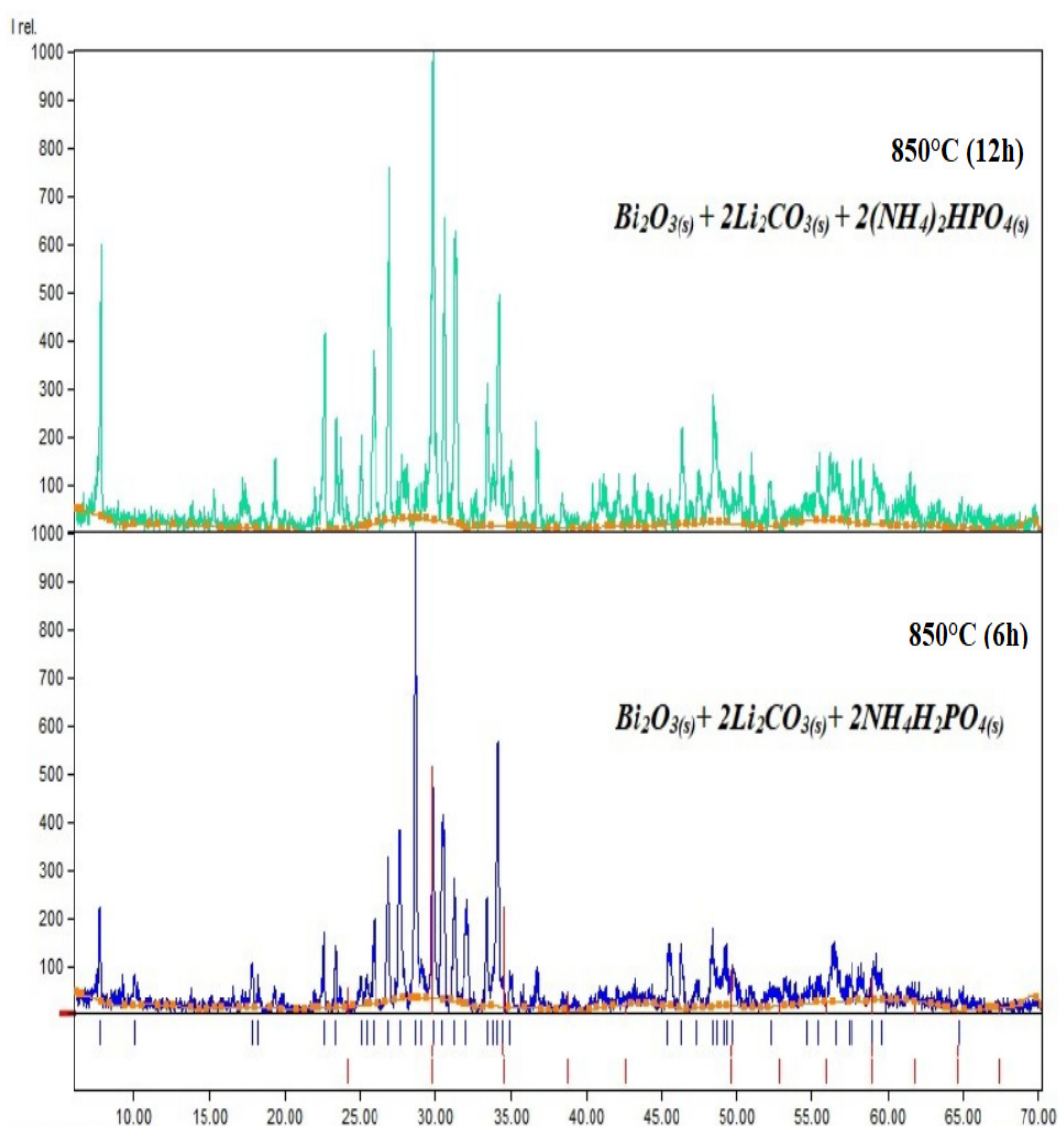


Figure 4.36. X-Ray Powder Diffraction Pattern of $\text{Bi}_2\text{O}_{3(s)} + 2\text{Li}_2\text{CO}_{3(s)} + 2(\text{NH}_4)_2\text{HPO}_{4(s)}$ at 850°C (12h) shown on the top of figure and $\text{Bi}_2\text{O}_{3(s)} + 2\text{Li}_2\text{CO}_{3(s)} + 2\text{NH}_4\text{H}_2\text{PO}_{4(s)}$ at 850°C (6h) shown on the below of figure.

5. CONCLUSIONS

The main purpose of this work was to synthesize and characterization of new alkali-bismuth oxyphosphates that formulated as $\text{Na}_2\text{BiOPO}_4$ and $\text{Li}_2\text{BiOPO}_4$. The novel type of orthorhombic $\text{Na}_2\text{BiOPO}_4$ compound was synthesized for the first time according to performed with different solid-state reactions.

Characterization process was done by Infrared Spectroscopy, X-Ray powder diffraction (radiation in the 2Θ range, $6-70^\circ$) and Scanning Electron Microscopy studies. The results of characterization processes showed that the compounds of $\text{Na}_2\text{BiOPO}_4$ and $\text{Li}_2\text{BiOPO}_4$ could be synthesized at 800°C .

All the unit cell parameters were calculated based on the currently marked peaks from Match! Software. And with making quantitative analyzes, ICDD and COD were taken as a reference. In this way, phase identifications for each heating were done. And then, with detected cell parameters from the powder crystal data of products, fitting refinement graphs of product profiles were drawn on Jana Software.

The all-solid-state reactions which studied in this work written in the followed list with their refined unit cell parameters and appropriate space groups.

1. The $\text{Na}_2\text{BiOPO}_4$ orthorhombic compound from the reaction of $\text{Bi}_2\text{O}_{3(s)} + \text{Na}_4\text{P}_2\text{O}_{7(s)}$ at $800^\circ\text{C}(12\text{h})$. The unit cell parameters are $a=15.4658$, $b=10.8601$, $c=12.6592$ Å and the space group determined as Pmm_2 .
2. The $\text{Na}_2\text{BiOPO}_4$ orthorhombic compound from the reaction of $\text{Bi}_2\text{O}_{3(s)} + 2\text{Na}_2\text{HPO}_{4(s)}$ at $800^\circ\text{C}(12\text{h})$. The unit cell parameters are $a=15.932$, $b=10.913$, $c=13.128$ Å and the space group determined as Pmm_2 .
3. The $\text{Na}_2\text{BiOPO}_4$ orthorhombic compound from the reaction of $\text{Bi}_2\text{O}_{3(s)} + 2\text{NH}_4\text{H}_2\text{PO}_{4(s)} + 2\text{Na}_2\text{CO}_{3(s)}$ at $800^\circ\text{C}(12\text{h})$. The unit cell parameters

are $a=15.3244$, $b=10.7467$, $c=13.0113$ and the space group determined as *Pnma*.

4. The $\text{Li}_4\text{P}_2\text{O}_7$ triclinic compound from the reaction of $2\text{Li}_2\text{CO}_{3(s)}+2\text{NH}_4\text{H}_2\text{PO}_{4(s)}$ at $750^\circ\text{C}(8\text{h})$ (Zaafouri, Megdiche, and Gargouri 2015). The unit cell parameters are $a=7.099$, $b=5.179$, $c=8.549\text{\AA}$, $\alpha=89.841$, $\beta=103.180$, $\gamma=111.342^\circ$ and the space group determined as P_{-1} .
5. The $\text{Li}_2\text{BiOPO}_4$ monoclinic compound from the reaction of $\text{Bi}_2\text{O}_{3(s)}+\text{Li}_4\text{P}_2\text{O}_{7(s)}$ at $800^\circ\text{C}(20\text{h})$. The unit cell parameters are $a=10.7380$, $b = 12.2486$, $c = 10.4148 \text{\AA}$, $\beta = 93.088$ and the space group determined as $P2_1$.
6. The $\text{Li}_2\text{BiOPO}_4$ monoclinic compound from the reaction of $\text{Bi}_2\text{O}_{3(s)} + 2\text{LiH}_2\text{PO}_{4(s)} + \text{Li}_2\text{CO}_{3(s)}$ at $850^\circ\text{C}(6\text{h})$. The unit cell parameters are $a=24.0345$, $b=4.3912$, $c=11.3362$, $\beta=101.802$ and the space group determined as $P2_1$.

Indexing of these unit cell parameters showed that these oxyphosphates (5. and 6.) were isomorphous with the monoclinic $\text{LiBi}_{7.37}\text{O}_7(\text{PO}_4)_3$ which is reported previously (Muktha, Darriet, and Guru Row 2008). It is proved and supported with the Rietveld process when the matched peaks were detected by indexing calculation.

Also, $\text{Li}_2\text{BiOPO}_4$ compounds were suggested to synthesize by the solid-state reactions of $\text{Bi}_2\text{O}_{3(s)} + 2\text{Li}_2\text{CO}_{3(s)} + 2\text{NH}_4\text{H}_2\text{PO}_{4(s)}$ and $\text{Bi}_2\text{O}_{3(s)} + 2\text{Li}_2\text{CO}_{3(s)} + 2(\text{NH}_4)_2\text{HPO}_{4(s)}$ with the same procedures. But hence the phase diffractions occurred, $\text{Li}_2\text{BiOPO}_4$ was not been observed properly by these reactions. It was decided that $\text{Li}_2\text{BiOPO}_4$ compounds can be obtained as a mixed phase (BiPO_4 , Li_3PO_4 , LiBiO_2) materials.

6. REFERENCES

- © Emsley John. 2011. "Phosphorus - Element Information, Properties, and Uses | Periodic Table." <http://www.rsc.org/periodic-table/element/15/phosphorus> (January 22, 2019).
- Abraham, F., O. Cousin, O. Mentre, and E. M. Ketatni. 2002. "Crystal Structure Approach of the Disordered New Compounds $\text{Bi}_{1.2}\text{M}_{1.2}\text{PO}_5.5$ (M=Mn, Co, Zn): The Role of Oxygen-Centered Tetrahedra Linkage in the Structure of Bismuth-Transition Metal Oxy-Phosphates." *Journal of Solid State Chemistry* 167(1): 168–81.
- Aksenov, Sergey M., et al. 2018. " $\text{Bi}_3(\text{PO}_4)_3\text{O}_3$, the Simplest Bismuth(III) Oxophosphate: Synthesis, IR Spectroscopy, Crystal Structure, and Structural Complexity." *Inorganic Chemistry* 57(12): 6799–6802.
- Arumugam, Nachiappan, Vincent Lynch, and Hugo Steinfink. 2007. "A New Pillared Lithium Bismuth Phosphate, $\text{LiBi}_7.37\text{P}_3\text{O}_{19}$, with Elliptical Channels." 1: 86–88.
- Averbuch-Pouchot, Marie-Thérèse M-T, and A Durif. 1996. "Topics in Phosphate Chemistry." *World Scientific*: 404. <https://leseprobe.buch.de/images-adb/97/51/975117ae-f9fd-4896-a9f3-6f57f78e3b83.pdf%0Ahttp://www.amazon.com/Topics-Phosphate-Chemistry-M-Averbuch-Pouchot/dp/9810226349>.
- Belharouak, Ilias, and Khalil Amine. 2005. "New Active Titanium Oxyphosphate Material for Lithium Batteries." *Electrochemistry Communications* 7(7): 648–51.
- Bierlein, John D., and Herman Vanherzeele. 1989. "Potassium Titanyl Phosphate: Properties and New Applications." *Journal of the Optical Society of America B* 6(4): 622. <https://www.osapublishing.org/abstract.cfm?URI=josab-6-4-622>.
- Birkner, Nancy. 2011. "How an FTIR Spectrometer Operates." *UC Davis ChemWiki*: 1–9. http://chemwiki.ucdavis.edu/Physical_Chemistry/Spectroscopy/Vibrational_Spectroscopy/How_an_FTIR_Spectrometer_Operates.
- "Bismuth: Applications and Uses-Metalpedia." *ASIAN METAL*. <http://metalpedia.asianmetal.com/metal/bismuth/application.shtml> (February 3, 2019).
- "Bismuth: Not Just for Heartburn | Seeking Alpha." <https://seekingalpha.com/article/123793-bismuth-not-just-for-heartburn?page=7> (January 31, 2019).

- Bolt, R. J., M. van der Mooren, and M. T. Sebastian. 1991. "Etching Experiments on Flux Grown Potassium Titanyl Phosphate KTiOPO_4 (KTP)." *Journal of Crystal Growth* 112(4): 773–80.
- Byrappa, K. 1986. "Preparative Methods and Growth of Rare Earth Phosphates." *Progress In Crystal Growth And Characterization* 13(3): 163–96.
- DeCoste Zumdahl. 2013. *General Chemistry 152*. [https://dynamic.libretexts.org/print/url=https://chem.libretexts.org/Bookshelves/General_Chemistry/Map%3A_Chemistry_\(Zumdahl_and_Decoste\)/18%3A_The_Representative_Elements/18.07%3A_The_Group_5A_Elements.pdf](https://dynamic.libretexts.org/print/url=https://chem.libretexts.org/Bookshelves/General_Chemistry/Map%3A_Chemistry_(Zumdahl_and_Decoste)/18%3A_The_Representative_Elements/18.07%3A_The_Group_5A_Elements.pdf) (January 22, 2019).
- Deriouche, W. et al. 2017. "A Vanadium Oxy-Phosphate $\text{Na}_4\text{VO}(\text{PO}_4)_2$ as Cathode Material for Na Ion Batteries." *Solid State Sciences* 72: 124–29. <https://doi.org/10.1016/j.solidstatesciences.2017.08.017>.
- Epp, J. 2016. Materials Characterization Using Nondestructive Evaluation (NDE) Methods *X-Ray Diffraction (XRD) Techniques for Materials Characterization*. Elsevier Ltd. <http://dx.doi.org/10.1016/B978-0-08-100040-3.00004-3>.
- Erhan, Sevim Z. 1946. "Industrial Uses Of." *Agriculture* 1: 1946.
- Essehli, Rachid et al. 2009. " $\text{Co}_0.5\text{TiOPO}_4$: Crystal Structure, Magnetic and Electrochemical Properties." *Materials Research Bulletin* 44(4): 817–21.
- Gautier, Romain et al. 2011. " $\text{VOPO}_4 \cdot \text{H}_2\text{O}$: A Stacking Faults Structure Studied by X-Ray Powder Diffraction and DFT-D Calculations." *Inorganic Chemistry* 50(10): 4378–83.
- Gonen, Z S, and M Kizilyalli. *Journal of Alloys and Compounds*, 2000. "Synthesis and Characterization of $\text{Na}_2\text{GdOPO}_4$ and $\text{Na}_2\text{LaOPO}_4$." vol 304: 416–20.
- Haynes, William Mickey. *CRC Handbook of Chemistry and Physics*. 92nd ed. CRC Press, 2011. [https://books.google.com.tr/books?id=pYPRBQAAQBAJ&pg=SA4-PA6&lpg=SA4-PA6&dq=1753+by+Claude+Geoffroy+the+Younger.+Bismuth+does+occur+free+in+nature+and+in+such+minerals+as+bismuthinite+\(Bi2S3\)+and+bismite+\(Bi2O3\).&source=bl&ots=LTeng5CS0r&sig=ACfU3U3bvYNEo](https://books.google.com.tr/books?id=pYPRBQAAQBAJ&pg=SA4-PA6&lpg=SA4-PA6&dq=1753+by+Claude+Geoffroy+the+Younger.+Bismuth+does+occur+free+in+nature+and+in+such+minerals+as+bismuthinite+(Bi2S3)+and+bismite+(Bi2O3).&source=bl&ots=LTeng5CS0r&sig=ACfU3U3bvYNEo) (January 22, 2019).
- House, James E., and Kathleen A. House. 2016. "Phosphorus, Arsenic, Antimony, and Bismuth." *Descriptive Inorganic Chemistry*: 215–34. <https://linkinghub.elsevier.com/retrieve/pii/B9780128046975000142>.
- Iwashita, Norio. 2016. "X-Ray Powder Diffraction." *Materials Science and Engineering of Carbon*: 7–25. <https://linkinghub.elsevier.com/retrieve/pii/B9780128052563000027>.
- Jeanmonod, Donald Jeanmonod, Rebecca, and Keisuke; et al. Suzuki. 2018. "We Are IntechOpen , the World's Leading Publisher of Open Access Books Built by Scientists, for Scientists TOP 1% Control of a Proportional Hydraulic System." *Intech open* 2: 64.

- Ketatni, El Mostafa, Marielle Huvé, Francis Abraham, and Olivier Mentré. 2003. "Characterization of the New Bi₆2Cu₆2O₈(PO₄)₅oxyphosphate; a Disordered Compound Containing 2- and 3-O(Bi, Cu)₄tetrahedra - Wide Polycationic Ribbons." *Journal of Solid State Chemistry* 172(2): 327–38.
- Ketatni, M., F. Abraham, and O. Mentré. 1999. "Channel Structure in the New BiCoPO₅. Comparison with BiNiPO₅. Crystal Structure, Lone Pair Localisation and Infrared Characterisation." *Solid State Sciences* 1(6): 449–60. <http://linkinghub.elsevier.com/retrieve/pii/S1293255800800977> (February 5, 2019).
- Ketatni, Mustafa et al. 1998. "Synthesis and Crystal Structure of Bi₆.67(PO₄)₄O₄ Oxyphosphate: The Bi₆M₂₊(PO₄)₄O₄ and Bi₆.5A+0.5(PO₄)₄O₄ Series." *Journal of Solid State Chemistry* (139): 274–80.
- McMurry, John., Robert C. Fay, and Logan. McCarty. 2004. *Chemistry*. Pearson Education.
- Mentré, O. et al. 2008. "Magnetic Structure and Analysis of the Exchange Interactions in BiMO(PO₄)(M = Co, Ni)." *Journal of Physics Condensed Matter* 20(41).
- Mizrahi, Ariane, Jean-pierre Wignacourt, and Hugo Steinfink. 1997. "Pb₂BiO₂PO₄, a New Oxyphosphate." 521(133): 516–21.
- Muktha, B., J. Darriet, and T. N. Guru Row. 2008. "Synthesis and Crystal Structure of a Novel Lithium Bismuth Phosphate, LiBi_{7.37}O₇(PO₄)₃." *Materials Research Bulletin* 43(11): 3017–25.
- Naito, Makio, Nobuhiro Shinohara, and Keizo Uematsu. 2003. "Raw Materials." *Handbook of Advanced Ceramics: Materials, Applications, Processing and Properties* 1–2: 81–129.
- Ouyang, Ruizhuo et al. 2016. "Potential Anti-Cancer Activity of a Novel Bi(III) Containing Thiosemicarbazone Derivative." *Inorganic Chemistry Communications* 73: 138–41. <http://dx.doi.org/10.1016/j.inoche.2016.10.020>.
- "Paints & Coatings." <https://phosphatesfacts.org/wp-content/uploads/2015/09/PaintsandCoatings.pdf> (January 28, 2019).
- Phosphates, What A R E. 2019. "(<https://Phosphatesfacts.Org>)." : 1–3.
- Pokapū Akoranga Pūtaiao. 2013. "The Phosphorus Cycle — Science Learning Hub." <https://www.sciencelearn.org.nz/resources/961-the-phosphorus-cycle> (January 22, 2019).
- Putz, Dr. H. and Dr. K. "Match! - Phase Identification from Powder Diffraction." <https://www.crystalimpact.de/match>.

- Selander, Richard B. 1991. "On the Nomenclature and Classification of the Meloidae (Coleoptera)." *InsectaMundi* 5(2): 65–94. <http://journals.fcla.edu/mundi/article/view/24672%5Cnhttp://journals.fcla.edu/mundi/article/view/24672/24003>.
- Seyyidođlu, Semih, Macit Özenbaş, and Aysen Yilmaz. 2008. "Investigation of Solid State Synthesis and Characterizations of Novel Sodium Rare-Earth Oxyphosphates." *Turkish Journal of Chemistry* 32(1): 35–54.
- Sumathi, Shanmugam, and Buvaneswari Gopal. 2015. "A New Insight into Biomedical Applications of an Apatite like Oxyphosphate - BiCa₄(PO₄)₃O." *Ceramics International* 41(3): 4852–60. <http://dx.doi.org/10.1016/j.ceramint.2014.12.043>.
- Toby, Brian H. 2006. "R Factors in Rietveld Analysis: How Good Is Good Enough?" *Powder Diffraction* 21(01): 67–70.
- Tordjman, Par i., R. Masse, and J.C. Guitel. 1974. "Structure Cristalline Du Monophosphate KTiPO₅." 139: 103–15.
- Uztetik Amour and M. Kızılyallı, *Journal of Solid State Chemistry*, vol. 120, pp. 275-278, 1995.
- Weeks, Mary Elvira. 1933. "The Discovery of the Elements. XXI. Supplementary Note on the Discovery of Phosphorus." *Journal of Chemical Education* 10(5): 302. <http://pubs.acs.org/doi/abs/10.1021/ed010p302>. 2000. "The Discovery of the Elements. II. Elements Known to the Alchemists." : 3.
- Wendus, Ayaka Hosoya, Toshiyuki Masui, and Nobuhito Imanaka. 2013. "Novel Environmentally Friendly Inorganic Blue Pigments Based on Amorphous Tungsten Oxyphosphate." *Chemistry Letters* 42(8): 906–8. <http://www.journal.csj.jp/doi/10.1246/cl.130314>.
- White (Firm), Samuel S. 1923. *Dental Cements: The Chemistry and Physics of Oxyphosphates / S.S. White Dental Mfg. Co.* Philadelphia: <http://hdl.handle.net/2027/mdp.39015029844597> (January 23, 2019).
- William W. Anku, Samuel O.B. Opong and, and Penny P. Govender. 2018. "We Are IntechOpen , the World ' s Leading Publisher of Open Access Books Built by Scientists, for Scientists TOP 1% Control of a Proportional Hydraulic System." *Intech open* 2: 64.
- Xia, Qi Neng et al. 2014. "Pd/NbOPO₄ Multifunctional Catalyst for the Direct Production of Liquid Alkanes from Aldol Adducts of Furans." *Angewandte Chemie - International Edition* 53(37): 9755–60.
- Xun, Xiumei. 2002. "Synthesis and Structure of New Transition Metal Containing Bismuth Oxides." Oregon State University. https://ir.library.oregonstate.edu/concern/graduate_thesis_or_dissertations/c534fr681.

Yang, Yang et al. 2015. "Review: Bismuth Complexes: Synthesis and Applications in Biomedicine." *Journal of Coordination Chemistry* 68(3): 379–97.

Yoshida, Akira, Yutaka Kaburagi, and Yoshihiro Hishiyama. 2016. "Scanning Electron Microscopy." *Materials Science and Engineering of Carbon - Characterization*: 71–92.

Zaafouri, A., M. Megdiche, and M. Gargouri. 2015. "Studies of Electric, Dielectric, and Conduction Mechanism by OLPT Model of Li₄P₂O₇." *Ionics* 21(7): 1867–79.

Zhao, Yun, Yong Chen, Ye Hua Zhang, and Shu Feng Liu. 2017. "Recent Advance in Black Phosphorus: Properties and Applications." *Materials Chemistry and Physics* 189: 215–29. <http://dx.doi.org/10.1016/j.matchemphys.2016.12.014>.





APPENDICES

7. APPENDICES

7.1. Appendix A FTIR Spectrums of Samples

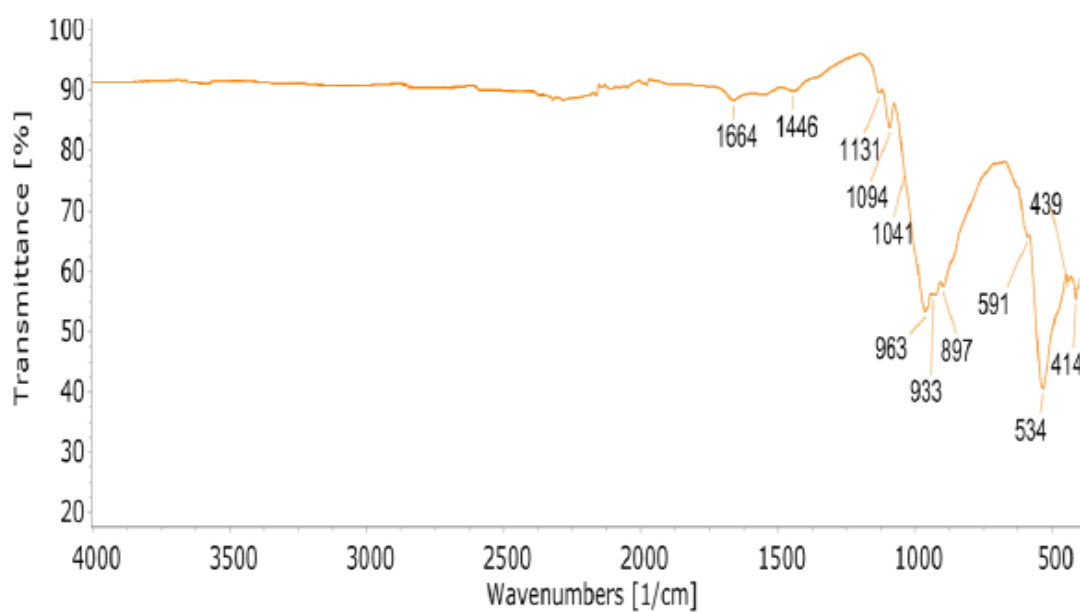


Figure A.1. IR Spectrum of the product of $Bi_2O_3 (s) + Na_4P_2O_7 (s)$ at $800^\circ C$ (12h).

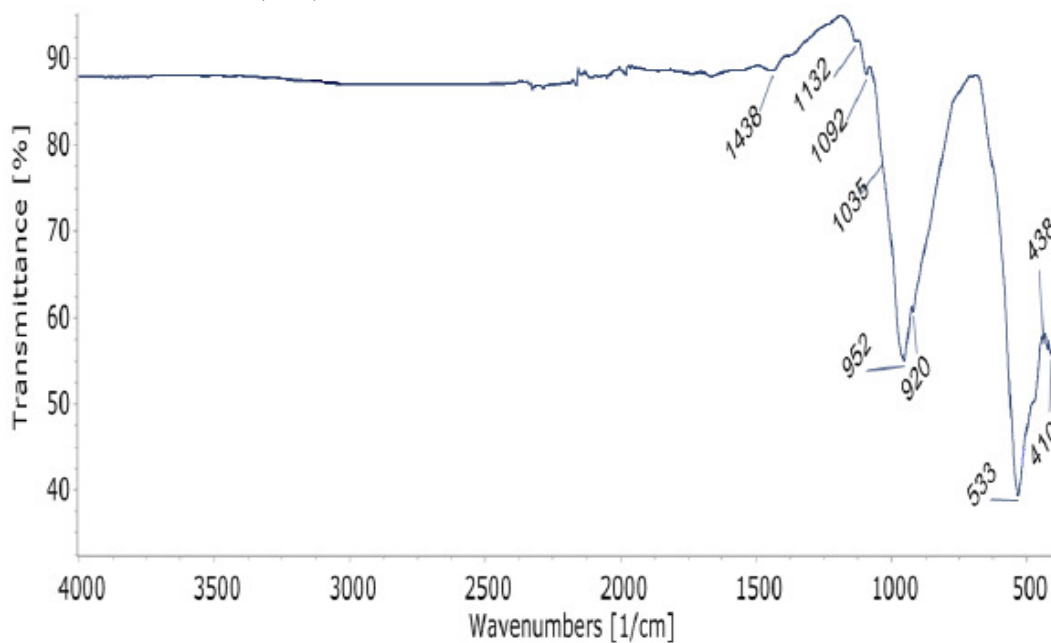


Figure A.2. IR Spectrum of the product of $Bi_2O_3 (s) + 2Na_2HPO_4(s)$ at $800^\circ C$ (12h).

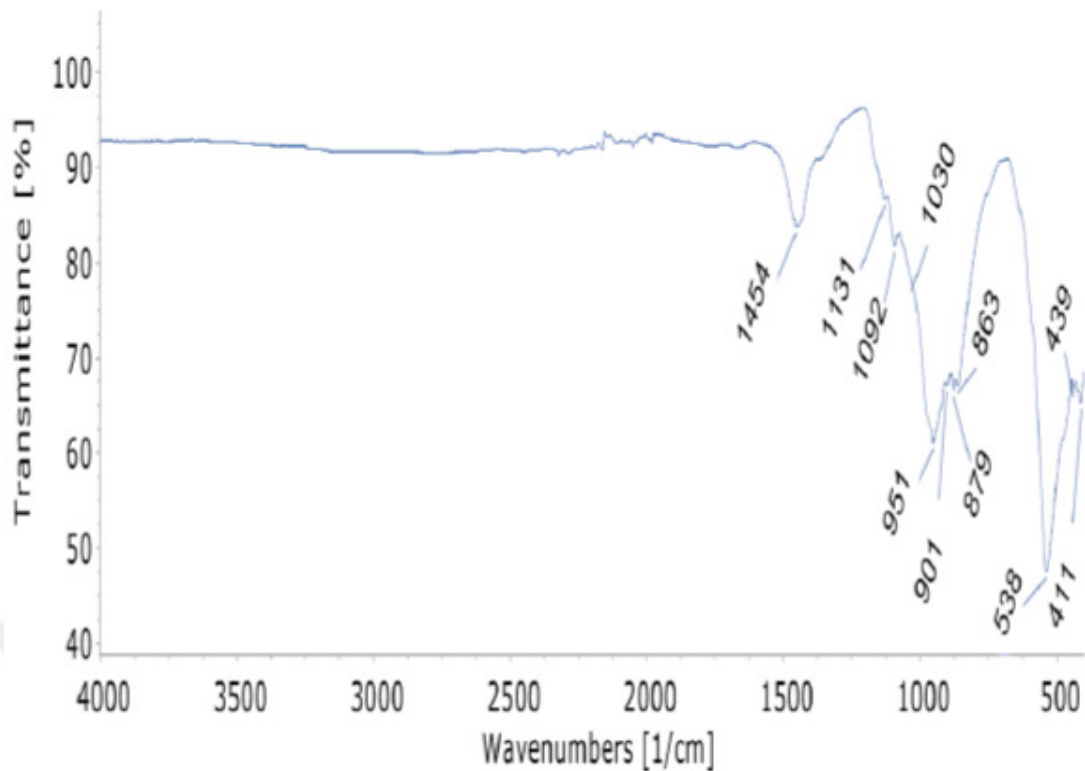


Figure A.3. IR Spectrum of the product of $Bi_2O_3(s) + 2NH_4H_2PO_4(s) + 2Na_2CO_3(s)$ at $800^\circ C$ (12h).

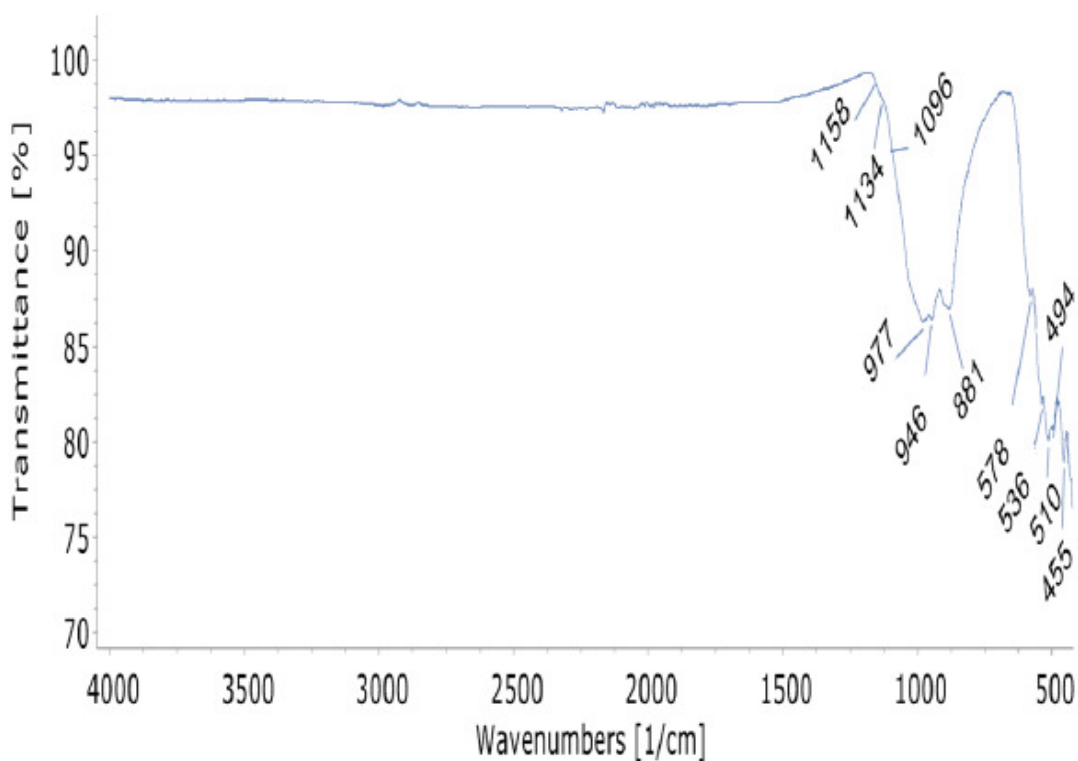


Figure A.4. IR Spectrum of the product of $Bi_2O_3(s) + Li_4P_2O_7(s)$ at $800^\circ C$ (20h).

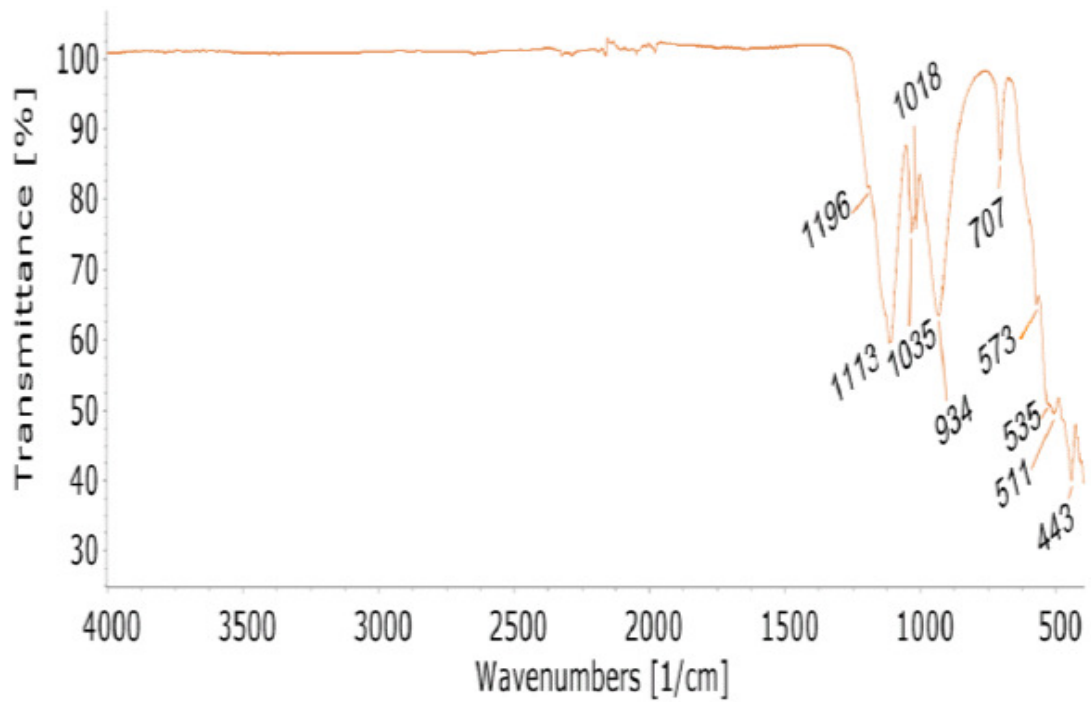


Figure A.5. IR Spectrum of the product of $Li_4P_2O_7(s)$ at $750^\circ C$ (8h).

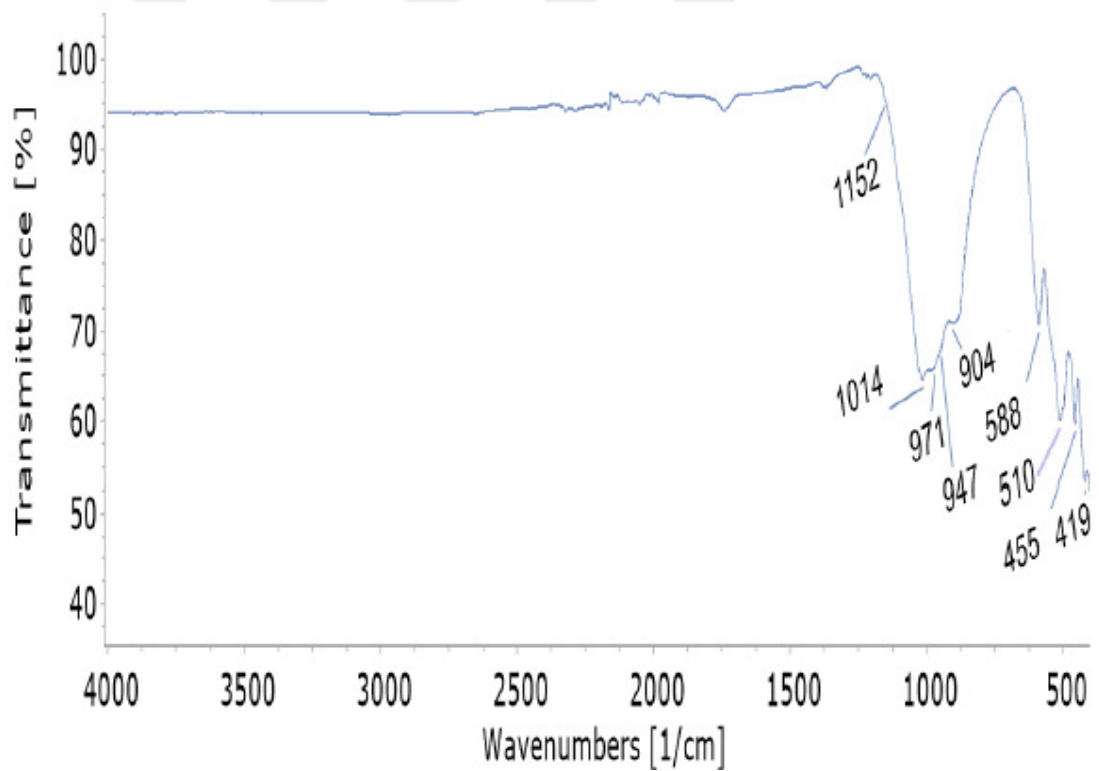


Figure A.6. IR Spectrum of the product of $Bi_2O_{3(s)} + LiH_2PO_{4(s)} + Li_2CO_{3(s)}$ at $850^\circ C$ (6h).

8. CURRICULUM VITAE

Name SURNAME : Burcu KARTAV

Place and Date of Birth : İstanbul, April 1993

University : Bolu Abant İzzet Baysal University

Bachelor's Degree : 2.33/4

MSc Degree : 3.27/4

e -mail : burcukartav@gmail.com